



universität  
wien

# DIPLOMARBEIT

Titel der Diplomarbeit

Analysis and characterisation of  
five novel Barentsz interactors in the context of  
nonsense-mediated mRNA decay

angestrebter akademischer Grad

Magistra der Naturwissenschaften (Mag. rer. nat.)

Verfasserin:	Ingrid Daniela Kieweg
Matrikel-Nummer:	0206085
Studienrichtung (lt. Studienblatt):	A490 Molekulare Biologie
Betreuer:	O. Univ.-Prof. Dr. Michael Kiebler

Wien, am 13.9.2008



# TABLE OF CONTENTS

ABSTRACT.....	1
INTRODUCTION .....	3
1. RNA decay.....	3
1.1. Nonsense-mediated mRNA decay (NMD).....	4
1.1.1. NMD in human diseases .....	5
1.1.2. Sources and definition of PTCs .....	5
1.1.3. Distinction between a normal stop codon and a PTC.....	5
1.1.4. The core NMD machinery .....	7
1.1.5. The mammalian exon-junction complex .....	9
1.1.6. Initiation and mechanism of NMD .....	12
1.1.7. Recognition of NMD targets occurs during different rounds of translation in distinct species .....	13
1.1.8. Translational termination upon recognition of NMD targets .....	14
1.1.9. Mechanism and location of the actual decay .....	16
2. RNA interference.....	18
2.1. Summary of RNAi mechanisms .....	19
2.2. Differences and similarities between miRNA and siRNA .....	20
2.3. Short hairpin RNA plasmids.....	21
3. Ideas, aims and working hypothesis .....	22
3.1. The idea behind the NMD assay.....	22
3.2. The experimental approach.....	26
3.3. Aim & working hypothesis.....	26
MATERIAL & METHODS .....	28
1. Material.....	28
1.1. Reagents & consumables .....	28
1.2. Enzymes.....	31
1.3. Antibodies .....	31
1.4. Plasmids & primers.....	33
1.5. Markers & ladders .....	37
1.6. Cells .....	38
1.7. Buffers & solutions .....	39
1.8. Equipment.....	44
2. Methods .....	46
2.1. Design, creation and testing of shRNA plasmids .....	46

2.1.1.	Design.....	46
2.1.2.	Cloning.....	47
2.1.3.	Selection and colony PCR.....	49
2.1.4.	Large-scale DNA isolation (Maxiprep).....	50
2.1.5.	Transfection of HeLa cells.....	52
2.1.6.	Protein lysate of HeLa cells.....	53
2.1.7.	Western Blot (WB).....	53
2.1.8.	Quantification of downregulation of proteins via Western blotting.....	54
2.2.	Immunocytochemistry.....	55
2.2.1.	Transient transfection of HeLa cells on coverslips using FuGENE <sup>®</sup> HD Transfection Reagent.....	55
2.2.2.	Immunofluorescence.....	55
2.2.3.	Microscopy of immunocytochemical preparations.....	55
2.3.	Semiquantitative PCR.....	56
2.3.1.	RNA isolation.....	56
2.3.2.	Reverse transcription PCR (RT-PCR).....	58
2.3.3.	Semiquantitative PCR.....	59
2.4.	Real-time PCR.....	61
2.4.1.	Temperature gradient PCR for optimisation of annealing temperature of primers.....	62
2.4.2.	Optimisation of real-time PCR conditions.....	63
2.4.3.	Optimised real-time PCR cycle scheme.....	63
2.4.4.	Neomycin selection.....	64
2.5.	Nucleofection of embryonic day 17 (E17) rat hippocampal neurons.....	65
	RESULTS.....	66
1.	Creation and testing of shRNAs for NMD assay candidates.....	66
1.1.	ShRNA plasmids targeting NPM1.....	71
1.2.	ShRNA plasmid targeting DDX5.....	75
1.3.	ShRNA plasmid targeting U5-116 kDa.....	77
1.4.	ShRNA plasmids targeting RBMX.....	79
1.5.	ShRNA plasmids targeting RBM4.....	82
2.	Establishment of an NMD Assay.....	84
2.1.	Essential controls for the NMD assay.....	84
2.2.	Establishment of the NMD assay in conventional HeLa cells using TCR- $\beta$ reporter constructs.....	87
2.2.1.	Optimisation of semiquantitative PCR for TCR- $\beta$ pre-mRNA in HeLa cells.....	88
2.2.2.	Test of different RNA isolation kits.....	90

2.2.3.	Optimisation of template amounts and internal standards for normalisation.....	92
2.2.4.	Optimisation of RT-PCR conditions.....	93
2.2.5.	Variability of cotransfections.....	97
2.3.	Cell lines stably expressing $\beta$ -Globin & real-time PCR.....	98
2.3.1.	Analysis of NMD assay candidates in TCR- $\beta$ and $\beta$ -Globin HeLa cell lines .....	99
2.3.2.	NPM1 downregulation in wt $\beta$ -Globin HeLa cells.....	101
2.3.3.	Neomycin selection to enrich transfected cells.....	105
2.3.4.	Establishment of the real-time PCR.....	107
2.3.5.	Real-time PCR of $\beta$ -Globin HeLa cell lines after neomycin selection.....	111
3.	Test of designed shRNA plasmids in E17 rat hippocampal neurons.....	113
	DISCUSSION.....	115
1.	Transfection of shRNA plasmids.....	115
2.	Downregulation and detection of selected protein candidates.....	117
2.1.	DDX5 detection with immunocytochemistry .....	117
2.2.	U5-116 kDa detection with immunocytochemistry .....	118
2.3.	RBMX and RBM4 detection on Western Blots.....	119
3.	Optimisation of RNA isolation & PCR setups .....	121
4.	Comparison of conventional and stable HeLa cells.....	122
5.	Neomycin selection.....	123
6.	Preliminary NMD assay results .....	124
7.	Conclusions & prospects .....	125
8.	Arrival at hypothesis.....	127
	ACKNOWLEDGEMENT .....	129
	APPENDIX I: ZUSAMMENFASSUNG .....	130
	APPENDIX II: REFERENCES .....	132
	APPENDIX III: CURRICULUM VITAE.....	147



## ABSTRACT

Nonsense-mediated mRNA decay (NMD) is a mechanism to post-transcriptionally regulate gene expression in eukaryotes. Beside quantity control, NMD also serves as quality control for transcripts. The latter function comprises the degradation of aberrant RNAs with a so-called premature termination codon (PTC). Otherwise, these RNAs would give rise to truncated proteins with potentially deleterious functions which is often the case in diseases like cancer.

In my diploma thesis, potential NMD components were investigated for their role in NMD. For this purpose, I especially established an assay in different HeLa cell lines. NMD is impaired, if an essential NMD component, like Barentsz (Btz) or the eukaryotic initiation factor 4A isoform 3 (eIF4AIII), is missing. This leads to accumulation of aberrant PTC-containing transcripts, because they are no longer degraded by NMD. Therefore, these two proteins served as positive controls for the establishment of the assay. As a next step, the impact of five putative protein-protein interactors of the RNA-binding protein Btz on NMD was analysed: Nucleophosmin 1 (NPM1), DEAD-box polypeptide 5 (DDX5), U5-116 kDa, RNA-binding motif protein - X-linked (RBMX) and RNA-binding motif protein 4 (RBM4). I generated short hairpin RNA (shRNA) plasmids directed against these proteins and tested them. Subsequently, I investigated whether the depletion of the respective proteins using shRNAs caused accumulation of PTC-containing NMD reporter constructs, as it is the case in the Btz knockdown. Upon depletion, the expression levels and the decay of exogenously provided T-cell receptor  $\beta$  (TCR- $\beta$ ) and  $\beta$ -Globin NMD reporter constructs with and without PTC were compared and measured using semiquantitative PCR and real-time PCR. In addition, neomycin/G418 selection was performed to enrich for successfully transfected, candidate-depleted cells. Finally, the obtained real-time PCR data indicated a crucial role of DDX5 and U5-116 kDa in NMD, because their knockdowns caused accumulation of aberrant transcripts. No firm conclusion was possible regarding NPM1, RBMX and RBM4, because their shRNA plasmids did not reduce the corresponding protein levels in the used stable HeLa cell lines. Further experiments for the analysis of these proteins are necessary. In this diploma thesis, I was able to identify two additional proteins which play a role in NMD: the potential Btz interactors DDX5 and U5-116 kDa.





# INTRODUCTION

## 1. RNA DECAY

Eukaryotic gene expression is a complex and highly regulated process. It consists of many subsequent and interconnected steps: transcription, 5'-cap formation, messenger RNA (mRNA) splicing, polyadenylation, mRNA export and transport, mRNA storage or translation, translational control and mRNA degradation. These different stages of gene expression assure that genes and their products are only expressed when needed. Differential gene expression is crucial to provide the cell with the necessary transcripts and proteins in various situations. This enables the cell to react to its environment, to develop and to promote its own survival.

For a cell, it is very important to keep its metabolism under tight control in order to minimise its energy requirement and conversion. Therefore, it is necessary to create different functional spaces, called compartments, for distinct reactions within a cell. One efficient way to achieve this is by tightly controlling local protein synthesis. In addition, it is very important for the cell to get rid of abnormal or no longer needed RNAs via RNA decay. Different kinds and forms of RNA decay have evolved within cells to adapt to the different requirements.

## 1.1. Nonsense-mediated mRNA decay (NMD)

Nonsense-mediated mRNA decay (NMD) is a post-transcriptional quality-control mechanism for gene expression in eukaryotes (for an overview see (Chang, Y. F. et al. 2007)). It is a highly conserved pathway present in all eukaryotes examined up to now. mRNAs that have premature-termination codons (PTCs) are degraded by this process. In higher eukaryotes, PTCs are defined by the “50 - 55 nucleotides” rule saying that a stop codon residing more than 50 - 55 nt upstream of the 3'-most exon-exon junction is a premature termination codon.

If mRNAs containing PTCs were translated, they would result in truncated proteins with dominant-negative or deleterious gain-of-function activities. In case the NMD process is impaired, which is often the case in diseases (e.g. cancer), harmful and non-functional mRNAs with PTCs accumulate in the cell leading to further derailing of the cell's metabolism. Approximately 3 -10% of the expression of the transcriptome are regulated via NMD in different species (reviewed in (Behm-Ansmant, I., Kashima, I. et al. 2007)).

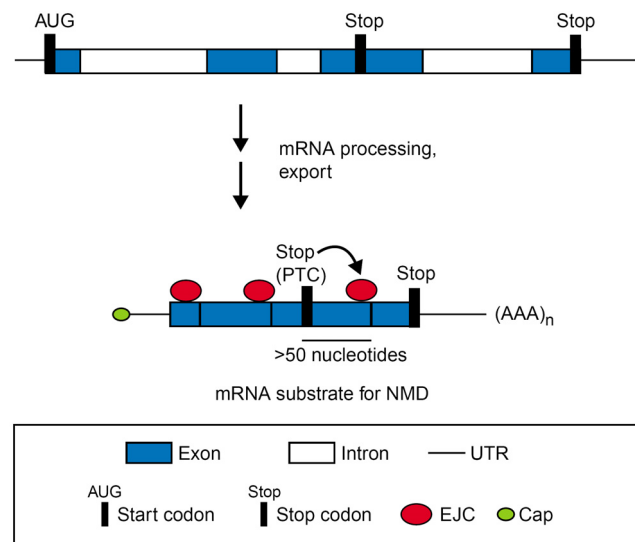


**Figure 1-1: The “50 - 55 nucleotides” rule for the definition of premature-termination codons (PTCs).** (Figure 1B from (Schell, T. et al. 2002)).

If a stop codon is located more than 50 - 55 nt upstream of the 3'-most exon-exon junction and respectively exon-junction complex (EJC), it is a premature termination codon.

### **1.1.1. NMD in human diseases**

NMD is an important RNA surveillance mechanism. Interestingly, derailing of NMD can cause or aggravate human illnesses as well as NMD can modulate or ease the phenotype and the symptoms of genetic diseases through inhibition of the synthesis of harmful or non-functional proteins (reviewed in (Holbrook, J. A. et al. 2004)). Approximately, 10 - 30% of PTC-containing transcripts escape NMD and produce physiological levels of truncated proteins that can mediate certain effects (reviewed in (Neu-Yilik, G. et al. 2004)). Current studies find that ~20.3% of the ~43,000 disease-associated single base pair mutations in coding genome sequences are nonsense mutations (according to the Human Gene Mutation Database in November 2007) (Mort, M. et al. 2008).

### **1.1.2. Sources and definition of PTCs**

In principle, there are three major ways how PTCs are introduced (for an overview see (Chang, Y. F. et al. 2007)). First, random nonsense and frameshift mutations emerge in the DNA. These mutated DNA sequences are then subsequently transcribed into mRNA. The second source of PTCs is programmed DNA rearrangement. This is a very useful mechanism to create big diversity with little genomic space. In mammals, for example the T-cell receptor (TCR) and the immunoglobulin (Ig) genes use DNA rearrangement to increase their repertoire of antigen receptors. The third possibility to generate PTCs is via errors in RNA splicing, including aberrant alternative splicing.

### **1.1.3. Distinction between a normal stop codon and a PTC**

For understanding the observed differences in NMD and its importance in various species, it is necessary to note that the NMD targets are not conserved and that the NMD effectors underwent functional diversification, at least in mammals (reviewed in (Behm-Ansmant, I., Kashima, I. et al. 2007)). Thus, NMD effectors can have slightly different or additional functions in NMD or other cellular processes in distinct species. Furthermore, a factor required for NMD in one organism might not even be necessary for decay in another organism.

### In mammals

An intron downstream of the PTC is a strong indication and signal for the cell that the mRNA might be aberrant. If the stop codon is normal, representing a so-called *bona fide* stop codon, it is usually localised in the last exon and therefore no intron follows. There are, however, exceptions from this rule. There is recent evidence that mammalian transcripts lacking introns are usually not targeted by NMD (Maquat, L. E. and Li, X. 2001; Brocke, K. S. et al. 2002). But how can an intron which is already removed in the nucleus play a role for NMD that depends on the cytoplasmic translation apparatus? Interestingly, introns downstream of the PTC have to be spliceable to trigger NMD (Carter, M. S. et al. 1996). This indicates that the spliceosome leaves an imprint on the mRNA which is recognised by ribosomes: the exon-junction complex (EJC) (for an overview see (Chang, Y. F. et al. 2007)).

### In invertebrates

In *S. cerevisiae*, *D. melanogaster* and *C. elegans*, PTC recognition to elicit NMD occurs independent of splicing and therefore of the EJC (reviewed in (Behm-Ansmant, I., Kashima, I. et al. 2007)). Three different triggers for NMD were observed in invertebrates (for an overview see (Behm-Ansmant, I., Kashima, I. et al. 2007)). First, loosely defined downstream elements (DSEs) can elicit NMD. Second, the poly(A)-tail or another mark generated during splicing contains positional information to recognise the PTC. Third, the so-called “faux 3’-UTR model” is involved in the activation of NMD. In this model, the “faux 3’-UTRs” have an altered protein composition compared to normal 3’-UTRs. These modified 3’-UTRs are recognised by ribosomes during translation. For example, the cytoplasmic poly(A)-binding protein PABPC1 (in metazoan) is a marker of normal 3’-UTRs (for an overview see (Amrani, N. et al. 2004; Behm-Ansmant, I., Gatfield, D. et al. 2007)). Interestingly, the binding of PABPC1 downstream of a PTC converts the PTC into a normal stop codon and therefore suppresses NMD. This indicates that an increased distance between the poly(A)-tail and the stop codon is crucial for PTC recognition. Therefore, long 3’-UTRs seem to trigger NMD under certain conditions. This PABPC1-dependent form of NMD also exists in mammals (reviewed in (Behm-Ansmant, I., Kashima, I. et al. 2007)).

#### 1.1.4. The core NMD machinery

The core of the NMD machinery consists of the up-frameshift (UPF) proteins, UPF1, UPF2 and UPF3 (reviewed in (Chang, Y. F. et al. 2007)). They serve as a platform for the attachment and interaction of additional NMD factors like EJC components.

UPF 1 is a phosphoprotein as well as a helicase of the group I family. The protein has an ATP-dependent 5'-to-3' helicase activity and an RNA-dependent ATPase activity (reviewed in (Chang, Y. F. et al. 2007)). UPF1 plays an important role in DNA and RNA stability pathways (reviewed in (Azzalin, C. M. et al. 2006)). It is predominantly localised in the cytoplasm, but shuttles also between the cytoplasm and the nucleus (reviewed in (Chang, Y. F. et al. 2007)). This factor plays a crucial role in NMD and other cellular processes (reviewed in (Azzalin, C. M. et al. 2006)). Beside NMD, UPF1 is also required in Staufen1-mediated RNA decay (SMD) (Kim, Y. K. et al. 2005) and mediates the decay of replication-dependent histone mRNAs together with Stem-Loop Binding Protein (SLBP) (reviewed in (Azzalin, C. M. et al. 2006; Behm-Ansmant, I., Kashima, I. et al. 2007)). Experiments showed that UPF1 is essential for survival in mammals, but is not absolutely necessary in lower eukaryotes (reviewed in (Chang, Y. F. et al. 2007)).

When translation is terminated, UPF1 is recruited to the mRNA. Its activities in NMD are driven and regulated by cycles of de-/phosphorylation of its serine residues (for an overview see (Chang, Y. F. et al. 2007)). UPF1 is de-/phosphorylated by the Suppressors with Morphogenetic effect on Genitalia (SMG) proteins which were first identified in *C. elegans*. SMG-1 is a kinase which is responsible for the phosphorylation, whereas the SMG-5/SMG-7 heterodimer and the SMG-6 protein promote dephosphorylation. None of the SMG proteins is a phosphatase. Instead, they mediate their action for example via recruitment of protein phosphatase 2A (PP2A) to UPF1 (e.g. (Anders, K. R. et al. 2003)). The SMG factors play also a role in the recruitment of UPF1 to processing bodies (P-bodies) (Unterholzner, L. et al. 2004; Fukuhara, N. et al. 2005). Experiments in *C. elegans* proved the importance of the SMG proteins for NMD (Pulak, R. et al. 1993). If their corresponding genes are mutated and the proteins are no longer functional, NMD is completely abolished.

UPF 3 has no known biochemical function to date (reviewed in (Chang, Y. F. et al. 2007)). Whereas mammals have two UPF3 genes, coding for UPF3a (also known as UPF3) and UPF3b (also UPF3X), lower eukaryotes possess only one UPF3 gene. In higher eukaryotes, UPF3a and UPF3b are recruited to the mRNA in the nucleus during splicing. They stay associated with the RNA-protein complex, also when the complex is exported into the cytoplasm. There they serve as a trigger for NMD as part of the EJC (for an overview see (Chang, Y. F. et al. 2007)).

UPF2 serves as an adaptor molecule to bring UPF1 and UPF3 together to start NMD. It is still unclear whether UPF2 is recruited to mRNAs in the nucleus or later to the perinuclear region in the cytoplasm (reviewed in (Chang, Y. F. et al. 2007)). UPF2 is like UPF3 part of the EJC and therefore elicits NMD (reviewed in (Chang, Y. F. et al. 2007)).

Interestingly, some of these NMD factors play also a role in telomere maintenance (for an overview see (Holbrook, J. A. et al. 2004)). Studies in yeast showed that if NMD is impaired, 35.9% of all open reading frames (ORFs) of the telomeric region are upregulated implicating a function of NMD in telomeric gene regulation (He, F. et al. 2003).

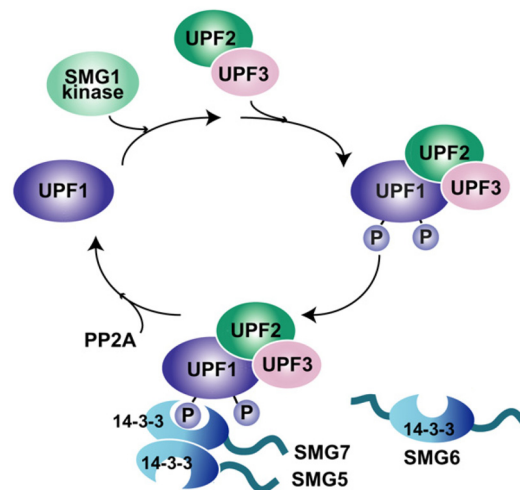


**Figure 1-2: Interactions of the core NMD machinery.** (Figure 1 from (Behm-Ansmant, I., Kashima, I. et al. 2007)).

The core of the NMD machinery consists of the three UPF proteins. UPF1, a conserved RNA helicase, is a key player in NMD. UPF1 is phosphorylated by the SMG-1 kinase at serine residues followed by association of UPF2 and UPF3. SMG-6 and the heterodimer SMG-5/SMG-7 bind phosphorylated UPF1 via 14-3-3 domains and recruit protein phosphatase 2A (PP2A) for dephosphorylation. The de- and phosphorylated state of UPF1 allow the binding and interaction of different factors which mediate and regulate NMD.

### 1.1.5. The mammalian exon-junction complex

This dynamic, multi-protein complex is deposited at the mRNA 20 -24 nt upstream of exon-exon junctions upon RNA splicing and serves as signal to trigger NMD. The core of the EJC consists of four proteins: Barentsz (Btz) or MLN51, the heterodimer MAGOH/Y14 and eIF4AIII (Tange, T. O. et al. 2005; Bono, F. et al. 2006). This protein core serves as a platform (Le Hir, H. et al. 2001) where transient EJC factors can associate and interact. For example, UPF2 and UPF 3b also associate to and are part of the EJC (reviewed in (Chang, Y. F. et al. 2007)).

The EJC stays attached to the messenger ribonucleoprotein particle (mRNP), a complex of mRNA and proteins, when they enter the cytoplasm. Thus, the EJC marks previous locations of introns relative to stop codons (reviewed in (Chang, Y. F. et al. 2007)). This information is still present in the cytoplasm - as long as translation has not yet occurred - and dictates whether an mRNA is an NMD target.

The main function of the EJC is to mediate NMD (reviewed in (Chang, Y. F. et al. 2007)). In addition, the complex mediates the export of mature, normally spliced mRNAs, their subcellular localisation and translational stimulation (reviewed in (Chang, Y. F. et al. 2007; Le Hir, H. et al. 2008)).

Two recent studies link the EJC's translation control activities with translation activation via the mTOR signalling pathway (Ma, X. M. et al. 2008) as well as with translation repression (repression of bulk translation after the first pioneer round of translation) during NMD (Isken, O. et al. 2008). This is not contradictory, but emphasises the central role of the EJC.

In normal transcripts, all EJCs are found upstream of the stop codon, so they can be displaced by the ribosomes. NMD mRNA targets have a stop codon in a premature position. This also results in the deposition of at least one EJC downstream of the PTC which is a clear signal that triggers NMD (reviewed in (Chang, Y. F. et al. 2007)).

Furthermore, there is recent data indicating that EJC-independent NMD is possible in rare cases (for an overview see (Chang, Y. F. et al. 2007)).

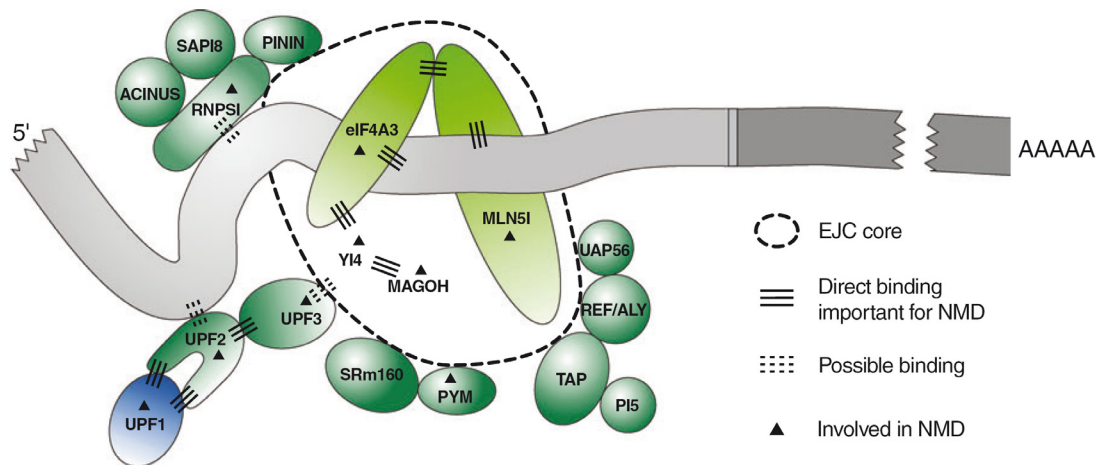


**Figure 1-3: The structure and composition of the exon-junction complex.** (Figure 1 from (Chang, Y. F. et al. 2007)).

The RNA-binding exon-junction complex (EJC) core consists of the four proteins: Y14, MAGOH, eIF4AIII and Barentsz (BTZ; also MLN51). In general, the EJC serves as a platform where other EJC and NMD factors (illustrated in dark green) can transiently associate and interact with the mRNP during its transportation from the nucleus into the cytoplasm. Possible and confirmed interactions of the core NMD machinery - consisting of the three UPF proteins - with the RNA and the EJC are also depicted. The N-terminal binding domains of the proteins are coloured darker compared to the lighter C-terminal binding domains. Interaction and relation of the proteins to each other are explained by the caption on the right.

The four essential protein core components of the EJC (with their synonyms in parentheses):

1. **Y14** (Y14: RBM8 – RNA-binding motif protein 8, tsu – tsunagi) &
2. **MAGOH** (MAGOH: mago-nashi homolog)

The proteins Y14 and MAGOH form a stable heterodimer via an RNA-binding domain (RBD). Both Y14 as well as MAGOH also directly bind to eIF4AIII (Shibuya, T. et al. 2004; Bono, F. et al. 2006).

3. **eIF4AIII** (eukaryotic initiation factor 4A isoform 3; DDX48 - DEAD (Asp-Glu-Ala-Asp) box polypeptide 48)

The ATP-dependent DEAD-box RNA helicase encloses one ATP molecule, directly binds Y14/MAGOH as well as spliced mRNA and anchors the EJC to its RNA substrate (Shibuya, T. et al. 2004). Thus, eIF4AIII serves as a clamp between the mRNA and the EJC and plays a central role in NMD (Palacios, I. M. et al. 2004).

eIF4AIII represents one of three eukaryotic translation initiation factors of the eIF4A family which are encoded by different genes and have distinct functions (Li, Q. et al.



1999). eIF4A, eIF4E and eIF4G form the trimeric eIF4F pre-initiation complex for eukaryotic translation (Svitkin, Y. V. et al. 2005).

#### 4. Btz (Barentsz; MLN51 - Metastatic lymph node protein 51, CASC3 - cancer susceptibility candidate 3 protein)

Btz is an RNA-binding protein (Degot, S. et al. 2004). In *D. melanogaster* Btz (van Eeden, F. J. et al. 2001), Y14/MAGOH, eIF4AIII and Staufen proteins orchestrate the localisation of *oskar* mRNA to the posterior pole of the oocyte (for an overview see (Chang, Y. F. et al. 2007)). In humans, Btz is overexpressed in breast cancer cells (Degot, S. et al. 2002). The protein was also shown to bind spliced mRNA *in vitro* and to localise to nuclear speckles - subnuclear structures enriched in pre-mRNA splicing factors – *in vivo* (Degot, S. et al. 2004; Ballut, L. et al. 2005). Btz directly interacts with the RNA through a single conserved residue, a phenylalanine, as well as with the proteins MAGOH and eIF4AIII (Chan, W. K. et al. 2007) via its speckle localiser and RNA-binding module (called SELOR domain; residues 137-283) (Ballut, L. et al. 2005; Bono, F. et al. 2006). The crucial role of Btz in NMD is already confirmed (Palacios, I. M. et al. 2004).



**Figure 1-4: The protein structure and different consensus motifs of Barentsz (Btz).** (Figure 3A from (Degot, S. et al. 2004)).

Btz protein is 703 amino acids and respectively 76 kDa in size. For its transportation und shuttling, the Btz protein has two nuclear localisation signals (NLS) - NLS1 and NLS2 – within the N-terminal half as well as one nuclear export signal (NES) within the C-terminal half. These sequences are conserved in miscellaneous species making Btz a nucleocytoplasmic protein. RNA binding is mediated by the speckle localiser and RNA binding module motif (SELOR domain; residues 137-283) which localises around the two NLSs in the N-terminal half. In addition, Btz has different potential protein-protein interaction domains: one coiled-coil domain, one SH2 domain binding site and four SH3 domain binding sites. Btz has a glycine-rich and a glutamine-rich region at the N-terminus and a proline-rich region at the C-terminus.

### 1.1.6. Initiation and mechanism of NMD

In the following, the chain of events is highlighted that marks an mRNA for decay (for an overview see (Chang, Y. F. et al. 2007)). Three signals and triggers are necessary to elicit NMD.

First, an mRNA must have a PTC to be marked for decay. Second, the EJC is deposited 20 – 24 nt before a splice donor site at the mammalian RNA during splicing. In *S. cerevisiae*, for example, specific mRNA downstream sequence elements and/or abnormally long 3'-UTRs serve as a second signal for NMD (Ruiz-Echevarria, M. J. et al. 1998). Third, the attachment of the NMD core machinery consisting of the UPF proteins is crucial for NMD. The activity of this complex is fine-tuned via de-/phosphorylation by the SMG proteins. The whole NMD process is then mediated by the binding and activity of additional protein interactors to both the EJC and the NMD core complex. Both complexes then in turn interact and communicate with each other.

In general, NMD is only elicited, if the EJC interacts with factors bound near or at the PTC. It is still unclear how the ribosome then orchestrates the dissociation of the EJC from the mRNA.

### **1.1.7. Recognition of NMD targets occurs during different rounds of translation in distinct species**

If a PTC-containing mRNA went through several rounds of translation before it was decayed by NMD, it would give rise to large amounts of harmful or not functional proteins. This would be a major disadvantage and cause a serious problem for a cell. Thus, it is important that mRNA NMD targets are already recognised during their first round of translation.

Interestingly, biochemical data support this idea showing that most mammalian mRNAs are already downregulated and decayed via NMD in the nuclear fraction (e.g (Carter, M. S. et al. 1996)). This implies that mRNAs are scanned for decay via NMD when they are in the nucleus or in the cytoplasm, but still attached to the nuclear envelope. Furthermore, this finding is also contributing to the discussion whether translation is exclusively proceeding in the cytoplasm or also occurring in the nucleus to some extent. Additional evidence, however, documents that also newly synthesised mRNAs are targeted by NMD during a unique pioneer round of translation (for an overview see (Chang, Y. F. et al. 2007)). The cap-binding complex, a heterodimer of the cap-binding proteins 20 and 80 (CBP20 and CBP80), is deposited at the 5' of pre-mRNAs during transcription (for an overview see (Izaurrealde, E. et al. 1995; Chang, Y. F. et al. 2007)). Therefore, CBC is a valid marker for newly synthesised mRNAs. CBC promotes RNA splicing and stays attached to the mRNA target until translation. If an mRNA has no NMD signals, CBC is replaced by the eukaryotic elongation factor eIF4E (for an overview see (Chang, Y. F. et al. 2007)). Then the pioneer round of translation can be followed by additional rounds of translation like on the assembly line, a process called bulk translation.

NMD is just executed on CBP80-marked mRNAs, but never on eIF4E-bound mRNAs (Ishigaki, Y. et al. 2001; Lejeune, F. et al. 2002). Additional findings and experiments support this data (reviewed in (Chang, Y. F. et al. 2007)).

Some publications, however, indicate that NMD can also occur without CBC, if the mRNAs have so-called internal ribosomal entry sites (IRES) (Wang, J. et al. 2002; Holbrook, J. A. et al. 2006). An IRES mediates the binding of the mRNA to the ribosome, usually when the 5'-cap is missing, and thereby initiates translation.

In contrast to mammals, *S. cerevisiae* seems to activate NMD in any round of translation. In general, NMD in yeast is very inefficient (Keeling, K. M. et al. 2004). Interestingly, NMD in yeast is still functional without Cbc1p (the yeast ortholog of mammalian CBP80) (Gao, Q. et al. 2005).

Taken together, the presented evidence indicates that higher and lower eukaryotes differ in the number of translational rounds which are necessary to recognise the signals and elicit NMD.

### **1.1.8. Translational termination upon recognition of NMD targets**

Translational termination occurs when the eukaryotic release factors eRF1 and eRF3 recognise a stop codon. These two factors probably recruit UPF1 followed by SMG-1 to the stop codon at the ribosome. The emerging complex is called SURF complex consisting of SMG-1, UPF1 and eRFs (Kashima, I. et al. 2006). Interaction between UPF1 in the SURF complex on one side and UPF2 in the EJC on the other side leads to the formation of a “super” complex consisting of SURF and EJC which mediates NMD (Kashima, I. et al. 2006). This probably stimulates SMG-1 to phosphorylate UPF1. Hence, this is considered to be the starting signal for NMD.

UPF1 phosphorylation probably triggers the recruitment of new NMD factors like SMG-7, dissociation from the mRNPs and therefore recycling of the eRFs and the ribosomal subunits. Biochemical data shows that phosphorylated UPF1 is predominantly present in polysome fractions (Pal, M. et al. 2001). Concerning all evidence to date, UPF1 can be seen as the central key player in mediating and eliciting mRNA decay.

Nevertheless, contradictory data to the SURF/EJC model exists. These data indicate UPF2- (Gehring, N. H. et al. 2003; Gehring, N. H. et al. 2005) and UPF3-independent (Chan, W. et al. 2005) NMD pathways. In addition, an NMD pathway independent of the EJC core, but dependent on the RNA-binding proteins RNPS1 (RNA-binding protein with serine-rich domain 1) and UPF2 was reported (Gehring, N. H. et al. 2005). These three alternative pathways are called non-classical NMD pathways.

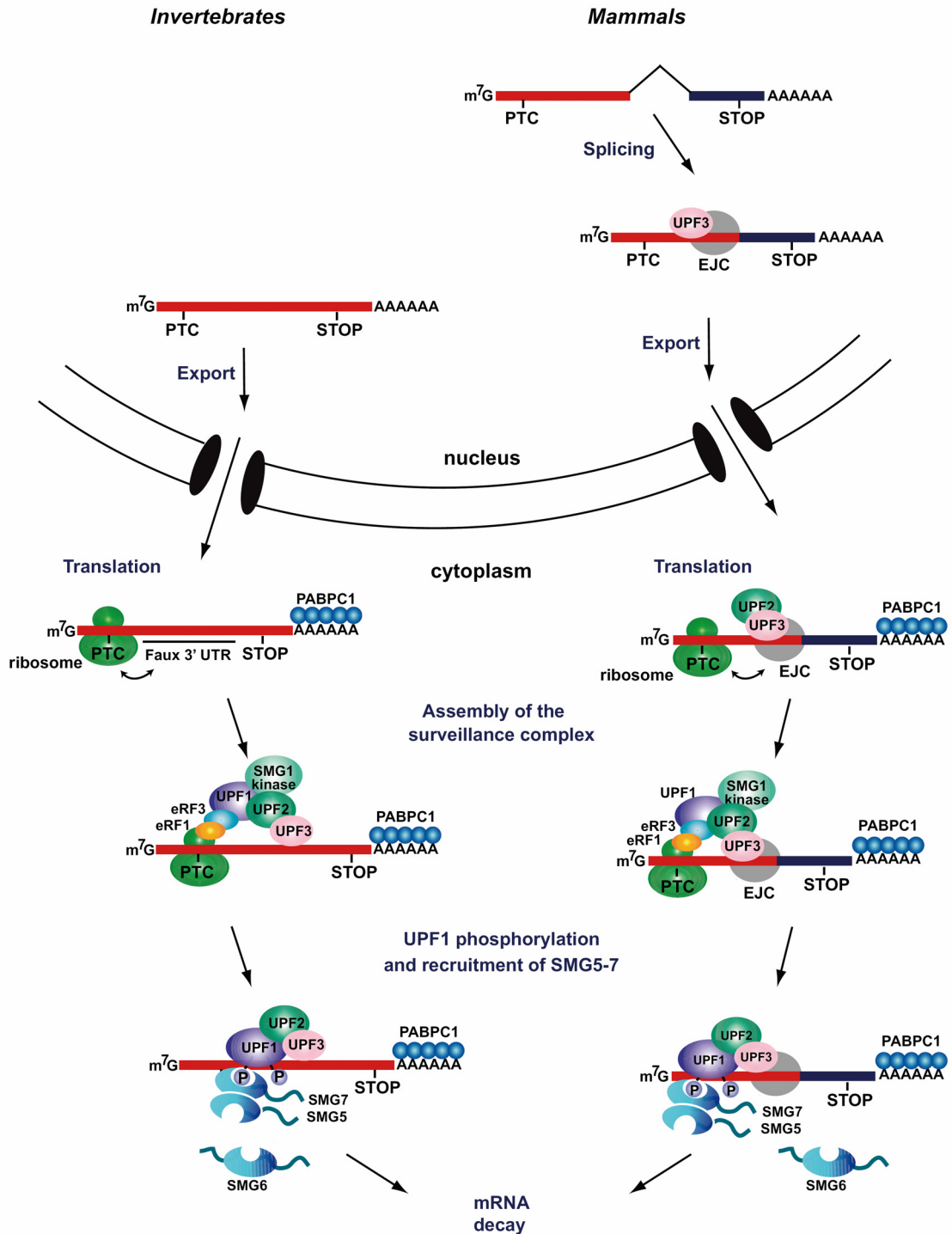


**Figure 1-5: NMD in invertebrates versus mammals.** (Figure 2 from (Behm-Ansmant, I., Gatfield, D. et al. 2007)).

The PTC is defined by its relative position to a cis-acting downstream signal. The signal varies across different species. In invertebrates like *S. cerevisiae*, *D. melanogaster* and *C. elegans*, the cis-acting signal is a so-called “faux 3'-UTR” where a different subset of proteins associates compared to normal 3'-UTRs. For example, cytoplasmic poly(A)-binding protein PABPC1 is a marker of normal 3'-UTRs flanking correct stop codons. PABPC1 is missing near PTCs. These signals elicit NMD. In mammals, the cis-acting signal is the exon-junction complex which is deposited at exon-exon boundaries during splicing. Translation termination is followed by subsequent events resulting in mRNA decay via NMD.

### 1.1.9. Mechanism and location of the actual decay

Phosphorylated UPF1 attracts SMG-7 for its dephosphorylation. SMG-7 is supposed to be the terminal effector in NMD.

Interestingly, the ribonucleases degrading normal or PTC-containing RNA are the same (reviewed in (Chang, Y. F. et al. 2007)). The decapping-dependent 5'-to-3' exoribonuclease pathway as well as the 3'-to-5' exoribonuclease pathway are used for NMD (reviewed in (Chang, Y. F. et al. 2007)).

It is still unclear, whether NMD is just a nuclear and/or a cytoplasmic process. Different data supporting both models exist (for an overview see (Chang, Y. F. et al. 2007)). But it seems that it is depending on the target itself where it is decayed. Therefore, NMD substrates can be divided into two classes, concerning whether they are already degraded in or associated with the nucleus or later on in the cytoplasm (for an overview see (Frischmeyer, P. A. et al. 1999; Maquat, L. E. and Carmichael, G. G. 2001; Wilkinson, M. F. et al. 2002)).

One possible site for NMD to take place in the cytoplasm are P-bodies. The C-terminus of SMG-7 was identified to localise mRNPs containing mRNAs with PTCs to P-bodies where they can be decayed (Unterholzner, L. et al. 2004).

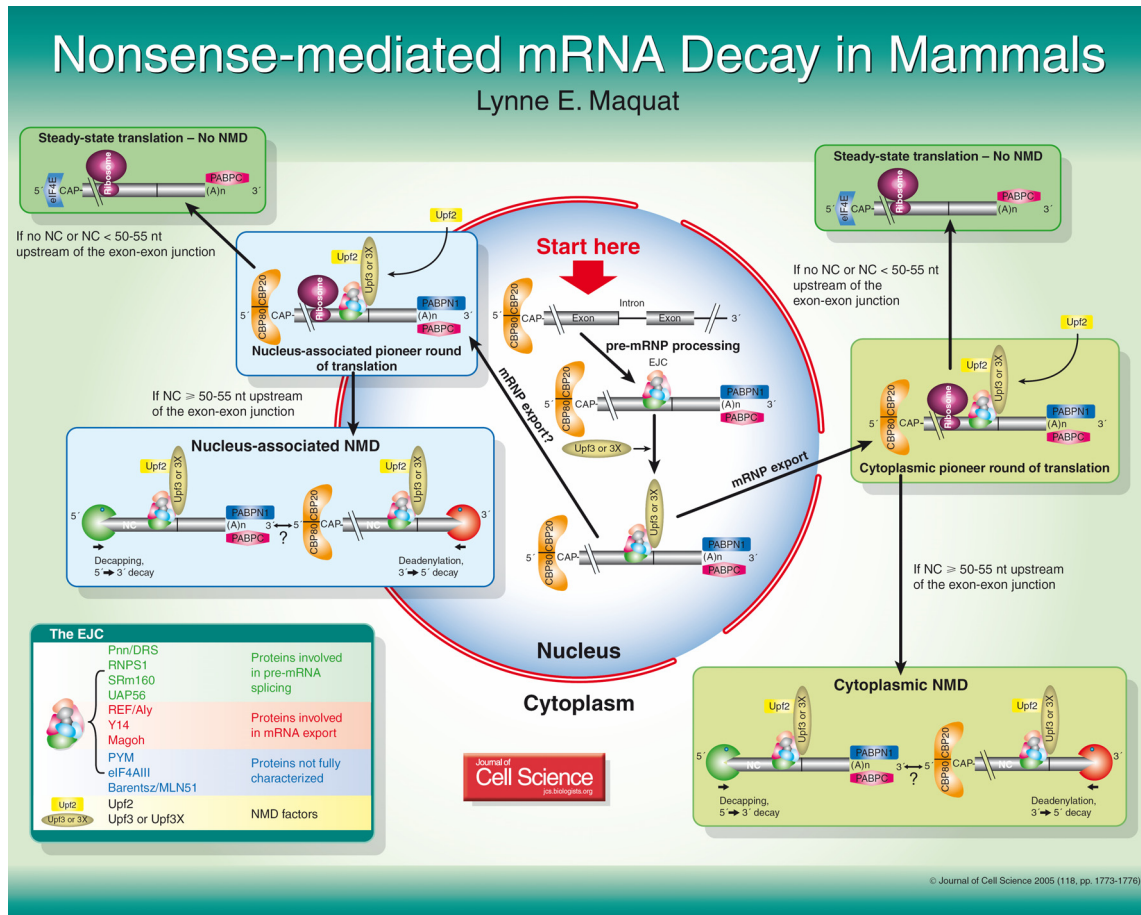


**Figure 1-6: Decision between translation and NMD in mammals.** (Figure from (Maquat, L. E. 2005)). Pre-mRNPs are processed in the nucleus. Introns are spliced out and the EJC assembles on exon-exon junctions. The 5' of the pre-mRNAs is marked by the cap-binding complex (CBC = CBP20 and CBP80). Mature mRNPs are then exported into the cytoplasm. The PTC (= NC = nonsense codon) and other protein signals for NMD are then recognised by the ribosome either in a nucleus-associated or a cytoplasmic pioneer round of translation. PTCs are defined via the “50 - 55 nucleotides“ rule. The ribosome is stalled and mRNA decay involving decapping and/or deadenylation takes place. In contrast, if the mRNA contains no PTC and no NMD signals, the CBC is replaced by the eukaryotic elongation factor eIF4E and steady-state translation (also called bulk translation) occurs.

## 2. RNA INTERFERENCE

The discovery of RNA interference (RNAi) has opened up a plethora of opportunities for its application and use. RNAi probably evolved as a protection mechanism against invading double-strand RNA (dsRNA) (reviewed in (Plasterk, R. H. 2002; Zamore, P. D. 2002; Wilkins, C. et al. 2005)) in fungi, plants and animals. It is an important mechanism to mediate gene regulation and silencing. Gene silencing was first discovered in plants by Napoli et al. in 1990 (Napoli, C. et al. 1990) and the mechanism was later confirmed by van Blokland (van Blokland, R., van der Geest, N., Mol, J., Kooter, J. 1994) who named it co-suppression, as transgene and endogenous gene were both repressed.

Systemic silencing was first of all described in plants in 1997 (Palauqui, J. C. et al. 1997; Voinnet, O. et al. 1997). In 1998, Fire et al. and Tabara et al. independently of each other identified siRNA-mediated suppression as an own intracellular mechanism via injection of dsRNA into *C. elegans* (Fire, A. et al. 1998; Tabara, H. et al. 1998). They found that dsRNA was more efficient in gene silencing than antisense RNA alone. Andrew Z. Fire and Craig C. Mello shared the Nobel Prize in Physiology or Medicine in 2006 for their work on RNA interference in *C. elegans* from 1998.

RNAi can be mediated by different RNA sources like RNA viruses, transposons, exogenously introduced dsRNAs called short interfering RNAs (siRNAs) and endogenous, small non-coding RNAs known as microRNAs (miRNAs) (for an overview see (Rana, T. M. 2007)). In general, two pathways trigger RNAi via introduction of dsRNA: siRNA and miRNA. In the case of siRNA, the outcome is predominantly target degradation, whereas translational suppression and enhancement of mRNA degradation are usually triggered by miRNAs. The specific actions of siRNAs or miRNAs are mediated via a multi-component complex called RNA-induced silencing complex (RISC) into which the small RNAs are incorporated.

Crucial components of the human RISC complex are for example Dicer, Argonaute proteins, TRBP (HIV-1 transactivation responsive element (TAR) double-stranded RNA-binding protein), dsRNA-binding protein PACT as well as FMRP (Fragile X mental retardation protein) and related proteins (for an overview see (Filipowicz, W.



2005)). The homologues of the RISC components are highly conserved between species (for an overview see (Meister, G. et al. 2004)).

An interesting finding is that miRISC components localise to P-bodies. P-bodies are storage and degradation sites of translational repressed RNAs in the cytoplasm. One such miRISC component is the general translation repressor protein RCK (also called p54 and DDX6). So the miRNA in the miRISC might provide the sequence specificity, whereas RCK could serve as an effector molecule that shuttles mRNA targets and therefore whole RNPs to P-bodies where they are either stored or degraded (for an overview see (Chu, C. Y. et al. 2006; Rana, T. M. 2007)).

## **2.1. Summary of RNAi mechanisms**

To sum it up, RNAi is triggered by dsRNA that is cropped by Dicer (for an overview see (Matzke, M. A. et al. 2004)). The small RNAs are then incorporated into different silencing effector complexes (RISCs). These complexes recognise and bind the target mRNA or also DNA to mediate mRNA degradation, translational repression or genome modification in order to silence genes. RNA-mediated gene silencing pathways are essential for development, chromosome structure and virus resistance in fungi, plants and animals.

For a global overview of RNAi, it shall also be mentioned that a third pathway of RNAi exists, regulating the heterochromatin silencing by small RNAs (Lippman, Z. et al. 2004). But despite the importance and the permanent use of RNAi, the underlying mechanisms are not yet fully understood.

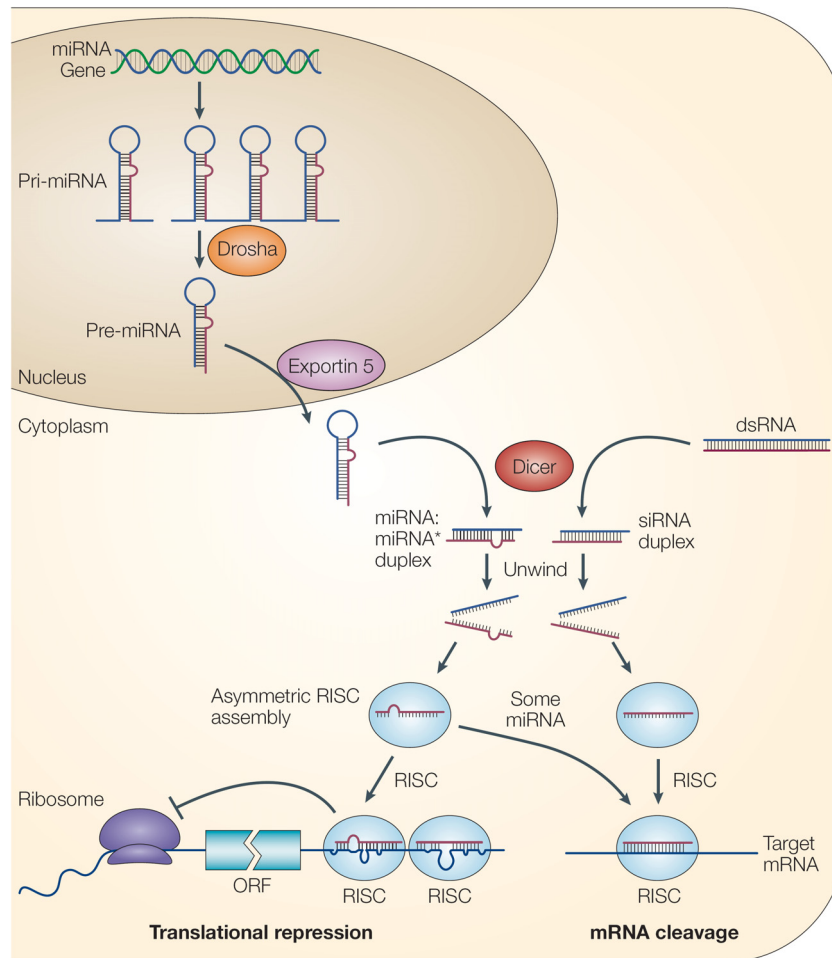


**Figure 1-7: Biogenesis and post-transcriptional suppression of miRNAs and siRNAs.** (Figure 2 from (He, L. et al. 2004)).

Pri-miRNAs are processed by the enzyme Drosha into ~ 70 nt pre-miRNAs inside the nucleus. These precursors are exported into the cytoplasm via Exportin 5 using GTP-hydrolysis. There, the enzyme Dicer produces miRNA:miRNA\* duplexes as well as it crops long dsRNAs into siRNA duplexes. Only one strand of the miRNA or siRNA duplex is then assembled into the RNA-induced silencing complex (RISC). The loaded RISC mediates translational repression when there are mismatches between the target and the small RNA. Upon perfect complementarity, mRNA cleavage is induced via the RISC. ORF, open reading frame.

## 2.2. Differences and similarities between miRNA and siRNA

An internal bulge is formed when miRISC binds to its target and this bulge makes miRISC unable to cleave its target. Interestingly, when the miRNA and the target mRNA sequence are perfectly complementary, miRISC can also cleave the mRNA target as siRISC usually does (e.g. (Hutvagner, G. et al. 2002)). Similarly, siRNAs can also act as miRNAs (e.g. (Saxena, S. et al. 2003)).

So as siRNAs and miRNAs seem to be functionally and chemically similar or maybe even identical, it is still unsolved, whether they consist of the same components and have the same enzymatic properties (reviewed in (Rana, T. M. 2007)). The so-called seed region from nucleotide number two till number eight on the siRNA or miRNA is crucial for the RNAi effect. Base pairing between the seed region and the target mediates the action of the siRNA or miRNA (for an overview see (Wu, L. et al. 2008)).

### **2.3. Short hairpin RNA plasmids**

Usually, silencing via siRNA is only transient. To overcome this limitation, siRNAs can be generated from cloned short hairpin RNAs (shRNAs) expressed from exogenously provided vectors (for an overview see (Kumar, L. D. et al. 2007)). The expressed shRNA is recognised and processed into the corresponding siRNA by the RNAi machinery (for an overview see (Kumar, L. D. et al. 2007)).

Different strategies with varied advantages can be used to finally obtain the desired siRNA. Sense and antisense siRNA sequence are hybridised and cloned into an expression vector with an RNA Polymerase III (Pol III) promoter (e.g. the pSUPERIOR.neo+gfp vector from OligoEngine used in this thesis, see also (Brummelkamp, T. R. et al. 2002)). For the design of the shRNA sequence which is inserted into this kind of vector, it is crucial to avoid strong secondary structures that would otherwise prematurely terminate the transcription by RNA Polymerase III (reviewed in (Kumar, L. D. et al. 2007)). This problem can be overcome by the use of vectors with dual Pol III promoters where the premature siRNA duplex is directly created from the selected 19 bp DNA sequence (for an overview see (Kumar, L. D. et al. 2007)). Inducible promoters can also be used and allow tight control of the expression of the shRNA and therefore of the knockdown of the investigated protein. Thus, short-hairpin-activated gene silencing (SHAGging) is a good alternative to normal siRNAs to study gene function in mammalian cells (Paddison, P. J. et al. 2002).

### **3. IDEAS, AIMS AND WORKING HYPOTHESIS**

#### **3.1. The idea behind the NMD assay**

An NMD assay for HeLa cells was designed and developed by Miles Wilkinson and coworkers (Carter, M. S. et al. 1995; Li, S. et al. 1997; Muhlemann, O. et al. 2001). They transiently transfected HeLa cells with an NMD reporter construct (TCR- $\beta$  or  $\beta$ -globin) for the expression of either a wild type (wt) or a premature termination codon (PTC)-containing mRNA (Carter, M. S. et al. 1995; Li, S. et al. 1997). The role of possible NMD factors for decay was then investigated via the expression and degradation of the reporter constructs.

With an NMD assay, new putative candidates can be investigated for their role in NMD. HeLa cells are a fast and convenient experimental model system. Therefore, HeLa cells are optimal to establish and set up an NMD assay which can later be used in more demanding primary cells or cell lines.

The RNA-binding protein Btz and eIF4AIII are core components of the EJC and play a major role in NMD (Palacios, I. M. et al. 2004). In Btz-depleted HeLa cells, the NMD process is no longer functional and mRNAs with PTCs accumulate, giving rise to truncated proteins (Palacios, I. M. et al. 2004). The same effect was also shown for UPF1 (Sun, X. et al. 1998) and eIF4AIII (Ferraiuolo, M. A. et al. 2004). Thus Btz and eIF4AIII were chosen as positive controls for the establishment of the NMD assay in this diploma thesis.

The candidates for the NMD assay were selected by Dr. Daniela Karra based on her work in our laboratory (Daniela Karra, PhD thesis 2008). In her PhD thesis, she isolated endogenous Btz-ribonucleoprotein particles (RNPs) from rat brain and identified the protein components via mass spectrometry in cooperation with Dr. Keiryn Bennett and Dr. Giulio Superti-Furga (CeMM, Vienna). In addition, she adopted a procedure that made it possible to distinguish between RNA-mediated and possible protein-protein interactors. In a first round of experiments, five putative protein-protein interactors were

chosen as candidates for the NMD assay: Nucleophosmin 1 (NPM1), DEAD(Asp-Glu-Ala-Asp)-box polypeptide 5 (DDX5), U5-116 kDa, RNA-binding motif protein - X-linked (RBMX) and RNA-binding motif protein 4 (RBM4). The proteins are described below with important synonyms in parentheses.

**NPM1 (Nucleophosmin 1; Nucleolar phosphoprotein B23; Nucleolar protein NO38; Numatrin)**

NPM1 was first identified as a multifunctional, predominantly nucleolar protein and chaperone (Feuerstein, N. et al. 1987; Schmidt-Zachmann, M. S. et al. 1987). Its cellular activities include cell proliferation, cytoplasmic/nuclear shuttle transportation, binding of single-stranded nucleic acids, ribonucleic cleavage and molecular chaperoning (reviewed in (Ye, K. 2005)). NPM1 is also involved in the assembly and transport of ribosomes (Nozawa, Y. et al. 1996). The protein is upregulated in cancer cells compared to normal cells (Nozawa, Y. et al. 1996). NPM1 is supposed to be crucial for the regulation of cancer growth via the p53/p14ARF/mdm2 stress response pathway (for an overview see (Ye, K. 2005; Gjerset, R. A. 2006)) and can therefore contribute to tumorigenesis (reviewed in (Yung, B. Y. 2007)). Therefore, the protein serves as a tumor marker acting through binding and suppressing various tumour suppressors.

Interestingly, NPM1 is reported to have both oncogenic and tumour suppressive functions (Grisendi, S. et al. 2005).

Overexpression of NPM1 was shown to counteract apoptosis (reviewed in (Ye, K. 2005)). The importance of NPM1 for proliferation, apoptosis and differentiation was also recently confirmed in neural stem cells (Qing, Y. et al. 2008). In addition, previous data in yeast indicates a possible function of NPM1 in NMD (Palaniswamy, V. et al. 2006).

**DDX5 (DEAD-box polypeptide 5; p68 - probable ATP-dependent RNA helicase DDX5)**

DDX5 is a multifunctional ATP-dependent RNA helicase which belongs to the DEAD-box (Asp-Glu-Ala-Asp) (DDX) family. The members of this protein family are highly conserved (reviewed in (Luking, A. et al. 1998; Fuller-Pace, F. V. 2006; Linder, P. 2006)) and have important roles in RNA metabolism (for an overview see (Fuller-Pace,

F. V. 2006)). Thus, DDX3 or DDX17 are highly related to DDX5 (Luking, A. et al. 1998; Ogilvie, V. C. et al. 2003; Abdelhaleem, M. 2005; Barbosa-Morais, N. L. et al. 2006; Fuller-Pace, F. V. 2006). The latter two RNA helicases even share 90% amino acid identity across the conserved core (Ogilvie, V. C. et al. 2003) and exist as a heterodimer in the cell (Lamm, G. M. et al. 1996).

DDX5 protein shows ATP-dependent RNA helicase and RNA-dependent ATPase activities *in vitro* (Ogilvie, V. C. et al. 2003). It functions in translational repression as well as activation via interaction with different cofactors (e.g. CBP/p300 or RNA Pol II for activation; histone deacetylase 1 (HDAC1) for repression) (reviewed in (Fuller-Pace, F. V. 2006)). In addition, DDX5 also mediates pre-mRNA and pre-rRNA processing, alternative splicing, mRNA decay and RNA interference (for an overview see (Fuller-Pace, F. V. 2006)). DDX5 expression is regulated during growth and development and correlates with organ differentiation (Stevenson, R. J. et al. 1998).

A previous publication also indicates that DDX5 plays a role in the regulation of incorrect transcripts and therefore NMD in yeast (Bond, A. T. et al. 2001).

### **U5-116 kDa (U5 snRNP-specific protein - 116 kD; EFTUD2 - elongation factor Tu GTP-binding domain containing 2)**

The best-characterised components of the spliceosome are the four small nuclear ribonucleoprotein particles (snRNPs) U1, U2, U4/U6, and U5 (Behrens, S. E. et al. 1991). These four snRNPs differ in their composition and therefore consist of distinct snRNAs and proteins (Behrens, S. E. et al. 1991). U5-116 kDa is a small nuclear RNP (Fabrizio, P. et al. 1997). Little is known about this protein. The U snRNPs are splicing factors and helicases (Fabrizio, P. et al. 1997). The spliceosome forms via orchestrated assembly of both snRNPs and other splicing factors on the pre-mRNA (Fabrizio, P. et al. 1997). U5-116 kDa is supposed to play a role in rearrangement steps during spliceosome assembly or the splicing process (Achsel, T. et al. 1998). The protein is a component of the 20S U5 snRNP (Behrens, S. E. et al. 1991). U5-116 kDa shows a high degree of homology with the ribosomal elongation factor EF-2, a ribosomal translocase and GTPase (Fabrizio, P. et al. 1997). Like EF-2, U5-116 kDa binds and hydrolyses GTP and might therefore play a crucial role either in splicing or the recycling of spliceosomal snRNPs (Fabrizio, P. et al. 1997). There is only one publication showing a predominantly nuclear localisation of U5-116 kDa where it colocalises with nuclear

speckles in HeLa cells (Fabrizio, P. et al. 1997).

Altogether, the role of U5-116 kDa in the splicing process makes it a promising candidate for NMD.

### **RBMX (RNA-binding motif protein - X-linked; hnRNP G - heterogeneous nuclear ribonucleoprotein G)**

RBMX is a heterogeneous, nuclear ribonucleoprotein of the RNA-binding motif (RBM) or RBMY family (Delbridge, M. L. et al. 1999; Elliott, D. J. 2004). It is localised on the X chromosome (Delbridge, M. L. et al. 1999). Very little is known about this protein so far. RBMX has an RNP-consensus RNA-binding domain (RBD) at the amino terminus and is rich in serines, arginines and glycines at the carboxyl terminus (Soulard, M. et al. 1993). Knockdown experiments were performed in zebrafish where the depletion of RBMX led to underdevelopment of the head and eyes as well as to a reduced body size compared to wt zebrafish (Tsend-Ayush, E. et al. 2005). Due to the study in zebrafish and a recently published study in *Xenopus laevis* (Dichmann, D. S. et al. 2008), RBMX plays an essential role in the development of the brain.

RBMX and RBMY are homologues which evolved from a common ancestor (Delbridge, M. L. et al. 1999). RBMY is located on the Y chromosome and displays a male-specific function in testis for spermatogenesis (Delbridge, M. L. et al. 1999).

There are publications indicating a role of the RBMY family proteins and therefore RBMX in pre-mRNA splicing (e.g. (Venables, J. P. et al. 2000)). In addition, RBMX is also considered to be a transcriptional regulator (Takemoto, T. et al. 2007). This role of RBMX in RNA processing and regulation might provide a link of the protein to NMD.

### **RBM4 (RNA-binding motif protein 4; LARK).**

RBM4 is an RNA-binding protein of the RNA recognition motif (RRM) class and a splicing factor (Markus, M. A. and Morris, B. J. 2006). RBM4 localizes in nuclear speckles and nucleoli and can be redistributed to perinucleolar clusters (Markus, M. A. and Morris, B. J. 2006). These findings indicate a potential role of RBM4 in RNA processing and/or splicing. Actually, RBM4 is also involved in alternative splicing (e.g. (Markus, M. A., Heinrich, B. et al. 2006; Lin, J. C. et al. 2007)). In addition, the protein acts as a suppressor of cap-dependent as well as an enhancer of IRES-mediated

translation in response to stress signals (Lin, J. C. et al. 2007). These RBM4 activities are regulated via phosphorylation (Lin, J. C. et al. 2007). Moreover, RBM4 is required for miRNA-guided gene regulation and therefore incorporated into a complex with Argonaute proteins (Hock, J. et al. 2007).

These facts are good indicators for a possible role of RBM4 in the NMD process.

### **3.2. The experimental approach**

The shRNA plasmids for the five candidates targeting both human (for use in HeLa cells) and rat (for use in primary hippocampal neurons) were designed and generated. First, these shRNA sequences were tested for their efficiency of downregulation of the corresponding protein in HeLa cells via Western Blot and immunofluorescence. Working shRNA plasmids were cotransfected together with a TCR- $\beta$  NMD reporter construct (either with or without a PTC). Total RNA was isolated and reverse transcribed into cDNA. Semiquantitative PCR was then performed to monitor differences in the expression level of the TCR- $\beta$  NMD reporters.

Subsequently, I also investigated the effects of the selected candidates on NMD using two cell lines stably expressing  $\beta$ -globin reporter constructs (again with or without PTC) and real-time PCR. Again the expression levels of the  $\beta$ -globin constructs were used to monitor the impact on and the integrity of NMD in cells depleted for an NMD candidate.

### **3.3. Aim & working hypothesis**

The aim of this diploma thesis was to investigate the role of the five selected putative Btz interactors - NPM1, DDX5, U5-116 kDa, RBMX and RBM4 - in NMD. Therefore, an NMD assay was established in the laboratory. Once the assay is set up, it is quick and easy to investigate the function of new, putative NMD components in different cell types and lines.



In theory, if an essential NMD component is missing, NMD is impaired and aberrant transcripts accumulate, because they are no longer degraded by NMD. This was already shown for Btz and eIF4AIII (Ferraiuolo, M. A. et al. 2004; Palacios, I. M. et al. 2004). As Btz and eIF4AIII are established NMD markers, they were chosen as positive controls for the establishment of the NMD assay in this diploma thesis. Since the five chosen NMD candidates (NPM1, DDX5, U5-116 kDa, RBMX and RBM4) are putative protein-protein interactors of Btz, the idea of this study was to test whether their depletion has a similar effect on NMD like Btz and therefore cause accumulation of PTC-containing reporter constructs. This effect would then indicate a role of the candidate in NMD. Thus, shRNAs were generated to downregulate those protein candidates first in HeLa cells and later on in rat hippocampal neurons in order to investigate their role in NMD.

# MATERIAL & METHODS

## 1. MATERIAL

### 1.1. Reagents & consumables

#### Reagents:

Acetic acid	Roth
Acrylamide mix, 30%	Roth
Agar	Sigma
Agarose	Roth
Ammonium peroxodisulfate (APS)	Roth
Ampicillin	Roth
$\beta$ -Mercaptoethanol	Sigma
Bio-Rad Protein Assay	Bio-Rad
Bovine serum albumin (BSA)	Calbiochem
Bromphenol blue	Serva
Complete, Mini, EDTA-free - protease inhibitor cocktail tablets	Roche
dATP, 100 mM	Fermentas
dCTP, 100 mM	Fermentas
Detector Block, 5x	KPL
dGTP, 100 mM	Fermentas
4',6-Diamidino-2-phenylindole dihydrochlorid (DAPI)	Roth
1,4-Diazabicyclo[2.2.2]octane (DABCO)	Sigma
Diethylpyrocarbonate (DEPC)	Sigma
Dithiothreitol (DTT)	Sigma
DMEM	Invitrogen
dTTP, 100 mM	Fermentas
Ethanol, absolute	Merck
Ethidium bromide solution (1% in H <sub>2</sub> O)	Fluka
Ethylendiamine tetraacetate (EDTA), Na-salt	Sigma
Fetal Calf Serum (FCS)	PAA
FuGENE <sup>®</sup> HD Transfection Reagent	Roche
Gelatin from cold water fish skin, ~ 45% in H <sub>2</sub> O	Sigma
GeneRuler <sup>™</sup> 1 kb DNA Ladder (0.5 $\mu$ g/ $\mu$ l)	Fermentas
GeneRuler <sup>™</sup> 100 bp DNA Ladder (0.5 $\mu$ g/ $\mu$ l)	Fermentas
Geneticin <sup>®</sup> G-418 Sulphate	Gibco
Glycerol	Sigma
Glycine	Biomol
Guanidine hydrochloride	Sigma
Hydrochloric acid	Roth
4-(2-Hydroxyethyl)piperazine-1-ethanesulfonic acid (HEPES)	Sigma
iQ <sup>™</sup> SYBR <sup>®</sup> Green Supermix	Bio-Rad

Isopropanol (2-Propanol)	Roth
Loading Dye Solution, 6x	Fermentas
Magnesium chloride (MgCl <sub>2</sub> ), 25 mM	Fermentas
MLV Reverse Transcriptase 5X Reaction Buffer	Promega
MOWIOL <sup>®</sup> 4-88 Reagent	Calbiochem
N,N,N',N'-Tetramethylethyldiamin (TEMED)	Roth
PageRuler <sup>™</sup> Prestained Protein Ladder	Fermentas
Paraformaldehyde (PFA)	Merck
10x PBS Dulbecco, w/o Ca <sup>2+</sup> Mg <sup>2+</sup>	Biochrom AG
Polyethylenimine (PEI), 50%	Sigma
Ponceau S	Merck
PROTRAN <sup>®</sup> -Nitrocellulose transfer membrane, 0.2 µm pore size	Schleicher & Schuell
Sodium chloride	Merck
Sodium dodecylsulfate (SDS)	Serva
Sodium hydroxide	Merck
Trichloric acid (TCA)	Merck
Tris(hydroxymethyl)-aminomethan (Tris)	Roth
Triton X-100	Roth
Tryptone	Roth
Tween 20	Roth
Whatman chromatography paper	Multimed
Yeast extract	Roth

RNA grade reagents:

Chloroform	Fluka
Ethanol, absolute	Merck
Glycogen, (20 mg/ml)	Fermentas
MLV Reverse Transcriptase 5x Reaction Buffer	Promega
2-Propananol (isopropanol), for molecular biology, min 99%	Sigma
RNaseZAP <sup>®</sup>	Sigma
Trizol <sup>®</sup> Reagent	Invitrogen
Random Primers, (0.5 µg/µl)	Promega
RiboLock <sup>™</sup> Ribonuclease Inhibitor (40 u/µl)	Fermentas

**Consumables:**

*DNA, RNA and protein handling*

Microtubes - PLASTIBRAND <sup>®</sup>
Biopur <sup>®</sup> Safe-Lock micro test tubes (DNase and RNase-free) - Eppendorf
15 ml and 50 ml PP Tubes, sterile - Greiner
Rotilabo <sup>®</sup> - Expendable Cuvettes, PS - Roth
8-strip 0.2 ml PCR tubes, colorless, thin walled - Eppendorf
Syringe Filter, 0.45 µm - Schleicher & Schuell
Rotilabo <sup>®</sup> -Petri dishes, Ø 90 mm, sterile, PS - Roth

*Cell culture*

Dishes Nunclon™Δ 60 x 15 - Nunc™  
Multidishes 12, non-treated - Nunc™  
Rotilabo®-Syringe filter sterile; 0.22 μm; PVDF - Roth

*Immunofluorescence*

Ø 10 mm glass coverslips, 0.13 – 0.16 mm - Marienfeld  
Microscope Slides, cut edges, ca. 76 x 26 mm - Roth

*Real-time PCR*

Thin-Wall PCR Plates, 96-well, 0.2ml - Bio-Rad  
Microseal® 'B' Film, optically clear - Bio-Rad  
Flat Cap Stripes, optical - Bio-Rad

*Kits:**Agarose gel purification*

QIAquick Gel Extraction Kit - Qiagen

*Cloning*

LigaFast™ Rapid DNA Ligation System - Promega

*DNA isolation (Maxiprep)*

EndoFree Plasmid Purification Kit - Qiagen  
PureYield™ Plasmid Maxiprep System - Promega

*RNA isolation*

RNeasy Midi Kit - Qiagen  
mirVana™ miRNA Isolation Kit - Ambion

*DNase digestion*

Deoxyribonuclease I - Sigma

*Reverse transcription PCR (RT-PCR)*

Moloney Murine Leukemia Virus Reverse Transcriptase, RNase H Minus, Point  
Mutant (M-MLV RT (H-)) - Promega  
First Strand cDNA Synthesis Kit - Fermentas  
iScript™ cDNA Synthesis Kit - Bio-Rad

*Real-time PCR*

iQ™ SYBR® Green Supermix (100mM KCl; 40 mM Tris-HCl; pH 8.4; 0.4 mM of each dNTP; dATP, dCTP, dGTP, dTTP; iTaq DNA polymerase; 50 u/ml; 6mM MgCl<sub>2</sub>; SYBR Green I; 20 nM fluorescein; and stabilisers) - Bio-Rad

**1.2. Enzymes**

*BglIII* (10 u/μl) - Fermentas

*HindIII* (10 u/μl) - Fermentas

*T4 DNA Ligase* (3 u/μl) - Promega

*Deoxyribonuclease I* - Sigma

*Moloney Murine Leukemia Virus Reverse Transcriptase, RNase H Minus, Point Mutant (M-MLV RT (H-))* (200 u/μl) - Promega

*Taq DNA Polymerase* (recombinant; 5 u/μl) - Fermentas

**1.3. Antibodies****Western Blot:**

All antibody dilutions for Western Blots were made in 1x Detector Block (KPL).

*Primary antibodies:*

Antigen	Size [kDa]	Species	Dilution	Company
U5-116 kDa	116	rabbit	1:1,000	Dr. Lührmann
Btz	115	rabbit (#8)	1:500	D. Karra, PhD thesis 2008
DDX5	68	rabbit	1:1,000	Aviva Systems Biology
α-Tubulin	55	mouse	1:5,000	Sigma
eIF4AIII	48	rabbit	1:1,000	Abcam
RBMX	43	goat	1:500	Santa Cruz Biotechnologies
RBM4	43	goat	1:500	Abcam
NPM1	38 (double band)	mouse, monoclonal	1:500	Abnova
EGFP	26	rabbit	≥ 1:1,000	P. Altrichter

Secondary antiodies:

Fluorophores:

IRDye 800 – green

IRDye 700 – red

Specificity	IRDye	Dilution	Company
donkey $\alpha$ rabbit	800	1:10,000	LI-COR Biosciences
donkey $\alpha$ rabbit	700	1:10,000	Rockland
goat $\alpha$ mouse	800	1:10,000	Rockland
donkey $\alpha$ mouse	700	1:10,000	LI-COR Biosciences
donkey $\alpha$ goat	700	1:10,000	Molecular Probes

Immunocytochemistry:

All antibody dilutions for immunofluorescence were made in 10% Blocking Solution.

Primary antibodies:

Antigen	Size [kDa]	Species	Dilution	Company
U5-116 kDa	116	rabbit	1:500	Dr. Lührmann
Btz	115	rabbit (#8)	1:500	D. Karra, PhD thesis 2008
DDX5	68	rabbit	1:500	Aviva Systems Biology
RBMX	43	goat	1:100	Santa Cruz Biotechnologies
NPM1	38	mouse, monoclonal	1:500	Abnova

Secondary antibodies:

Specificity	Fluorophore	Dilution	Company
goat $\alpha$ mouse	CY3 (red)	1:1,000	Dianova
goat $\alpha$ rabbit	CY3 (red)	1:1,000	Dianova
donkey $\alpha$ goat	CY3 (red)	1:2,000	Dianova

## 1.4. Plasmids & primers

### Plasmid:



**pSUPER RNAi System™**

VECTOR: pSUPERIOR.neo+GFP  
 CATALOG#: VEC-IND-0007/0008

Length: 5430 bp

#### Key Sites

BglII: 3182  
 HindIII: 3188  
 EcoRI: 2960  
 Sall: 3203  
 XhoI: 3209

#### Vector Features

f1(+) origin: 135-441  
 PGK promoter: 2840-2442  
 Neo ORF: 1684-715  
 EGFP ORF: 2424-1691  
 H1 promoter: 2965-3167  
 Ampicillin resistance ORF: 5302-4445

T3 primer (ATTAACCCTCACTAAAG): 3259-3243

M13 reverse primer (AACAGCTATGACCATG): 3292-3277

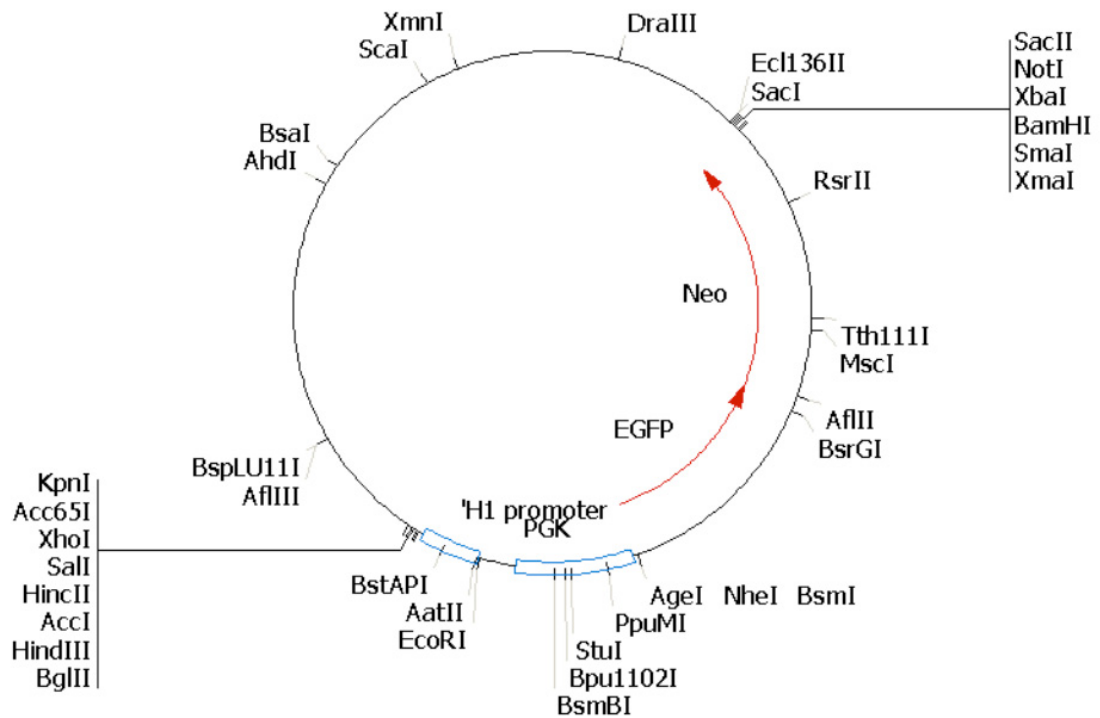


**Figure 2-1:** Picture of the pSUPERIOR.neo+gfp vector map taken from <http://www.oligoengine.com>.

**Primers (5'-3'):***Sequences of shRNA primers and plasmids that were designed in this study:*

Target & notation	Plasmid number	Species	19 nt specific sequence	Designed by	Working in HeLa cells
<b>Controls</b>					
Btz					
siBtz_1650	#283	human & rat	GGACCAATCTATACCCATG	D. Karra, PhD thesis 2008	+
eIF4AIII					
sieIF4A_3'-UTR	#291	human	GCAGCAGATCAGTGGGATG	D. Karra, PhD thesis 2008	+
<b>NMD assay candidates</b>					
DDX5					
siDDX5_580	#298	human & rat	TGTCGCTTGAAGTCTACTT	D. Karra	-
siDDX5_275-293	#329	human, rat & mouse	GGGTTTGGTGCACCTCGAT	I. Kieweg	-
siDDX5_1827-1845	#330	human, rat & mouse	ATGGTGTTTACAGTGCTGC	I. Kieweg	-
siDDX5_ORF838	#339	human & rat	CAACACCTGGAAGACTGAT	I. Kieweg	+
siDDX5_ORFDani	#340	human & rat	CTCCTATTCTGATTGCTAC	D. Karra	-
RBMX (hnRNP G)					
siRBMX-5'-UTR	#308	human	CCTCGTCCCGGCAGTAT	I. Kieweg	not detectable on WB
siRBMX-448	#309	human	AAGGTGGAACAAGCCACCA	I. Kieweg	not detectable on WB



U5-116 kDa (EFTUD2)						
siU5-116 kDa (EFTUD2)-CDS1	#310	human & rat	GGACCAGAGCTTGATTCTG	I. Kieweg	-	
siU5-116 kDa (EFTUD2)-CDS2	#311	human & rat	TGGAGCTGAAGCTGCCTCC	I. Kieweg	-	
siU5-116 kDa_147-165	#331	human & rat	GATCTTGATGAGATGGATG	I. Kieweg	-	
siU5-116 kDa_1298-1316	#332	human & rat	GCTCAGGCTGGTCTGCAAA	I. Kieweg	-	
siU5-116 kDa_3'-UTR_3044	#341	human	CAGAGAGTGTCTGGAAGCT	I. Kieweg	-	
siU5-116 kDa_3'-UTR_3283	#342	human	GGTTTGCAAGTGAACAGAA	I. Kieweg	+	
NPM1						
si NPM1-CDS1	#312	human & rat	TCGATGGACATGGACATGA	I. Kieweg	+	
si NPM1-CDS1	#317	human & rat	GGAAAGATGCAGAGTCAGAA	I. Kieweg	+	
RBM4 (LARK)						
siRBM4 Exon1	#320	human & rat	GTGGAGGCCATCAGGGGCC	I. Kieweg	-	
siRBM4 Exon2	#321	human & rat	GTCCCAAGCTGCCACAAGTC	I. Kieweg	-	
siRBM4_#1	#343	human	TTACGGCTTTGTGCACATA	(Hock, J. et al. 2007)	-	
siRBM4_#2	#344	human	GGAGCTTCGAGCCAAGTTT	(Hock, J. et al. 2007)	-	

- + working shRNA plasmids
- not working shRNA plasmids

All of these primers were cloned into the pSUPERIOR.neo+gfp mammalian expression vector, using the pSUPERIOR RNAi System™ from OligoEngine (Brummelkamp, T. R. et al. 2002; Brummelkamp, T. R. et al. 2002) (see 2.1.1 *Design* and 2.1.2 *Cloning*).

Plasmid #100 is an empty pSUPERIOR.neo+gfp vector without shRNA insert that was used as a control together with plasmid #283.

*Colony PCR primers*

Notation	Orientation	Sequence
pSUPER2101f	forward	ACACAGGAAACAGCTATGAC
pSUPER-2390rv	reverse	GCGCCCTGGCAGGAAGATGG

*Primers for semiquantitative PCR of TCR- $\beta$  pre- and mRNA:*

Notation	Orientation	Sequence	Reference
TCR- $\beta$ -mRNA for	forward	GACTGACTGTTCTCGAGG	C. Giorgi, personal communication
TCR- $\beta$ -pre-mRNA	forward	GTACCTGATCCAGACAGTTA	
TCR- $\beta$ -REV	reverse	GTCAAGGTGTCAACGAGGAA	

*Primers for semiquantitative PCR used as internal standards for normalisation of TCR- $\beta$  PCR products:*

Notation	Orientation	Sequence
GAPDHfor	forward	GAGCTGAACGGGAAGCTCAC
GAPDHrev	reverse	GGAGAGTGCTCAGTGTGGG
$\beta$ tubulin for	forward	AGACCGCATCATGAACACCT
$\beta$ tubulin rev	reverse	TCTTGGAGTCGAACATCTGC

*Primes for real-time PCR:*

Target & notation	Orientation	Sequence	Resulting fragment size	Reference
$\beta$ -Globin				
<b><math>\beta</math>-globin-Morris-for</b>	forward	TTGGGGATCTGTCCACTCC	277 bp	(Morris, C. et al. 2007)
<b><math>\beta</math>-globin-Morris-rev</b>	reverse	CACACCAGCCACCACTTTC		(Morris, C. et al. 2007)
GAPDH				
<b>Gap-F-2</b>	forward	ATTCTTCCACCTTTGATGC	104 bp	Y. Xie
<b>Gap-R-2</b>	reverse	GTCCACCACCCTGTTGCTGTA		
Tubulin				
<b>Tub-F-2</b>	forward	TGTCTTCCATCACTGCTTCC	150 bp	Y. Xie
<b>Tub-R-2</b>	reverse	TGTTTCATGGTAGGCTTTCTCAG		

Primers were in any case order from Sigma with exception of the Random Primers (0.5  $\mu$ g/ $\mu$ l; Promega) for the RT-PCR.

## 1.5. Markers & ladders

### Agarose gels:

- GeneRuler™ 1 kb DNA Ladder (0.5 µg/µl) – Fermentas

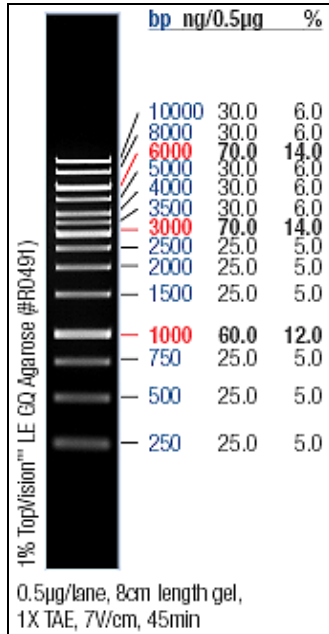


Figure 2-2: Picture taken from <http://www.fermentas.com>.

- GeneRuler™ 100 bp DNA Ladder (0.5 µg/µl) – Fermentas

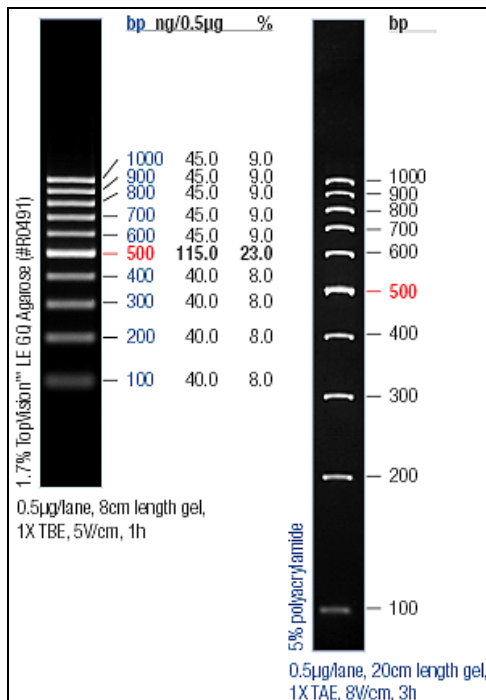


Figure 2-3: Picture taken from [www.fermentas.com](http://www.fermentas.com).

**SDS-PA gels:**

- PageRuler™ Prestained Protein Ladder - Fermentas

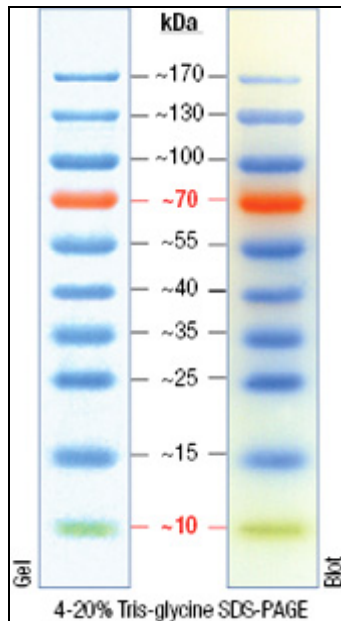


Figure 2-4: Picture taken from <http://www.fermentas.com>.

**1.6. Cells**

- *Top 10 E. coli* - Invitrogen
- *Conventional HeLa cells* – DSMZ Heidelberg
- *Stable HeLa cell lines for real-time PCR experiments* (from Dr. Oliver Mühlemann (Institute of Cell Biology, University of Bern, Switzerland))

$\beta$ -Globin cell lines:

Notation	Construct	Reference
HeLa wt $\beta$ -Globin	PTC-	(Thermann, R. et al. 1998)
HeLa NS39 $\beta$ -Globin	PTC+	(Thermann, R. et al. 1998)

TCR- $\beta$  cell lines:

Notation	Construct	Reference
HeLa 290F	PTC-	(Muhlemann, O. et al. 2001)
HeLa 593C	PTC+	(Muhlemann, O. et al. 2001)

## 1.7. Buffers & solutions

### Cloning & transfection:

<i>Ampicillin stock</i>	100 mg ampicillin in 1 ml sterile water → The stock is sterile-filtrated with a syringe through a 0.45 µm filter unit, aliquoted and stored at -20°C for further use.
<i>Annealing Buffer</i>	100 mM NaCl 50 mM HEPES pH 7.4
<i>LB (for 1 l)</i>	10 g Tryptone 5 g Yeast extract 10 g NaCl → fill up with ddH <sub>2</sub> O and autoclave
<i>LB plates</i>	400 ml LB medium 6 g agar → heat in microwave until agar is completely solved → cool down to ~ 50°C → add 400 ml of ampicillin stock and pour plates
<i>Polyethylenimine (PEI)</i>	PEI is dissolved in pre-heated ddH <sub>2</sub> O at 80°C to a final concentration of 1 mg/ml → cool to RT → carefully adjust to pH 7.0 with HCl → filter sterilise (0.45 µm pore size) → aliquots stored at -80°C + 150 mM NaCl (autoclaved + filter-sterilised (0.45 µm pore size))
<i>TE Buffer (Qiagen)</i>	10 mM Tris (to pH 8.0 with HCl) 1 mM EDTA

### Cell culture:

<i>HeLa medium</i>	DMEM + 10% (v/v) FCS
--------------------	----------------------

HeLa lysate & Western Blot:

<i>Blocking solution (Western Blot)</i>	1x Detector™ Block, KPL
<i>10x Blotting Buffer (Towbin)</i>	250 mM Tris 1.92 M Glycine
<i>1x Blotting Buffer</i>	→ dilute from 10x Blotting Buffer
<i>4x Laemmli Buffer (SDS-PAGE)</i>	200 mM Tris HCl pH 6.8 200 mM DTT 8% SDS 0.04% bromphenol blue 40% glycerol
<i>2x Laemmli Buffer (SDS-PAGE)</i>	400 µl ddH <sub>2</sub> O 100 µl 1 M Tris HCl pH 8.5 500 µl 4x Laemmli Buffer
<i>Lysis Buffer for HeLa cells</i>	50 mM Tris pH 7.5 150 mM NaCl 1 mM EDTA 1% (v/v) Triton X-100
<i>1x PBS Dulbecco, w/o Ca<sup>2+</sup> Mg<sup>2+</sup>, from Biochrom AG</i>	→ dilute from 10x PBS Dulbecco, w/o Ca <sup>2+</sup> Mg <sup>2+</sup> , from Biochrom with ddH <sub>2</sub> O 140 mM NaCl 2.7 mM KCl 16 mM disodium hydrogen phosphate 1.8 mM potassium dihydrogen phosphate → adjust pH to 7.1 with HCl
<i>Ponceau-S solution</i>	0.2% (w/v) Ponceau S 3% TCA (w/v) in ddH <sub>2</sub> O
<i>10% SDS (for 1l)</i>	100g SDS → fill up with ddH <sub>2</sub> O
<i>10x SDS Running Buffer</i>	0.25 M Tris 1.92 M Glycine 1% SDS
<i>1x SDS Running Buffer</i>	→ dilute from 10x SDS Running Buffer with ddH <sub>2</sub> O
<i>10x TBS</i>	150 mM Tris pH to 7.5 1.5 M NaCl
<i>1x TBS</i>	→ dilute from 10x Blotting Buffer

*TBS-T* 1x TBS with 0.1% (v/v) Tween 20

*RNA & protein isolation:*

*DEPC water* ddH<sub>2</sub>O including 0.1% of DEPC is constantly stirred for 6 h and subsequently autoclaved

*75% ethanol (v/v) (for 50 ml)* 37.5 ml ethanol absolute  
12.5 ml DEPC H<sub>2</sub>O

*6 M guanidine hydrochloride* 28.7 g guanidine hydrochloride  
→ fill up with DEPC H<sub>2</sub>O to 50 ml

*0.3 M guanidine hydrochloride (for 50 ml)* 2.5 ml 6 M guanidine hydrochloride  
47.5 ml ethanol absolute

*PCR:*

*dNTPs (10 mM each)* 10 µl of each dNTP (dATP, dCTP, dGTP, dTTP, 100 mM, Fermentas)  
60 µl ddH<sub>2</sub>O or DEPC H<sub>2</sub>O (for RT-PCR)

*Agarose gel:*

*Ethidium bromide working solution* – 0.2 mg/ml → final concentration in gel – 0.02 µg/ml

1 ml Ethidium bromide solution (1% in H<sub>2</sub>O)  
50 ml ddH<sub>2</sub>O

*50x TAE (2 l)* 484 g Tris  
114.2 ml Acetic acid  
200 ml EDTA (0.5 M, pH 8.0)  
→ adjust pH to 7.5 to 7.8 with HCl

*1x TAE* → dilute from 50x TAE with ddH<sub>2</sub>O

Immunocytochemistry:

<i>Blocking Solution</i>	2% (v/v) FCS 2% (v/v) BSA 0.2% (v/v) Gelatin from cold water fish skin, ~ 45% in H <sub>2</sub> O 10x PBS (10ml for 100 ml) → make aliquots and store them at -20°C
<i>10% Blocking Solution</i>	→ dilute from Blocking Solution with 1x PBS
<i>DAPI</i>	500µl DAPI (2mg/ml) in 500 ml 1x PBS → mix and protect from light with tin foil
<i>Mowiol</i>	2.4 g MOWIOL <sup>®</sup> 4-88 Reagent 6 g glycerol → stir to mix for 5 – 10 min + 6 ml ddH <sub>2</sub> O → leave at RT o/n + 12 ml 0.2 M Tris pH 8.5 – 8.8 → heat to 50°C with occasional stirring + 2.5% DABCO (w/v) in ddH <sub>2</sub> O (12 mg/ 500 µl Mowiol) when at 37°C and dissolve → centrifuge 15 min at 5,000 g → make aliquots and store them at -20°C
<i>16% PFA</i>	16 g PFA 70 ml ddH <sub>2</sub> O → heat to 60°C while stirring → add 1 -2 pellets NaOH +10 ml 10x PBS → adjust at RT to pH 7.4 with HCl → fill up with ddH <sub>2</sub> O to 100 ml → make aliquots and store them at -20°C
<i>4% PFA</i>	→ dilute from 16% PFA with 1x PBS
<i>1% Triton X-100</i>	→ dilute in 1x PBS



**Gels:**2% agarose gel:

For 1 gel

- 2 g agarose
- 100 ml 1x TAE
- heat in microwave
- stir until cooled down to hand-hot
- clean and prepare gel chamber
- + 10 µl ethidium bromide working solution – 0.2 mg/ml → final concentration in gel - 0.02 µg/ml
- pour gel
- gel is run in 1x TAE at 100 V

1.5 mm 10% PA gel:

→ gel is run in 1x SDS Running Buffer at 130 V for 1 h and 20 min

<i>10% Separation gel (8 ml/gel)</i>	
for 10 ml [ml]	
H <sub>2</sub> O	4.0
30% Acrylamide	3.3
1.5 M Tris pH 8.8	2.5
10% SDS	0.1
	mix well
10% APS	0.1
TEMED	0.004

<i>5% Stacking gel (3 ml/gel)</i>	
for 3 ml [ml]	
H <sub>2</sub> O	2.1
30% Acrylamide	0.5
1.0 M Tris pH 6.8	0.38
10% SDS	0.03
	mix well
10% APS	0.03
TEMED	0.003

## 1.8. Equipment

### Thermomixer

Eppendorf Thermomixer comfort - Eppendorf

### Vortexer

Vibrofix VF1 - Janke & Kunkel IKA

### pH Meter

MP225 - Mettler Toledo

### Shaker

GFL 3015 - GFL<sup>®</sup>

### Waterbath

GFL<sup>®</sup>

### Incubator

Unitron - INFORS HT<sup>®</sup>

### Balances

KERN ABS - KERN<sup>®</sup>

KERN 440-49N - KERN<sup>®</sup>

### Spectrophotometer

GeneQuant Pro spectrophotometer - Amersham Pharmacia  
Cuvette Suprasil, 10 mm - Hellma

### Power supplies

Power Pac 300 power supply for electrophoresis - Bio-Rad

Power Pac HC power supply for electrophoresis - Bio-Rad

### Western Blot

Mini-Protean<sup>®</sup> 3 Cell SDS-PAGE-System - Bio-Rad

Trans-Blot Cell blotting chamber - Bio-Rad

### Scanner for WB membranes

Odyssey<sup>®</sup> Infrared Imaging System - LI-COR<sup>®</sup> Biosciences;  
software: Odyssey<sup>®</sup> Application Software 2.1

### Agarose gels

Horizontal DNA Electrophoresis Gel Boxes - Bio-Rad

### UV/IR imaging system

Peqlab imaging system with UV/IR interference filter type F590 - Peqlab

**Microcentrifuges**

Eppendorf Centrifuge 5417 C - Eppendorf  
Eppendorf Centrifuge 5417 R - Eppendorf

**Centrifuge Avanti J-25<sup>TM</sup>, Beckman Coulter**

Rotor JLA10.500 - Beckman  
Rotor JA-25.50 - Beckman

**Microscopes**

Leica MZ 16F - Leica; software: Leica Application Suite Version 2.6.0 R1  
[Build 1192] - Leica  
Axioplan - Zeiss; software: analySIS<sup>B</sup> - Olympus

**-80°C freezer**

Herafreeze - Heraeus Instruments

**PCR cycler**

PTC-200 Peltier DNA Engine Thermal Cycler - MJ Research

**Real-time PCR machine**

MyiQ<sup>TM</sup> Single Color Real-Time PCR Detection System - Bio-Rad;  
software: iQ5 Optical System Software (Version 2.0) - Bio-Rad

## 2. METHODS

### 2.1. Design, creation and testing of shRNA plasmids

#### 2.1.1. Design

The sequences for new shRNAs were either designed using the “Target Design Option: Stealth™ RNAi“ of the “BLOCK-iT™ RNAi Designer” from Invitrogen (<http://rnaidesigner.invitrogen.com/rnaiexpress/>) or by alignment of the sequences found in the NCBI (<http://www.ncbi.nlm.nih.gov/>) and Ensembl (<http://www.ensembl.org/index.html>) data bases with the computer program Lasergene from DNASTAR (Version 7.1.0 (44)).

Criteria for the design of shRNA sequences (Johanna Barbara Munding, PhD thesis 2006):

- Avoid the third quarter of the whole target gene
- shRNA sequences targeting the 3'-UTR (3' - untranslated region) are as efficient for knockdown as sequences from the coding region (CDR) of the target gene (Hsieh, A. C. et al. 2004)
- Choose optimal guanine/ cytosine content of 30 – 52%
- Adenine/ uracil base pairs at the 5'-UTR have a low internal stability for the binding and directed incorporation into the RNA-induced Silencing Complex (RISC)
- A high melting temperature ( $T_m$ ) facilitates the folding of the hairpin structure
- Avoid internal repeats and palindromes which would interfere with the hairpin structure
- Analysis of shRNA sequences with high silencing efficiencies lead to the following structural similarities: Adenine at position 3 and 19, Uracil at position 10, no Guanine at position 13 and neither Guanine nor Cytosine at position 19 (Reynolds, A. et al. 2004)

For a table of all used and tested shRNA sequences see *1.4 Plasmids & primers* in the *Material section*.

##### 2.1.1.1. Manual design of shRNAs using Lasergene

Sequences found in the NCBI (<http://www.ncbi.nlm.nih.gov/>) and Ensembl (<http://www.ensembl.org/index.html>) databases of the desired genes were aligned with the computer program Lasergene (DNASTAR, Version 7.1.0 (44)). After alignment, 19 nucleotides were selected manually and blasted for their specificity using the NCBI database. The blast hits on the query sequence were identified using the NCBI, the iHOP (Information Hyperlinked over Proteins) (<http://www.ihop-net.org>) and the ExpASY (<http://www.expasy.org>) database, checking for the different nomenclatures of the identified genes and proteins.

When the specificity of the sequence was confirmed, the fragment was inserted into the following primer structures:

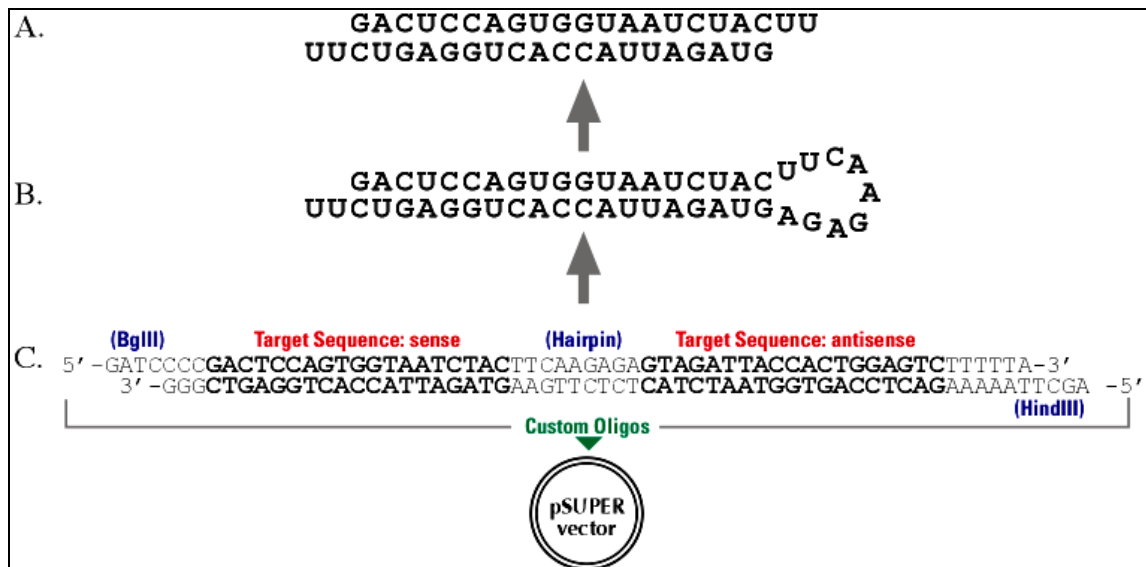


**Figure 2-5:** Transcription of a 60 nt oligo to a hairpin RNA which is processed to a functional siRNA (picture taken from <http://www.oligoengine.com>).

These two 60 nt primers per each new shRNA plasmid were then ordered from Sigma-Aldrich.

### 2.1.1.2. “BLOCK-iT™ RNAi Designer” from Invitrogen

In addition to the manually designed target sequences, shRNAs were designed using the “Target Design Option: Stealth™ RNAi” of the “BLOCK-iT™ RNAi Designer” from Invitrogen (<http://rnaidesigner.invitrogen.com/rnaiexpress/>). The nucleotide sequences or the gene accession number was filled into the form of the search engine and possible shRNA sequences were detected by a highly effective, proprietary algorithm.

19 nt were picked from the received sequences and blasted with the NCBI database for their specificity.

### 2.1.2. Cloning

Chosen sequences were cloned into the pSUPERIOR RNAi System™ from OligoEngine (Brummelkamp, T. R. et al. 2002; Brummelkamp, T. R. et al. 2002). The two 60 nt primer constructs contain a *BglIII* and a *HindIII* restriction site that allowed cloning them into the pSUPERIOR.neo+gfp expression vector according to the manufacturer’s protocol.

This mammalian expression vector has a *Polymerase-III* H1-RNA gene promoter. The recombinant vector gives rise to a 19 base pair stem-loop structure which is cleaved into a functional siRNA inside the cell. The produced short RNAs have no polyadenosine tail, but a prominent transcription and termination signal of 5 consecutive thymidines. So cleavage at the termination site occurs after the second uridine, leading to a 3’ overhang of 2 U or T as in synthetic siRNAs (Brummelkamp, T. R. et al. 2002).

It was shown that even a single mismatch in the 19 nt targeting sequence restores the expression of the targeted gene (Brummelkamp, T. R. et al. 2002).

The EGFP of the expression vector allows an easy monitoring of transfection and the transfection efficiency. The ampicillin and the neomycin resistance genes of the plasmid can be used for selection of transfected cells.

### 2.1.2.1. Primer annealing

3 µg of each primer pair (forward and reverse; diluted in sterile, nuclease-free H<sub>2</sub>O) were incubated in 48 µl Annealing Buffer (100 mM NaCl, 50 mM HEPES pH 7.4) at 90°C for 4 min in the PCR cycler. The annealing mix was then cooled down in 10°C steps for 4 min each (except for a 10 min step at 70°C) until 40°C were reached. Then two further steps, one with 37°C for 10 min and one with 10°C for 4 min were added, until the mix was cooled down to 4°C. Either the annealed primers were immediately used in a ligation reaction or put at -20°C for longer storage.

### 2.1.2.2. Ligation

2 µl of the mix of annealed primers (see 2.1.2.1 *Primer annealing*) were then inserted into the pSUPERIOR.neo+gfp vector linearised with *HindIII* and *BglII* (the same restriction sites as for the primers). The digested vector was purified from a 1% agarose gel using the QIAquick Gel Extraction Kit (Qiagen). Ligation was done using the LigaFast™ Rapid DNA Ligation System (Promega).

#### 1x ligation reaction mix:

Annealed primers	2 µl
pSUPERIOR.neo+gfp (linearised with <i>HindIII</i> and <i>BglII</i> ; 0.2 – 0.5 µg/µl)	1 µl
2x Rapid Ligation Buffer (Promega)	5 µl
ddH <sub>2</sub> O	1 µl
<i>T4 DNA Ligase</i> (3 u/µl; Promega)	1 µl
<hr/>	
Σ	10 µl

Ligation reaction was either performed for 2 h at RT or at 4°C o/n.

### 2.1.2.3. Digestion with *BglII* restriction enzyme

If the primers were cloned into the vector correctly, the *BglII* restriction sites are destroyed. In order to get rid of false-positive bacterial clones, *BglII* digestion was performed, because the enzyme can just cut self-ligated pSUPERIOR.neo+gfp plasmids without the inserted primers.

1 µl *BglII* enzyme (Fermentas) was added to the ligation reaction and incubated for 30 min at 37°C.

#### 2.1.2.4. Transformation into Top10 *E. coli*

A 100  $\mu$ l aliquot of Top10 *E. coli* competent cells (Invitrogen) was thawed on ice. 2  $\mu$ l of the ligation were then added to the bacteria and gently mixed with the pipette tip. This mixture was kept on ice for 30 min. A heat shock in a water bath at 42°C for 1 min was performed to infiltrate the cells with the DNA. Cells were again cooled on ice for 2 min, before 700  $\mu$ l LB medium were added to the bacteria. The bacterial suspension was now incubated for 1h at 37°C on the shaker at 400 rpm to allow the bacteria to recover and to develop the antibiotic resistance. To increase the concentration and density of the bacterial suspension, cells were spun down at 4,000 g (Eppendorf Centrifuge 5417 C or Eppendorf Centrifuge 5417 R - Eppendorf). 600  $\mu$ l of the supernatant were removed and the bacterial pellet was resuspended in the remaining 200  $\mu$ l of medium. This cell suspension was then sterilely plated onto LB-Amp (ampicillin; 100  $\mu$ g/ml) agar plates. The dishes were incubated at 37°C o/n to facilitate bacterial growth.

### 2.1.3. Selection and colony PCR

#### 2.1.3.1. Selection

Only bacteria containing the desired plasmids for the shRNA have antibiotic resistances (ampicillin and neomycin) and can therefore be selected using LB-Amp agar plates.

#### 2.1.3.2. Colony PCR

Colony PCR is a special and quick form of PCR to screen bacterial colonies for the desired genetic background. Positive bacterial clones are those containing the desired plasmid construct. The reaction volume is 25  $\mu$ l. Single bacterial colonies were taken from the original plate with a tip, partially transferred to another, marked LB-Amp plate and afterwards the tip was dumped into a PCR tube containing 25  $\mu$ l of the PCR mix (see below). The bacterial colonies were released into the PCR tube by gently blowing remaining liquid out of the tips with a pipette. During the initial denaturation step of the PCR, bacteria break open and their DNA content is released. The PCR was performed according to the listed cycle scheme below.

The primers used for colony PCR are binding outside the insert in the vector's sequence:

Notation	Orientation	Sequence
pSUPER2101f	forward	ACACAGGAAACAGCTATGAC
pSUPER-2390rv	reverse	GCGCCCTGGCAGGAAGATGG

These primers give a 317 bp fragment for vectors with the insert and a 261 bp fragment for vectors without insert.

1x reaction volume:

10x Taq buffer (Fermentas)	2.5 μl
MgCl <sub>2</sub> (25mM; Fermentas)	1.5 μl
dNTPs (10 mM for dATP, dCTP, dGTP, dTTP; Fermentas)	0.5 μl
pSUPER2101f (10 μM; Sigma)	0.7 μl
pSUPER-2390rv (10 μM; Sigma)	0.7 μl
<i>Taq DNA Polymerase</i> (5 u/μl; Fermentas)	0.2 μl
ddH <sub>2</sub> O	18.85 μl
<b>+ bacterial colony</b>	
Σ	25 μl

For screening of several colonies a mastermix was prepared.

PCR cycle scheme:

- 94°C 30 sec	1 cycle
- 94°C 30 sec	} 30 cycles
- 58°C 30 sec	
- 72°C 1 min 20 sec	
- 4°C for ever	

Vectors containing the desired inserts were larger and therefore running above the empty vectors on the gel. 5 μl 6x Loading Dye (Fermentas) were added to each PCR tube and 18 μl were loaded onto a 2% agarose gel. To identify positive clones 12 μl of the GeneRuler<sup>TM</sup> 100 bp DNA Ladder (Fermentas) were loaded in parallel. 100 V were applied for 30 min. Afterwards pictures of the gel were taken using an UV/IR imaging system (Peqlab imaging system with UV/IR interference filter type F590 – Peqlab).

### 2.1.4. Large-scale DNA isolation (Maxiprep)

Positive bacterial clones, containing the shRNA sequence insert, were inoculated o/n in 200 ml LB medium with ampicillin (100 μg/ml) for plasmid DNA amplification. As a backup for further use a glycerol stock with 1 ml bacterial culture and 0.5 ml glycerol was prepared before each maxiprep for every new positive clone. Two different Maxiprep kits were used for plasmid DNA isolation during this diploma thesis.

#### 2.1.4.1. EndoFree Plasmid Purification Kit - Qiagen

This kit was mainly used in the course of this diploma thesis, because it yields very pure DNA of high concentration which guarantees high transfection efficiency (Weber, M. et al. 1995; Zeitelhofer, M. et al. 2008).

Cells were harvested at 6,000 g and 4°C for 15 min (Avanti J-25<sup>TM</sup> Centrifuge - Beckman Coulter, rotor JLA10.500). Meanwhile, two 50 ml Falcon tubes were prepared per sample and Buffer P1 and P3 were cooled on ice. The bacterial pellet was



resuspended in 10 ml P1 (with RNase A) and transferred to one of the 50 ml tubes. 10 ml Buffer P2 were added and mixed by inverting 4-6x. This mixture was incubated at RT for 5 min. Lysis was stopped with 10 ml Buffer P3, again inverted 4-6x and then immediately poured into a QIAfilter Cartridge. An incubation for 10 min at RT should allow the bacterial debris as well as the genomic DNA and the proteins to separate from the aqueous phase. The screwtop of the cartridge was removed and the lysate was filtrated via plunger into the second 50 ml tube. 2.5 ml ER were added, mix was inverted 10x and cooled on ice for 30 min for removal of endotoxins.

A QIAGEN-tip 500 was equilibrated by flow-through of 10 ml Buffer QBT. Then the lysate was loaded onto the QIAGEN-tip 500. 50 ml centrifugation tubes were sterilised with 10 ml isopropanol and QIAGEN-tip 500 was washed twice with 30 ml Buffer QC. Now the DNA was eluted into the sterile centrifugation tubes with 15 ml Buffer QN. First the DNA in the tube was precipitated by addition of 10 ml isopropanol and mixed carefully. Second the DNA precipitate was pelleted by centrifugation at 14,000 g and 4°C for 35 min (Avanti J-25<sup>TM</sup> Centrifuge - Beckman Coulter, rotor JA-25.50). After centrifugation the supernatant was discarded and the white DNA pellet was resuspended in 500 µl 70% ethanol to remove salts and transferred into a sterile 1.5 ml tube. The suspension was then spun down at 20,000 g and 4°C for 5 min (Eppendorf Centrifuge 5417 C or R - Eppendorf). After centrifugation the supernatant was discarded again and the DNA pellet was washed with 200 µl 70% ethanol. Again the DNA was precipitated by centrifugation at 20,000 g and 4°C for 5 min (Eppendorf Centrifuge). The residual pellet was then dried on air for 5 - 10 min and dissolved in 180-200 µl TE or nuclease-free water. DNA concentration was measured by UV spectrophotometry at 260 nm and DNA purity was also monitored by using the 260 nm:280 nm ratio, where the optimum is a value of 1.8. Finally, the purified DNA was aliquoted for further use and stored at -20°C.

#### **2.1.4.2. PureYield<sup>TM</sup> Plasmid Maxiprep System – Promega**

Cells were harvested at 6,000 g and 4°C for 15 min (Avanti J-25<sup>TM</sup> Centrifuge - Beckman Coulter, rotor JLA10.500). The pellet was then resuspended in 12 ml Resuspension Solution and transferred into a sterile 50 ml centrifugation tube. 12 ml Cell Lysis Solution were added to start the lysis of the bacteria. The suspension was gently inverted 3 - 5x and incubated at RT for 3 min. Lysis was stopped by addition of 12 ml Neutralisation Solution inverting the mixture for 10 - 15x. Sufficient mixing is essential in this step to ensure precipitation of the cellular debris. The mixture was then centrifuged at 14,000 g and RT for 20 min (Avanti J-25<sup>TM</sup> Centrifuge - Beckman Coulter, rotor JA-25.50) to deposit the debris. Now a blue PureYield<sup>TM</sup> Clearing Column was placed on the top of a white, silica-membrane PureYield<sup>TM</sup> Maxi Binding Column. This column stack was fixed onto a special vacuum manifold (Vac-Man<sup>®</sup> Laboratory Vacuum Manifold - Promega). Approximately half of the lysate was poured into the blue clearing column and maximal vacuum was applied until the liquid passed both columns. Then the remainder of the lysate was also added to the columns. DNA should have bound to the binding membrane of the column by this procedure. Now the vacuum was slowly released to remove the clearing column, the binding column remained on the vacuum manifold. The binding column was then washed by addition of 5 ml Endotoxin Removal Wash to get rid of endotoxins, RNA and protein, and appliance of the vacuum. 20 ml of Column Wash were added and passed through the membrane. The membrane was dried for 10 or more min by applying the vacuum onto

the empty binding column. Ethanol was removed from the tip and the outside of the column with a paper towel. Afterwards the binding column was inserted inside the elution device on the top of a sterile 1.5 ml tube. This construct was again placed on the vacuum manifold. 600  $\mu$ l of sterile, nuclease-free water were added and DNA was eluted by applying the vacuum.

DNA concentration was measured by UV spectrophotometry at 260 nm and DNA purity was also monitored by using the 260 nm:280 nm ratio, where the optimum is a value of 1.8. Finally the maxiprep was aliquoted for further use and stored at -20°C.

### **2.1.5. Transfection of HeLa cells**

Transfections were usually performed using the FuGENE<sup>®</sup> HD Transfection Reagent from Roche. Polyethylenimine (PEI) was also tested for transfection (PEI:DNA ratio [ $\mu$ l: $\mu$ g] of 3:1) (Boussif, O. et al. 1995).

#### **2.1.5.1. Transient transfection of HeLa cells using FuGENE<sup>®</sup> HD Transfection Reagent**

For lipofection, a FuGENE<sup>®</sup> HD Transfection Reagent (Roche):DNA [ $\mu$ l: $\mu$ g] ratio of 8:3 was used. The whole procedure was performed under a sterile hood.

350,000 HeLa cells per  $\varnothing$  6 cm dish were cultured with 5 ml of DMEM with 10% FCS for 24 h. Before starting the procedure, HeLa Medium and OPTI-MEM<sup>®</sup> (GIBCO) were pre-warmed in a water bath at 37°C for at least 30 min. Then the medium was changed (5 ml per dish) and cells were put back into the incubator (37°C, 5% CO<sub>2</sub>) to adjust them to the new medium for 30 – 60 min. In the meantime, 230  $\mu$ l pre-warmed OPTI-MEM<sup>®</sup> (serum-free medium) were put into a sterile 1.5 ml tube and 7.5  $\mu$ g of purified plasmid DNA were added.

For transfection of single plasmids, 7.5  $\mu$ g plasmid DNA were used. Cotransfections were carried out with 7.5  $\mu$ g of the plasmid DNA of interest together with 100 ng of plasmids either for wt TCR- $\beta$  mRNA (plasmid #333) or TCR- $\beta$  mRNA with a premature termination codon (PTC) (plasmid #337) (Li, S. et al. 1997) which serve as targets for NMD decay.

The glass vial with the FuGENE<sup>®</sup> HD Transfection Reagent was vortexed. 20  $\mu$ l of FuGENE<sup>®</sup> HD Transfection Reagent consisting of lipids and other components in 80% ethanol were then added to the OPTI-MEM<sup>®</sup> and the DNA. It is essential in this step to avoid contact with the plastic tube wall, because chemical residues can decrease the biological activity of the transfection reagent. The mix was carefully vortexed for 15 sec to mingle. Then the mixture was incubated for 15 min at RT to allow lipid vesicles to form around the DNA. The mixture was added drop by drop to the cells in the dish and evenly distributed. Cells were then put back into the incubator and 24 h after the procedure the transfection efficiency was evaluated according to the EGFP expression under the microscope (Leica MZ 16F Microscope).

### 2.1.6. Protein lysate of HeLa cells

Protein lysates of HeLa cells were usually performed 3 days after transfection to allow downregulation by shRNAs to take place efficiently. Transfection efficiency was evaluated according to the EGFP expression under the microscope (Leica MZ 16F Microscope - Leica). Cells were also checked for morphology. The lysate was only made if the cells looked healthy. Pictures of the transfected cells were taken (Leica Application Suite Version 2.6.0 R1 [Build 1192]) to compare different samples and their transfection rates. Afterwards, pictures were assembled and arranged with Adobe Photoshop CS3 and/or Adobe InDesign CS2. Images were not modified other than adjustment of levels, brightness, contrast and magnification.

First PBS was pre-warmed, 1 protease inhibitor tablet (Roche) was added to the prepared Lysis Buffer and a microcentrifuge (Eppendorf Centrifuge 5417 C or R - Eppendorf) was pre-cooled. Second, the medium was taken off and the cells were once washed with pre-warmed PBS. All following steps were then performed on ice or cooled to limit protease activities. 250 µl of the Lysis Buffer (50 mM Tris pH 7.5, 150 mM NaCl, 1 mM EDTA, 1% Triton X-100) were added per Ø 6 cm dish. Cells were scraped from the dish and lysis was promoted by pipetting up and down 10 times. The lysate was transferred into a 1.5 ml tube. Then a centrifugation step at 20,000 g and 4°C for 5 min separated the lysate from the cellular debris. The supernatant was transferred into a new 1.5 ml tube. Protein concentration was ascertained by the Bradford Assay (Bio-Rad Protein Assay - Bio-Rad). This assay is based on the binding of the sulfonate groups of the dye Coomassie Brilliant Blue G-250 to the positively charged groups of the protein at a low pH. Due to the binding, the absorption maximum of the dye shifts from 465 nm (anionic form) to 595 nm (ionic form). After protein measurement, 100 µl 4x Laemmli Buffer were added to the lysate and the proteins were denatured at 95°C for 10 min. Afterwards the lysate was either immediately used for a Western Blot or stored at -20°C for later use.

### 2.1.7. Western Blot (WB)

A Western Blot was then made to confirm the downregulation of a protein by the corresponding, designed shRNA.

#### 2.1.7.1. SDS (Sodium dodecyl sulphate)-polyacrylamid gel (SDS-PA gel) and SDS-polyacrylamid gel electrophoresis (SDS-PAGE)

SDS binds proteins thereby yielding negatively charged complexes that now run according to their molecular size. Due to this fact, proteins can be separated under the term of their molecular weight by applying electric power. Protein samples move towards the anode through the gel pores as soon as the electric current is applied. Thereby small proteins are much faster than larger ones. These facts lead to a separation with the large proteins closer to the slots of the gel and the small proteins closer to the lower edge of the gel.

Based on Laemmli, 1.5 mm thick 10% PA gels for SDS-PAGE were prepared as described in the *Material section* (Laemmli, U. K. 1970).

Usually 75 µg of the HeLa lysates (see 2.1.6 *Protein lysate of HeLa cells*) and equal

volumes of proteins isolations with TRIzol<sup>®</sup> Reagent (see 2.3.1.1 *Total RNA & protein isolation with TRIzol<sup>®</sup> Reagent (Invitrogen)*) were denaturated at 95°C for 10 min before loading into the gel slots (always together with untreated, untransfected control samples). 3 µl of PageRuler<sup>™</sup> Prestained Proteins Ladder (Fermentas) were used as molecular weight marker. Constant electric voltage of 130 V was applied for 1 h and 20 min (Power Pac HC and Power Pac 300 power supply for electrophoresis - Bio-Rad) to separated the proteins.

#### **2.1.7.2. Western Blot**

Proteins separated by a SDS-PAGE were then transferred on a nitrocellulose membrane (0.2 µm pore size; Schleicher & Schuell) as Western Blot. For the transfer and Western blotting, the tank blotting system from Bio-Rad was used. First 2 sponges, the filter papers and the membrane were soaked and equilibrated in cold 1x Blotting Buffer. Second the sandwich was assembled in the following order starting from the cathode: sponge, 3 filter papers, gel, membrane, 3 filter papers and sponge. So the negatively charged proteins move towards the anode and thereby attach to the membrane. Proteins were blotted at constant amperage of 250 mA for 90 min (Power Pac HC or 300 power supplies, Bio-Rad) in the cold room at 4°C and additionally cooled with ice. To confirm the quality of the transfer and for later cutting of the membrane at the desired molecular sizes, the membrane was then stained with Ponceau S. Usually a photo (using the Peqlab imaging system with UV/IR interference filter type F590 – Peqlab) was taken to make sure that equal amount of the samples were loaded (also confirmed by an  $\alpha$ -Tubulin staining later on). The membrane was then cut according to the marker for the following probing of the proteins of interest. Blocking of the membrane was performed for at least 30 min at RT in Detector Block solution (KPL) while shaking (shaker GFL 3015 – GFL<sup>®</sup>). Thereby, unspecific binding sites were saturated to reduce the background of the detection. Incubation with the specific primary antibody was either done for 2 h at RT (shaking) or o/n at 4°C (shaking). Afterwards the membrane stripes were washed 3x 5 min with TBS-T Buffer (see 1.7 *Buffers & solutions*). The secondary antibody was now added for 45 min at RT (shielded from light). Finally, the blot was washed as previously described and scanned using the Odyssey<sup>®</sup> Infrared Imaging System (LI-COR<sup>®</sup> Biosciences; software: Odyssey<sup>®</sup> Application Software 2.1). Pictures were then assembled and arranged with Adobe Photoshop CS3 and/or Adobe InDesign CS2. Images were not modified other than adjustment of levels, brightness, contrast and magnification.

#### **2.1.8. Quantification of downregulation of proteins via Western blotting**

Western Blot Quantifications were performed using the Odyssey<sup>®</sup> Infrared Imaging System (LI-COR<sup>®</sup> Biosciences) with the Odyssey<sup>®</sup> Application Software 2.1 (see manufacturer's manual).

## 2.2. Immunocytochemistry

Once the knockdown of the desired protein was confirmed by Western Blot, immunofluorescence was performed to look at the downregulation *in situ*.

### 2.2.1. Transient transfection of HeLa cells on coverslips using FuGENE<sup>®</sup> HD Transfection Reagent

For lipofection, a FuGENE<sup>®</sup> HD Transfection Reagent (Roche):DNA [ $\mu\text{l}:\mu\text{g}$ ] ratio of 8:3 was used. The whole procedure was performed under a sterile hood. 350,000 HeLa cells per  $\varnothing$  6 cm dish containing 8 sterile  $\varnothing$  10 mm glass coverslips (CSs) were cultured with DMEM and 10% FCS for 24 h. The CSs were transferred to a 12-well plate, 1 CS per well. 1 ml of fresh medium was added per well. The transfection procedure was then carried out as in 2.1.5 *Transfection of HeLa cells* using 50  $\mu\text{l}$  pre-warmed OPTI-MEM<sup>®</sup> (serum-free medium), 1.5  $\mu\text{g}$  of plasmid DNA from a maxiprep and 4  $\mu\text{l}$  of FuGENE<sup>®</sup> HD Transfection Reagent per CS and well.

### 2.2.2. Immunofluorescence

3 days after transfection of normal HeLa cells and 5 days after transfection of the stable  $\beta$ -Globin HeLa cell lines (see 1.6 *Cells*), cells were fixed and stained.

First the medium was taken off and the CSs were washed with pre-warmed PBS (see 1.7 *Buffers & solutions*). Cells were then fixed with 4% paraformaldehyde (PFA) in PBS for 15 min at RT. CSs were washed 3x for 5 min with PBS while shaking (shaker GFL 3015 – GFL). Permeabilisation was achieved using 1% Triton X-100 in PBS for 5 min at RT. Again cells were washed as described. Blocking Solution was added for at least 30 min at RT. The following antibody solutions were always diluted in 10% Blocking Solution in PBS. Incubation with the primary antibody (see 1.3 *Antibodies*) was either done for 2 h at RT or o/n at 4°C. Cells were washed as previously. The secondary antibody (see 1.3 *Antibodies*) was applied for 45 min at RT and secured from light. CSs were washed again and incubated in DAPI solution in the dark for 3 min to visualise nuclei. Finally, the CSs were washed with PBS as previously and then once with ddH<sub>2</sub>O and mounted with 8  $\mu\text{l}$  of Mowiol onto object glass slides (Roth).

### 2.2.3. Microscopy of immunocytochemical preparations

Stained CSs were then investigated using an Axioplan microscope (Zeiss). Pictures of the stained untransfected and transfected cells were taken using analySIS<sup>B</sup> software (Olympus) and assembled with Adobe Photoshop CS3 and/or Adobe InDesign CS2. Images were not modified other than adjustment of levels, brightness, contrast and magnification.

## 2.3. Semiquantitative PCR

Conventional HeLa cells were cotransfected (see 2.1.5.1 *Transient transfection of HeLa cells using FuGENE<sup>®</sup> HD Transfection Reagent*) with the respective shRNA plasmid and a plasmid coding for TCR- $\beta$  mRNA, either wt (plasmid #333) or with a PTC (plasmid #337)(Li, S. et al. 1997), to monitor NMD.

### 2.3.1. RNA isolation

72 h after cotransfection, HeLa cells were washed once with pre-warmed PBS. Total RNA and proteins were usually isolated using the TRIzol<sup>®</sup> Reagent (Invitrogen) according to the manufacturer's protocol. Two other RNA isolation kits were also tested in order to fine-tune the quality and the amount of the isolated RNA: the RNeasy Midi Kit (Qiagen) and the mirVana<sup>™</sup> miRNA Isolation Kit (Ambion). These 2 kits were used according to the manufacturer.

#### RNA handling in general:

To avoid RNase contamination when working with RNA samples the following precautions were taken:

- The working space was cleaned with ethanol and RNaseZAP<sup>®</sup> (Sigma<sup>®</sup>)
- Gloves were worn and frequently cleaned with 75% ethanol or frequently disposed
- Water was treated with 0.1% diethylpyrocarbonate (DEPC)
- RNA grade chemicals were used to prepare solutions
- Barrier tips and pipettes reserved for RNA work only were used for pipetting
- RNase-free tubes were used for RNA experiments (Biopur<sup>®</sup> Safe-Lock micro test tubes – Eppendorf)
- Total RNA was stored at -80°C in DEPC-treated water with RiboLock<sup>™</sup> Ribonuclease Inhibitor (Fermentas)

#### 2.3.1.1. Total RNA and protein isolation with TRIzol<sup>®</sup> Reagent (Invitrogen)

The TRIzol<sup>®</sup> Reagent is a mono-phasic solution of phenol and guanidine isothiocyanate and is an improvement of the single-step RNA isolation (Chomczynski, P. et al. 1987). Handling of samples containing TRIzol<sup>®</sup> Reagent, chloroform or guanidine hydrochloride was always done under a chemical fume hood. Using the TRIzol<sup>®</sup> Reagent allows to isolate total RNA and protein simultaneously from the same sample.

72 h after transfection the viability, the morphology of the cells as well as the transfection efficiency according to their EGFP expression was analyzed using the Leica MZ 16F microscope (Leica). Pictures were taken using the Leica Application Suite Version 2.6.0 R1 [Build 1192] software (Leica) to record the state of the cells.

### *RNA isolation*

The medium was discarded and cells were 1x washed with pre-warmed PBS. 1.6 ml of TRIzol<sup>®</sup> Reagent were added. After 2 – 3 min of incubation cells were resuspended in TRIzol<sup>®</sup> Reagent by pipetting up and down. The suspension was transferred into a sterile, RNase-free 2 ml tube (Biopur<sup>®</sup> Safe-Lock micro test tubes - Eppendorf), vortexed for 15 sec and incubated at RT for 10 min. TRIzol<sup>®</sup> Reagent disrupts cells and dissolves cell components, but maintains the integrity of the RNA, DNA and the proteins. 320 µl of chloroform were added. The mixture was again vortexed for 15 sec and incubated at RT for 5 min before it was centrifuged in a microcentrifuge at 12,000 g and 4°C for 15 min to allow the pink organic phase, the interphase and the aqueous phase to separate. After centrifugation the upper, aqueous phase containing the RNA, which should be ~ 60% of the initial TRIzol<sup>®</sup> Reagent volume, was transferred into an RNase-free 1.5 ml tube (Biopur<sup>®</sup> Safe-Lock micro test tubes - Eppendorf). 1 µl of glycogen (20 µg/µl) diluted in diethylpyrocarbonate (DEPC)-treated H<sub>2</sub>O which facilitates the precipitation and 800 µl of isopropanol were added. This mix was incubated for 10 min at RT. The RNA was now precipitated by centrifugation at 12,000 g and 4°C for 10 min. Afterwards the RNA pellet at the bottom of the tube was washed with 1.5 ml 75% ethanol. RNA was again pelleted by centrifugation at 7,600 g and 4°C for 7 min. The pellet was air-dried for 5 – 10 min. It is important that the RNA pellet does not dry out completely, otherwise it can hardly be re-dissolved in DEPC water afterwards. To facilitate this step, the DEPC water (15 µl each pellet) was pre-warmed at 50°C. RNA was completely solved at 50°C, shaking at the thermomixer (Eppendorf) at 350 rpm for 5 min.

### *Protein isolation*

Proteins were isolated in parallel from the organic phase after the addition of chloroform according to the manufacturer's protocol.

The aqueous phase was removed completely. 500 µl of absolute ethanol were added to precipitate the DNA from the interphase. The mixture was 5x inverted and incubated for 2 – 3 min at RT. DNA was pelleted in a microcentrifuge (Eppendorf Centrifuge 5417 C or R - Eppendorf) at 2,000 x g and 4°C for 5 min. The phenol-ethanol supernatant (~800 µl) was then transferred into two 2 ml tubes and 1.5 ml isopropanol were added per tube. The mix was inverted 5x and incubated at RT for 10 min. Proteins were pelleted at 12,000 g and 4°C for 10 min in a microcentrifuge. The pellet was washed with 2 ml 0.3 M guanidine hydrochloride in 95% ethanol for 20 min at RT. After centrifugation at 7,600 g and 4°C for 5 min the supernatant was discarded. This washing procedure was performed 3x in total. During the last guanidine hydrochloride washing step the 2 protein pellets of the same sample were fused in one 2 ml tube. 2 ml absolute ethanol were added for the last washing step to remove salts, vortexed and incubated for 10 min at RT. Again the samples were centrifuged at 7,600 g and 4°C for 5 min. The protein pellet was air-dried until it started to get transparent. 4x Laemmli Buffer was now added according to the pellet size. The protein pellet was resuspended at the thermomixer (Eppendorf) at 95°C and 450 rpm for 10 min. Afterwards the protein suspension was either immediately used for a Western Blot (see 2.1.7 Western Blot) or stored at -20°C for later use.

### 2.3.1.2. DNase digestion

Possible DNA contaminations of the RNA isolation were reduced using *Deoxyribonuclease I* (Sigma) according to the manufacturer.

RNA concentration was measured using UV spectrophotometry at 260 nm and RNA purity was also monitored by using the 260 nm:280 nm ratio, where the optimum is a value of 2.

### 2.3.2. Reverse transcription PCR (RT-PCR)

Usually 1 – 3 µg of total RNA (see 2.3.1.1 *Total RNA & protein isolation with TRIzol<sup>®</sup> Reagent (Invitrogen)*) were transcribed using Moloney Murine Leukemia Virus Reverse Transcriptase, RNase H Minus, Point Mutant (M-MLV RT (H-); Promega) ((Roth, M. J. et al. 1985) and Sambrook J., Fritsch E. F., Maniatis T.; *Molecular Cloning: A Laboratory Manual*; Cold Spring Harbor Laboratory; Cold Spring Harbor; 1989).

The First Strand cDNA Synthesis Kit (Fermentas) and the iScript<sup>™</sup> cDNA Synthesis Kit (Bio-Rad) were also used for some samples according to the manufacturer's protocol.

#### 2.3.2.1. RT-PCR using random primers or TCR-β reverse primers

RNA solution (1 – 3 µg total RNA)	1 µl
Random Primers (0.5 µg/µl; Promega)	1 µl
DEPC H <sub>2</sub> O	15 µl
<hr/>	
Σ	17 µl

These reactions were prepared in a 0.2 ml PCR tube (Eppendorf). To melt secondary structures within the template, the mix was heated at 70°C for 5 min using the PCR cycler. Afterwards the mix was cooled down to 4°C for 5 min to prevent reformation of secondary structures.

In some experiments, specific TCR-β reverse primers were used instead of the random primers in order to enrich the PCR products with the desired TCR-β fragments. This mix was then also heated at 70°C for 5 min, but incubated afterwards at 58°C, which is the annealing temperature of the TCR-β reverse primer, for 10 min.

The following reagents were now added to each PCR tube:

MLV Reverse Transcriptase 5X Reaction Buffer (Promega)	5 µl
dNTPs (10 mM for dATP, dCTP, dGTP, dTTP; Fermentas)	1.5 µl
RiboLock <sup>™</sup> Ribonuclease Inhibitor (40 u/µl; Fermentas)	0.5 µl
<i>M-MLV RT (H-)</i> (200 u/µl; Promega)	1 µl
<hr/>	
Σ	25 µl



PCR cycle scheme:

- 25°C for 10 min
- 40°C for 1 h
- 70°C for 15 min
- 4°C for ever

The PCR scheme was modified for the specific TCR- $\beta$  reverse primer.

Modified PCR cycle scheme:

- 25°C for 10 min
- 55°C for 1 h
- 70°C for 15 min
- 4°C for ever

**2.3.3. Semiquantitative PCR**

PCR was performed to amplify TCR- $\beta$  pre- and mRNA to monitor the efficiency and continuance of the NMD process.

1x reaction volume:

10x Taq buffer (Fermentas)	5 $\mu$ l
MgCl <sub>2</sub> (25 mM; Fermentas)	3 $\mu$ l
dNTPs (10 mM for dATP, dCTP, dGTP, dTTP; Fermentas)	1 $\mu$ l
TCR- $\beta$ forward primer (10 $\mu$ M; Sigma)	1 $\mu$ l
TCR- $\beta$ reverse primer (10 $\mu$ M; Sigma)	1 $\mu$ l
ddH <sub>2</sub> O	38.5 – x $\mu$ l
cDNA	x $\mu$ l
Taq DNA Polymerase (5 u/ $\mu$ l; Fermentas)	0.5 $\mu$ l
<hr/>	
$\Sigma$	50 $\mu$ l

Primers (5'-3'):

Notation	Orientation	Sequence	Reference
TCR- $\beta$ -mRNA for	forward	GACTGACTGTTCTCGAGG	C. Giorgi, personal communication
TCR- $\beta$ -pre-mRNA	forward	GTACCTGATCCAGACAGTTA	
TCR- $\beta$ -REV	reverse	GTCAAGGTGTCAACGAGGAA	

The resulting PCR product for the TCR- $\beta$  pre-mRNA was ~200 nt and for the TCR- $\beta$  mRNA ~150 nt long. These fragments were analysed by agarose gel electrophoresis.

In some experiments, GAPDH or tubulin primers were added as an internal standard in order to normalize PCR products. The GAPDH and tubulin PCR products have a size of ~500 bp each.

Notation	Orientation	Sequence
GAPDHfor	forward	GAGCTGAACGGGAAGCTCAC
GAPDHrev	reverse	GGAGAGTGCTCAGTGTTGGG
$\beta$ tubulin for	forward	AGACCGCATCATGAACACCT
$\beta$ tubulin rev	reverse	TCTTGGAGTCGAACATCTGC

PCR cycle scheme:

- 94°C for 40 sec      1 cycle
- 94°C for 40 sec
- 58°C/60°C for 40 sec } 30 cycles
- 72°C for 1 min
- 72°C for 5 min      } 1 cycle
- 4°C for ever

Annealing temperatures for PCR:

TCR- $\beta$  pre-mRNA  $\rightarrow$  60°C

TCR- $\beta$  mRNA  $\rightarrow$  58°C

After PCR 8  $\mu$ l 6x Loading Dye (Fermentas) were added to each PCR reaction and 30  $\mu$ l of this PCR mixture were then loaded onto a 2% agarose gel. 15  $\mu$ l of the GeneRuler™ 100 bp DNA Ladder (Fermentas) were loaded in parallel in order to determine the size. 100 V were applied for 50 min. Afterwards pictures of the gels were taken using an UV/IR imaging system (Peqlab imaging system with UV/IR interference filter type F590 – Peqlab). Pictures were then assembled and arranged with Adobe Photoshop CS3 and/or Adobe InDesign CS2. Images were not modified other than adjustment of levels, brightness, contrast and magnification.

## 2.4. Real-time PCR

For the real-time PCR experiments, instead of the conventional HeLa cells 2 stable HeLa cell lines were used, which express NMD mRNA targets ( $\beta$ -Globin or TCR- $\beta$ ) with or without PTC. These stable cell lines were a generous gift from Dr. Oliver Mühlemann (Institute of Cell Biology, University of Bern, Switzerland).

### Stable HeLa cell lines:

#### $\beta$ -Globin HeLa cell lines:

Notation	Construct	Reference
HeLa wt $\beta$ -Globin	PTC-	(Thermann, R. et al. 1998)
HeLa NS39 $\beta$ -Globin	PTC+	(Thermann, R. et al. 1998)

#### TCR- $\beta$ HeLa cell lines:

Notation	Construct	Reference
HeLa 290F	PTC-	(Muhlemann, O. et al. 2001)
HeLa 593C	PTC+	(Muhlemann, O. et al. 2001)

In order to increase the efficiency of the downregulation of the NMD assay candidates, cells were also selected with neomycin (see 2.4.4 *Neomycin selection*).

### 2.4.1. Temperature gradient PCR for optimisation of annealing temperature of primers

Real-time primer (5'-3'):

Target & notation	Orientation	Sequence	Resulting fragment size	Reference
$\beta$ -Globin				
<b><math>\beta</math>-globin-Morris-for</b>	forward	TTGGGGATCTGTCCACTCC	277 bp	(Morris, C. et al. 2007)
<b><math>\beta</math>-globin-Morris-rev</b>	reverse	CACACCAGCCACCACTTTC		(Morris, C. et al. 2007)
GAPDH				
<b>Gap-F-2</b>	forward	ATTCTTCCACCTTTGATGC	104 bp	Y. Xie
<b>Gap-R-2</b>	reverse	GTCCACCACCCTGTTGCTGTA		
Tubulin				
<b>Tub-F-2</b>	forward	TGTCTTCCATCACTGCTTCC	150 bp	Y. Xie
<b>Tub-R-2</b>	reverse	TGTTTCATGGTAGGCTTTCTCAG		

1x reaction volume:

10x Taq buffer (Fermentas)	2.5 $\mu$ l
MgCl <sub>2</sub> (25 mM; Fermentas)	1.5 $\mu$ l
dNTPs (10 mM for dATP, dCTP, dGTP, dTTP; Fermentas)	0.5 $\mu$ l
$\beta$ -globin-Morris-for (400 nM; Sigma)	2 $\mu$ l
$\beta$ -globin-Morris-rev (400 nM; Sigma)	2 $\mu$ l
ddH <sub>2</sub> O	38.5 – x $\mu$ l
cDNA (0.5 $\mu$ g from wt $\beta$ -Globin cell line)	x $\mu$ l
Taq (5 u/ $\mu$ l; Fermentas)	0.5 $\mu$ l
$\Sigma$	50 $\mu$ l

PCR cycle scheme:

- 95°C for 4 min            1 cycle
  - 95°C for 30 sec
  - Increasing temperature gradient with each cycle for 45 sec
  - 72°C for 45 sec
- } 30 cycles
- 
- 72°C for 5 min
  - 4°C for ever
- } 1 cycle

After the PCR, 5 µl 6x Loading Dye (Fermentas) were added to each PCR tube and 18 µl of the PCR mixture were loaded onto a 2% agarose gel in parallel with 15 µl of the GeneRuler™ 100 bp DNA Ladder (Fermentas). 100 V were applied for 50 min. Afterwards, pictures were taken, assembled and modified as described in 2.3.3 *Semiquantitative PCR*.

### 2.4.2. Optimisation of real-time PCR conditions

The template amounts, primer concentrations, setup for the dilution series and the sealing method (Microseal® 'B' Film (optically clear) and Flat Cap Stripes (optical) – Bio-Rad) of the PCR plates were also optimised for real-time PCR.

### 2.4.3. Optimised real-time PCR cycle scheme

#### Template amount:

200 ng cDNA (see 2.3.2 *Reverse transcription PCR (RT-PCR)*) of wt or NS39 β-Globin HeLa cells were used for real-time PCR.

#### 1x reaction volume:

iQ™ SYBR® Green Supermix (Bio-Rad)	12.5 µl
β-globin-Morris-for (200 nM; Sigma)	1.5 µl
β-globin-Morris-rev (200 nM; Sigma)	1.5 µl
ddH <sub>2</sub> O	9.5 - x µl
cDNA (200 ng)	x µl
<hr/>	
Σ	25 µl

Samples and dilution series were analysed in triplicates, therefore mastermixes were prepared. Dilution series were made by a dilution factor of 4. In total, 300 nM of each β-globin primer and 400 nM of the GAPDH and tubulin primers were used on 200 ng cDNA template. The 96-well plates were sealed using Flat Cap Stripes (optical) (Bio-Rad) preventing evaporation.

PCR cycle scheme:

- 95°C for 3 min                      1 cycle
- 95°C for 15 sec                    } 55 cycles
- 55°C for 40 sec                    }

*Melting curve*

- 55°C - 95°C (+0.5°C per cycle) for 30 sec for each temperature                    } 81 cycles

After the PCR, 5 µl 6x Loading Dye (Fermentas) were added to each PCR tube and 20 µl of the PCR mixture were loaded onto a 2% agarose gel in parallel with 12 µl of the GeneRuler™ 100 bp DNA Ladder (Fermentas). 100 V were applied for 50 min. Afterwards, pictures were taken, assembled and modified as described in 2.3.3 *Semiquantitative PCR*.

#### 2.4.4. Neomycin selection

The reasons to pick neomycin (neo) for selection were the following: neo selection is a common used tool for the generation of stable cell lines and selection of the desired genotype. For example, the tested stable TCR-β cell lines were also created via neo and respectively geneticin (G418) selection (Muhlemann, O. et al. 2001). Neo and geneticin were also suggested for selection in the manual of the pSUPERIOR.neo+gfp vector from OligoEngine.

Neo is an aminoglycoside antibiotic. In pro- and eukaryotic cells, this antibiotic blocks the protein synthesis by binding ribosomal subunits and inhibiting the translocation of the peptidyl-tRNA from the A-site to the P-site. This also causes misreading of the mRNA hindering the cell to synthesise proteins vital to its survival and growth.

G418 is also an aminoglycoside antibiotic which blocks protein synthesis more efficiently than neo in eukaryotic cells. Therefore, geneticin is used instead of neo for selection in eukaryotic cells.

After transfection (see 2.1.5 *Transfection of HeLa cells*) of the β-Globin HeLa cell lines, the cells were kept in medium (DMEM + 10% FCS) containing the transfection reagent (FuGENE® HD Transfection Reagent - Roche) and the plasmid DNA for 24 hours. Then selection was induced using Geneticin® G-418 Sulphate (Gibco®) diluted in ddH<sub>2</sub>O (sterile filtrated; Rotilabo®-Syringe filter sterile; 0.22 µm; PVDF - Roth) which was applied to the medium (600 µg/ml final concentration). The medium and the neo solution were exchanged every 24 h for 7 days in total. Untransfected control dishes were treated equally with G418 in parallel to monitor the occurrence of spontaneous or persistent antibiotic resistant cells. Transfected cell samples were incubated with G418 until almost all cells in the controls were killed.

Transfection efficiency was evaluated according to the EGFP expression under the microscope (Leica MZ 16F Microscope - Leica). In addition, the cells were checked for their morphology and their physiological status. Pictures of the transfected cells and controls were taken (Leica Application Suite Version 2.6.0 R1 [Build 1192]) and assembled with Adobe Photoshop CS3 and/or Adobe InDesign CS2. Images were not modified other than adjustment of levels, brightness, contrast and magnification.

## **2.5. Nucleofection of embryonic day 17 (E17) rat hippocampal neurons**

Nucleofection is a method of transfection with high efficiency, especially for post-mitotic cells such as hippocampal neurons. In general, neurons are very sensitive to mechanical and physiological stress, so handling of the cultures should be quick and careful. The time span between the recovery of the neurons and the nucleofection should be as short as possible. In order to obtain high transfection efficiencies and to prohibit cellular stress or death, plasmid DNA preparations have to be very pure. The removal of endotoxins is also crucial for the survival of the neurons. Hence, the Endofree Plasmid Maxi Kit (Qiagen) was exclusively used for DNA preparation. Air bubbles in the culture suspension shall also be avoided during nucleofection, because they interfere with the flow of the electrical currents. To limit the stress after nucleofection, the neurons were transferred from the nucleofection cuvettes into poly-L-lysine-coated culture dishes with equilibrated medium as fast as possible. The neurons were then incubated for 3 days at 37°C and 5% CO<sub>2</sub>. This incubation step allows the expression of the transgenes and the knockdown of the corresponding proteins. In these experiments, 10 and 20 µg plasmid DNA were tested for their transfection efficiencies, which were checked under the Leica MZ 16F Microscope (Leica). Pictures were taken to monitor the differences. Nucleofection was carried out with the O-003 program in any case (included in Nucleofector II “S” software version S4-4 or above; Amaxa).

## RESULTS

### 1. CREATION AND TESTING OF shRNAs FOR NMD ASSAY CANDIDATES

The aim of this diploma thesis was to establish a nonsense-mediated decay (NMD) assay in the laboratory. The design of the assay was based on the method and assay developed by Miles Wilkinson and coworkers (Carter, M. S. et al. 1995; Li, S. et al. 1997; Muhlemann, O. et al. 2001). They transiently transfected HeLa cells with a NMD reporter construct (TCR- $\beta$  or  $\beta$ -globin) for the expression of either a wild type (wt) or a premature termination codon (PTC)-containing mRNA (Carter, M. S. et al. 1995; Li, S. et al. 1997).

With this NMD assay, I wanted to investigate the role of new putative candidates for the NMD process. In a first step, the NMD assay should be established in HeLa cells as shown by other groups (Miles Wilkinson and coworkers and (Carter, M. S. et al. 1995; Li, S. et al. 1997; Muhlemann, O. et al. 2001)). In addition this is cheaper, faster and experimentally easier to set up. In a second step, which is not part of this diploma thesis, the assay can then be adapted for hippocampal neurons, which are the main focus of the laboratory.

Usually RNAs harbouring PTCs are recognised and degraded by the NMD machinery. This mechanism is essential to prohibit the translation of truncated proteins with dominant-negative or deleterious gain-of-function activities (for a summary and overview see (Chang, Y. F. et al. 2007)). So if the NMD process is impaired, which is often the case in diseases e.g. cancer, harmful and non-functional mRNAs with PTCs accumulate in the cell leading to further derailing of the cell's metabolism. The so-called up-frameshift (UPF) proteins are the core components of the NMD machinery (Lykke-Andersen, J. et al. 2000). These UPF proteins are recruited to the PTC-containing mRNA via interactions with the exon junction complex (EJC) components (Lykke-Andersen, J. et al. 2000; Kashima, I. et al. 2006). The EJC plays a major role in the decay of incorrect transcripts and therefore in the NMD process (Palacios, I. M. et al. 2004).



The RNA-binding protein Btz is a core component of the EJC (Degot, S. et al. 2004; Palacios, I. M. et al. 2004; Tange, T. O. et al. 2005). As a component of the EJC, Btz plays a major role in NMD (Palacios, I. M. et al. 2004). In Btz-depleted HeLa cells, the NMD process is no longer functional and mRNAs with PTCs accumulate, giving rise to truncated proteins (Palacios, I. M. et al. 2004). The same effect was also shown for Upf1 (Sun, X. et al. 1998) and eIF4AIII (Ferraiuolo, M. A. et al. 2004). So if an essential component of the NMD machinery is missing, the process will be impaired.

The candidates for the NMD assay were selected based on previous work in our laboratory by Dr. Daniela Karra (Daniela Karra, PhD thesis 2008). In her PhD thesis, she isolated endogenous Btz-ribonucleoprotein particles (RNPs) from rat brain and identified the protein components via mass spectrometry in cooperation with Dr. Keiryn Bennett (CeMM, Vienna). In addition, she adopted a procedure that made it possible to distinguish between RNA-mediated and possible protein-protein interactors. In a first round of experiments, only putative protein-protein interactors were chosen as candidates for the NMD assay.

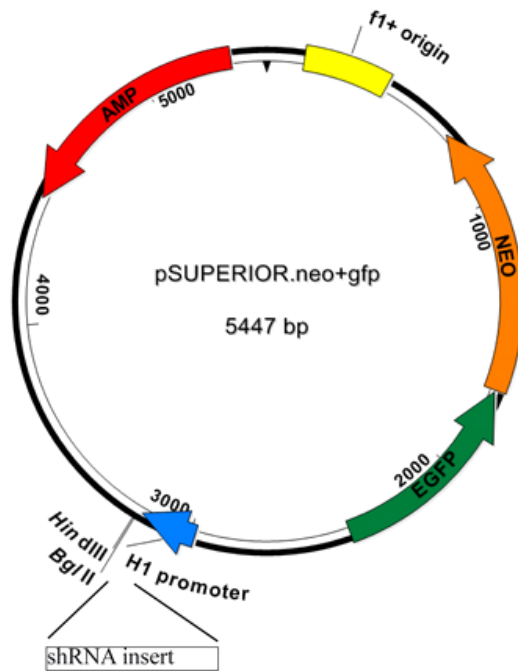
The candidates for the NMD assay were: NPM1, DDX5, U5-116 kDa, RBMX and RBM4. For NPM1 and the RNA helicase DDX5, previous data indicated a possible function in the regulation of incorrect transcripts (Bond, A. T. et al. 2001; Palaniswamy, V. et al. 2006).

In order to investigate the role of those candidates in NMD, shRNA plasmids were designed. These plasmids express shRNAs, which selectively inactivate the corresponding proteins via RNA interference (RNAi) (Brummelkamp, T. R. et al. 2002; Brummelkamp, T. R. et al. 2002). I designed and cloned the shRNA plasmids for the selected candidates as described in the *Methods section*. Whenever possible, shRNAs were designed to target human and rat sequences, so that the assay could first be established in HeLa cells and later on also be used to knock down the respective protein in primary rat hippocampal neurons. The selected shRNA sequences were cloned into the pSUPERIOR.neo+gfp vector (OligoEngine) shown in **Figure 3-1A**. False positive clones were removed by *BglIII* digestion, which only cuts the empty vector lacking any insert. Successful cloning of the desired shRNA sequence into the vector was then proven by colony PCR. The PCR products were loaded onto a 2% agarose gel. The little

shift in the size of the PCR product indicates the successful and accurate cloning (**Figure 3-1B**). The bands on the gel always had different intensities. So either the expression level of the shRNA construct varied from clone to clone and was for example especially low in clone 1 (CL1), or the differences were just due to different DNA amounts in the PCR reaction.

According to the gel picture positive clones were chosen, the plasmid DNA was amplified in bacteria, isolated, concentration measured and the DNA was stored in small aliquots at -20°C for later use.

A



B

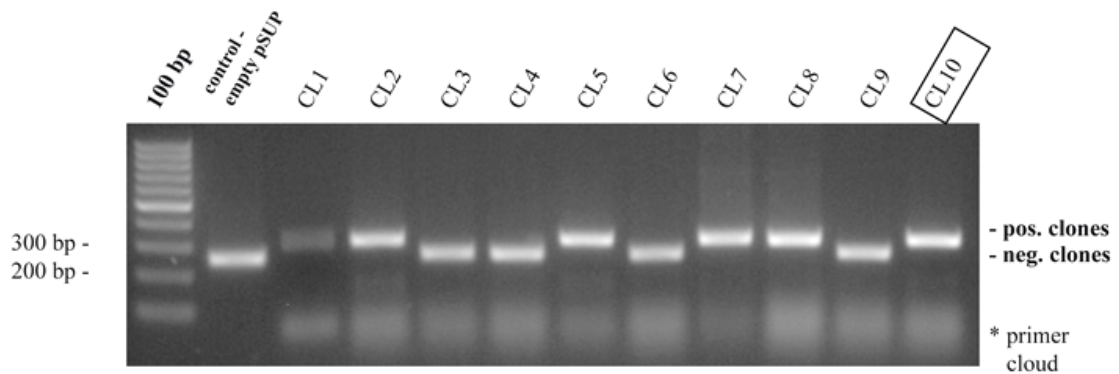


**Figure 3-1: Generation of shRNA constructs.**

**(A) pSUPERIOR.neo+gfp vector map.** The pSUPERIOR.neo+gfp (OligoEngine) vector map was created using the computer program Lasergene (DNASTAR, Version 7.1.0 (44)). Oligos were designed, hybridised and cloned into this vector to get new shRNA plasmids. **(B) Colony PCR.** The picture shows an agarose gel from colony PCR, in this case for shNPM1 plasmid (#317). Clone 10 (CL10) was chosen for further experiments. 18  $\mu$ l of each PCR reaction including 6x Loading Dye (Fermentas) were separated on a 2% agarose gel in parallel with 12  $\mu$ l of the GeneRuler™ 100 bp DNA Ladder (Fermentas). Primers were added in excess (\* indicates the primer cloud). A vector containing the shRNA insert results in a 317 bp PCR product (pos. clone). Without the insert, the PCR fragment is 261 bp long (neg. clone). The PCR product of an empty pSUPERIOR.neo+gfp vector was loaded as a control to detect the size shift of the fragments on the gel.

AMP, ampicillin; H1 promoter, *Polymerase-III* H1-RNA gene promoter for expression of shRNAs; EGFP, Enhanced Green Fluorescent Protein; NEO, neomycin; f1(+) origin, origin for bacterial replication; CL, bacterial clone.

The purity and quantity of the plasmid DNA was crucial for the transfection efficiency, as previously shown (Zeitelhofer, M. et al. 2008).

Usually, the quality of the plasmid DNA obtained with the maxiprep kit from Promega was not as convincing as the plasmid DNA from the maxiprep kit from Qiagen, although both kits include an endotoxin removal step. The purity and the concentration of the DNA were lower with the Promega kit, which resulted in lower transfection efficiencies (data not shown and (Zeitelhofer, M. et al. 2008)). So for all final and crucial experiments, exclusively the kit from Qiagen was used.

The newly created shRNA plasmids were transiently transfected into conventional HeLa cells to test their potential to downregulate their corresponding proteins. Cells were lysed after 72 h and the knockdown of the corresponding protein was analysed via Western blotting. Quantification was performed using the Odyssey<sup>®</sup> Application Software 2.1 (see *Methods section* and the respective manual). ShRNA samples were always compared to an untransfected control lysate (=100% protein expression) and normalised to Tubulin. The EGFP signals on the Western Blots were also quantified and served as an indicator for the transfection efficiency.

The subcellular localization of the candidate proteins in HeLa cells was analysed by immunostainings using commercially available antibodies against the respective protein. In order to visualize the effect of the shRNA plasmids in single cells and to overcome low transfection efficiencies immunocytochemistry experiments were performed. Therefore, HeLa cells on coverslips were transfected with the investigated shRNA plasmid and fixed 72 h after transfection. The staining procedure was performed as described in the *Material section*.

## 1.1. ShRNA plasmids targeting NPM1

NPM1 was first identified as a multifunctional, predominately nucleolar protein and chaperone (Feuerstein, N. et al. 1987; Schmidt-Zachmann, M. S. et al. 1987). Its cellular activities include cell proliferation, nucleo-cytoplasmic shuttling, nucleic acid binding, ribonucleic cleavage and molecular chaperoning (Ye, K. 2005).

**Figures 3-2A** and **3-3A** show Western Blots for testing the effects of two distinct shRNA plasmids targeting NPM1 (shNPM1, plasmid #312 and #317). NPM1 proteins give a double band on the Western Blot, representing the unphosphorylated and phosphorylated NPM1, respectively.

Using the shNPM1 plasmid #312, I observed a downregulation of NPM1 of 26.02% compared to the protein level in the untransfected control sample (UT=100%) (**Figure 3-2B**). This meant that the usual expression level of NPM1 was reduced by 73.98%. Tubulin served as a loading control for the normalisation of the quantification. So the shNPM1 plasmid #312 had a strong effect on the expression of its corresponding protein. The EGFP signal normalised to the Tubulin signal indicated the high transfection efficiency of the shRNA shNPM1 plasmid #312.

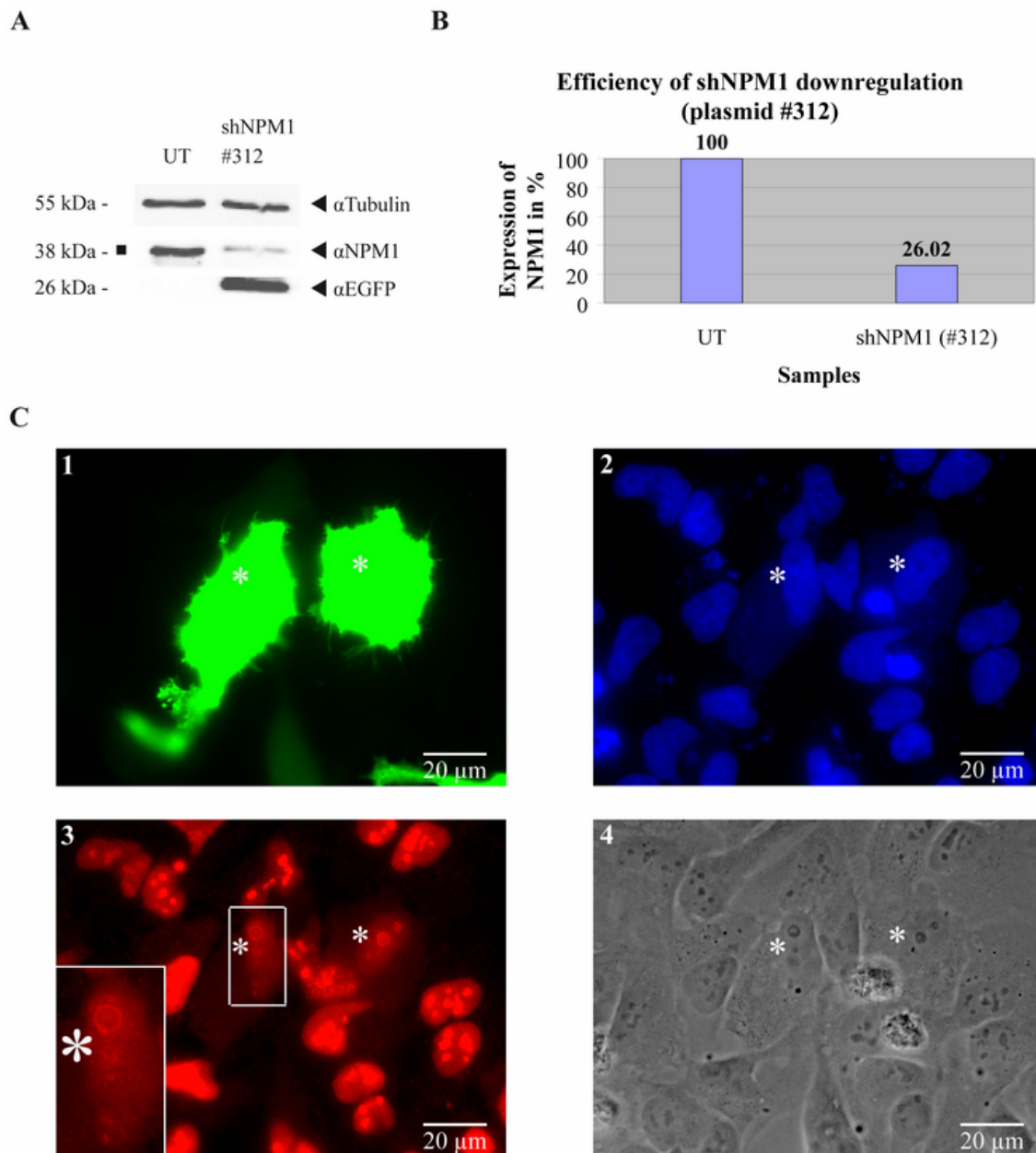


**Figure 3-2: Testing of one shNPM1 plasmid in HeLa cells.**

**(A) Test of protein downregulation on Western Blot.** Western Blot showing the downregulation of NPM1 protein upon transfection of HeLa cells with the shNPM1 plasmid (#312). NPM1 gives a double band on the Western Blot, representing the phosphorylated and unphosphorylated NPM1 (marked with ■). The corresponding molecular weights are indicated on the left side, the chosen antibodies for protein detection on the right side. **(B) Quantification of downregulation.** Quantification was done using the Odyssey® Application Software 2.1 (see manufacturer's manual). Protein level of NPM1 are compared to the level of untransfected cells (=100%) and normalised to Tubulin. **(C) Immunocytochemistry.** Immunostainings to test for NPM1 downregulation in fixed cells. Transfection and staining procedure as described in the *Methods section*. (1) HeLa cells transfected with the shNPM1 plasmid (#312) strongly expressing EGFP are marked with \*. Expression levels of EGFP differ from cell to cell. (2) DAPI staining of the DNA to visualise nuclei. (3) Antibody staining for NPM1 to visualise downregulation in transfected cells. Transfected HeLa cells are depleted for NPM1: the puncta of NPM1 in the nuclei are reduced or abolished. The inset on the left indicates a 2fold magnification of the selected cell area. (4) Phase contrast picture of the cells to check their morphology and their physiological status. UT, untransfected; #312, shNPM1 plasmid; α, anti.

The protein expression level of NPM1 upon transfection with the shNPM1 plasmid #317 was 17.94% on average (**Figure 3-3B**). According to the Western Blot data in **Figure 3-3A** the transfection efficiency of plasmid #317 was lower than those of #312. Both shNPM1 plasmids downregulated the corresponding protein, but the degree of downregulation was even a little stronger with plasmid #317.

Subsequently, downregulation of NPM1 upon transfection with plasmids # 312 and #317 was also investigated by immunostaining using specific antibodies against NPM1 (**Figure 3-2C** and **Figure 3-3C**).

The specificity of the observed NPM1 antibody staining pattern was as previously reported (Yung, B. Y. et al. 1990; Iggo, R. D. et al. 1991; Bocker, T. et al. 1995; Wu, M. H. et al. 1995; Nozawa, Y. et al. 1996; Zatsepina, O. V. et al. 1997; Cordell, J. L. et al. 1999). NPM1 is preferentially found in the nucleolus and also in the nucleoplasm (Cordell, J. L. et al. 1999). The protein shuttles continuously between the cytoplasm and the nucleolus, thereby functioning as a carrier of newly synthesised ribosomal proteins into the nucleolus (Borer, R. A. et al. 1989; Cordell, J. L. et al. 1999). Nucleolar labelling is not always observed due to the fixation procedure (Cordell, J. L. et al. 1999), but the cytoplasm is usually diffusely stained (Cordell, J. L. et al. 1999).

Based on the antibody staining, the transfected HeLa cells were clearly depleted for NPM1. Also the puncta of NPM1 in the nuclei were reduced or abolished which is especially visible in the magnified insets (**Figures 3-2C** and **3-3C**). In the cell periphery, NPM1 seemed to be completely removed. The transfected cells are identified by their EGFP expression. The nuclei were intact as confirmed by DAPI staining. Moreover, the morphology was good, which was also a clear parameter whether the cells were stressed or even dead (see **Figures 3-2C4** and **3-3C4**, phase contrast images).

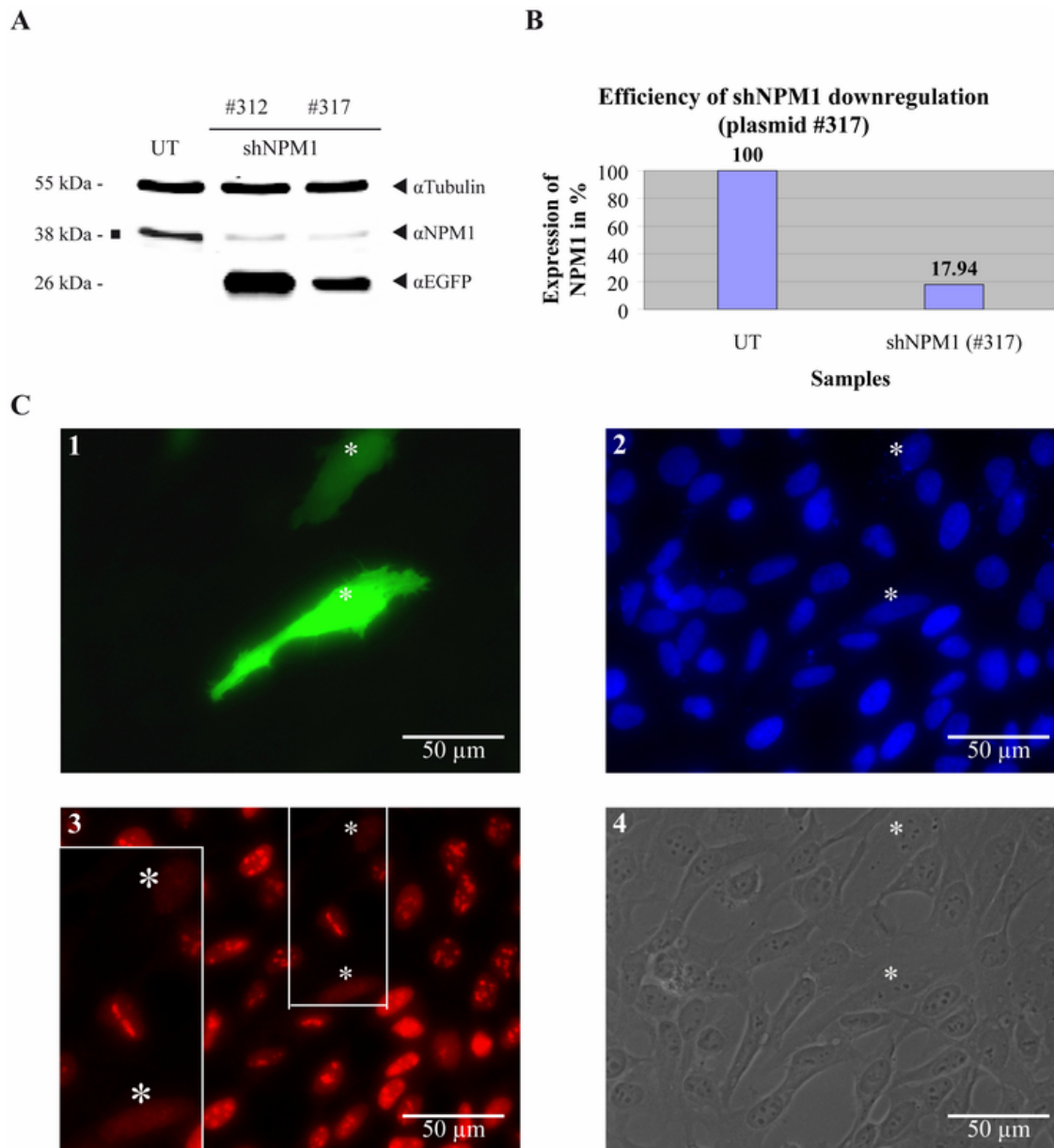


**Figure 3-3: Testing of two different shNPM1 plasmids in HeLa cells.**

**(A) Test of protein downregulation on Western Blot.** Western Blot showing the downregulation of NPM1 protein upon transfection of HeLa cells with two different shNPM1 plasmids (#317 and #312, respectively) in comparison. Double band of NPM1 as described in Figure 3-2 marked with  $\blacksquare$ . The corresponding molecular weights are indicated on the left side, the chosen antibodies for protein detection on the right side. **(B) Quantification of downregulation.** Quantification was done using the Odyssey® Application Software 2.1 (see manufacturer's manual). Protein levels of NPM1 are compared to the level of untransfected cells (=100%) and normalised to Tubulin. **(C) Immunocytochemistry.** Immunostainings to test for NPM1 downregulation in fixed cells. Transfection and staining procedure as described in the *Methods section*. For description of pictures see also Figure 3-2. (1) HeLa cells transfected with the shNPM1 plasmid (#317) expressing EGFP are marked with \*. Expression levels of EGFP differ from cell to cell as can be seen from the 2 transfected cells shown. (2) DAPI staining. (3) Antibody staining for NPM1 to visualise downregulation in the transfected cells. Transfected HeLa cells are depleted of NPM1: the puncta of NPM1 in the nuclei are reduced or abolished. The inset on the left indicates a 1.5fold magnification of the selected cell area. (4) Phase contrast picture.

UT, untransfected; #312, shNPM1 plasmid; #317, shNPM1 plasmid;  $\alpha$ , anti.



## 1.2. ShRNA plasmid targeting DDX5

DDX5 is a member of the DEAD-box (DDX) family and shows ATP-dependent RNA helicase and RNA-dependent ATPase activities *in vitro* (Ogilvie, V. C. et al. 2003). Previous data showed that DDX5 plays a role in the regulation of incorrect transcripts in yeast and therefore in the NMD process (Bond, A. T. et al. 2001).

**Figure 3-4A** shows the analysis of the newly generated shRNA plasmid targeting DDX5 (plasmid #339) via Western Blot. The quantification in **Figure 3-4B** displays the efficiency of DDX5 downregulation with plasmid #339. The protein level of DDX5 was reduced to 79.71% compared to the UT sample.

The observed DDX5 antibody staining pattern seemed to be not specific (Iggo, R. D. et al. 1991; Lamm, G. M. et al. 1996; Kahlina, K. et al. 2004) (see *Discussion section*). Published DDX5 staining patterns showed a predominantly nucleolar or nucleoplasmic localisation of the protein depending on the cell cycle stage (Iggo, R. D. et al. 1991; Lamm, G. M. et al. 1996; Ogilvie, V. C. et al. 2003; Kahlina, K. et al. 2004). In this diploma thesis, no obvious differences between the transfected and untransfected HeLa cells were observed in the immunocytochemistry experiment. Small puncta were evenly distributed across the cell areas and the downregulation of DDX5 was not visible in the transfected cells, although the same antibody has been used as for the Western Blots experiment (**Figure 3-4C**). The transfected cells shown in **Figure 3-4C1** demonstrated the variability of the EGFP expression in single HeLa cells. The nuclei and the morphology of the cells were analysed as in **Figure 3-2C**.

However, downregulation of DDX5 via the respective shRNA (plasmid #339) was confirmed on the Western Blots, but could not be visualised in the immunostaining (see *Discussion section*).

In addition, other created shDDX5 plasmids (see *1.4 Plasmids & primers* in the *Material section*) have been tested, but did not downregulate DDX5 (data not shown), before the working plasmid #339 was identified.

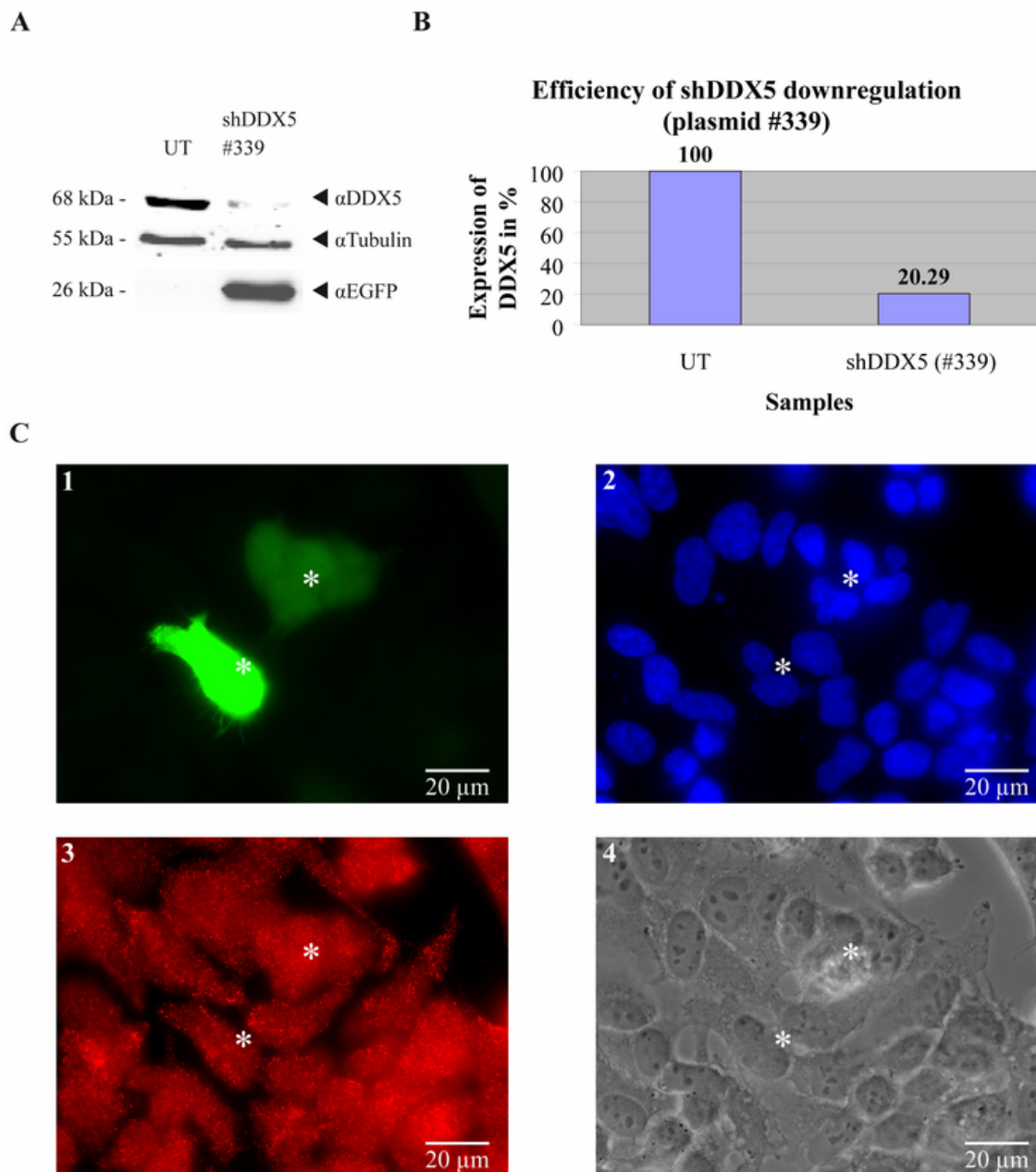


**Figure 3-4: Testing of the shDDX5 plasmid in HeLa cells.**

**(A) Test of protein downregulation on Western Blot.** Western Blot showing the downregulation of DDX5 protein upon transfection of HeLa cells with the shDDX5 plasmid (#339). The corresponding molecular weights are indicated on the left side, the chosen antibodies for protein detection on the right side. **(B) Quantification of downregulation.** Quantification was done using the Odyssey® Application Software 2.1 (see manufacturer's manual). DDX5 expression is compared to the expression level of an untransfected control (=100%) and normalised to Tubulin. **(C) Immunocytochemistry.** Immunostainings to visualise DDX5 downregulation in fixed cells. Transfection and staining procedure as described in the *Methods section*. For description of pictures see also Figure 3-2. (1) HeLa cells transfected with the shDDX5 plasmid (#339) expressing EGFP are marked with \*. Expression levels of EGFP differ from cell to cell as can be seen here. (2) DAPI staining. (3) Antibody staining for DDX5 to visualise downregulation in the transfected cells. Depletion of DDX5 in the transfected HeLa cells is not obvious in this example. (4) Phase contrast picture.

UT, untransfected; #339, shDDX5 plasmid;  $\alpha$ , anti.

### 1.3. ShRNA plasmid targeting U5-116 kDa

Very little is known about U5-116 kDa which is a small nuclear ribonucleoprotein (snRNP) (Fabrizio, P. et al. 1997). U5-116 kDa is supposed to play a role in rearrangement steps during spliceosome assembly or the splicing process (Achsel, T. et al. 1998).

**Figure 3-5A** shows a representative Western Blot exploring the efficiency of shU5-116 kDa to downregulate its corresponding protein. When quantified, a 54.33% reduction was observed compared to an untransfected sample (**Figure 3-5B**).

Immunostaining experiments were also performed to show the shRNA mediated knockdown of U5-116 kDa in HeLa cells (**Figure 3-5C**). In this thesis, the antibody staining for U5-116 kDa showed a significant downregulation in the transfected cells. Depletion of U5-116 kDa was visible especially in the periphery of the cell (see the 2x magnification of the cell area).

The EGFP signal was so strong that there was even bleed through in the DAPI channel. The transfected HeLa cell had an intact nucleus and morphology which were indicators for the cell's liveliness.

However, downregulation of U5-116 kDa upon transfection with its corresponding shRNA was visible on the Western Blots as well as in the immunofluorescence experiments.

Literature search revealed only one publication indicating a different staining pattern for U5-116 kDa (Fabrizio, P. et al. 1997) with a predominantly nuclear localisation of the protein. So the observed antibody staining seems not specific, according to the previously published subcellular localisation pattern (see *Discussion section*).

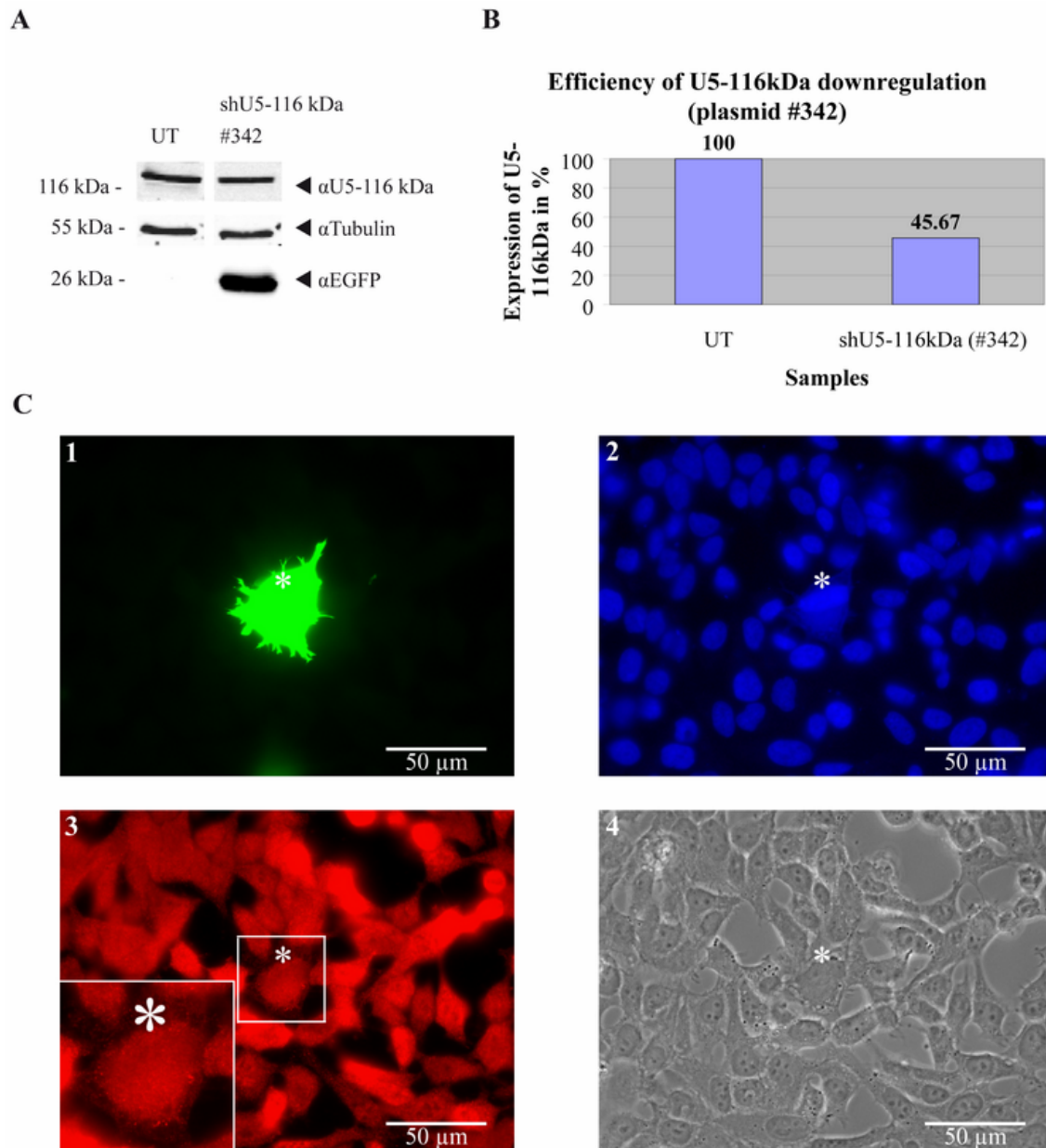


**Figure 3-5: Testing of the shU5-116 kDa plasmid in HeLa cells.**

**(A) Test of protein downregulation on Western Blot.** Western Blot showing the downregulation of U5-116 kDa protein upon transfection of HeLa cells with the shU5-116 kDa plasmid (#342). The corresponding protein molecular weights are indicated on the left side, the chosen antibodies for protein detection on the right side. **(B) Quantification of downregulation.** Quantification was done using the Odyssey® Application Software 2.1 (see manufacturer's manual). Protein levels of U5-116 kDa are compared to the level of untransfected cells (=100%) and normalised to Tubulin. **(C) Immunocytochemistry.** Immunostainings to visualise U5-116 kDa downregulation in fixed cells. Transfection and staining procedure as described in the *Methods section*. For description of pictures see also Figure 3-2. (1) HeLa cells transfected with the shU5-116 kDa plasmid (#342) expressing EGFP are marked with \*. (2) DAPI staining. (3) Antibody staining for U5-116 kDa to visualise downregulation in transfected cells. Depletion of U5-116 kDa in the transfected HeLa cells is visible especially in the periphery of the cell. The inset on the left indicates a 2fold magnification of the selected cell area. (4) Phase contrast picture. UT, untransfected; #342, shU5-116 kDa plasmid; α, anti.

## 1.4. ShRNA plasmids targeting RBMX

RBMX is a heterogeneous, nuclear ribonucleoprotein of the RNA-binding motif (RBM) family (Elliott, D. J. 2004). Very little is known about this protein so far. Knockdown experiments were performed in zebrafish, where the depletion of RBMX led to underdevelopment of the head and eyes as well as to a reduced body size compared to wt zebrafish (Tsend-Ayush, E. et al. 2005). Due to the study in zebrafish (Dichmann, D. S. et al. 2008) and a recently published study in *Xenopus laevis* (Dichmann, D. S. et al. 2008), RBMX plays an essential role in the development of the brain.

As RBMX was not detectable with the commercial antibody on the Western Blots to test the downregulation via corresponding shRNAs (data not shown), another Western Blot was made to investigate the protein expression level of RBMX in HeLa cells. To check whether in conventional HeLa cells the RBMX protein was maybe expressed in very low amounts, a Western Blot was made with 50 – 150 µg of an untreated HeLa cell lysate (UT). The protein was not detected under any condition, so its expression level in HeLa cells might simply be below the detection sensitivity of a Western Blot (see *Discussion section*). Therefore, the shRBMX plasmids could not be tested for their downregulation of RBMX in HeLa cells by Western blotting. The detection of RBMX (~43 kDa) on Western Blots was not possible with the used antibody (**Figure 3-6A**).

But as RBMX is a nuclear ribonucleoprotein (Elliott, D. J. 2004), its concentration in the cell's cytoplasm might simply be too low to be detected on a Western Blot. Most likely, the buffer used to lyse the cells in this diploma project was not strong enough to solubilise nuclei (see also *Discussion section*).

The immunostaining experiment performed with the same antibody as used for the Western Blots is shown in **Figure 3-6B**. Transfection was confirmed by the expression of EGFP, the transfected HeLa cells had intact nuclei as confirmed by DAPI staining and the morphology was also normal as shown by the phase contrast image.

The obtained RBMX staining pattern, however, seems rather diffuse and not very specific. Since there is no data published on RBMX in HeLa so far, there was no way to confirm the specificity of the antibody staining. If the staining pattern for RBMX was specific, it indicated that most RBMX protein is mainly concentrated in the nuclei and just to a

little extent cytoplasmic, which is a typical subcellular localisation pattern for hnRNPs (see *Discussion section*). With the antibody used for these experiments, there was no down regulation of RBMX detectable, neither on the Western Blot nor in the immunocytochemistry experiment. So it is unclear whether the shRBMX is working or not (**Figure 3-6B**).

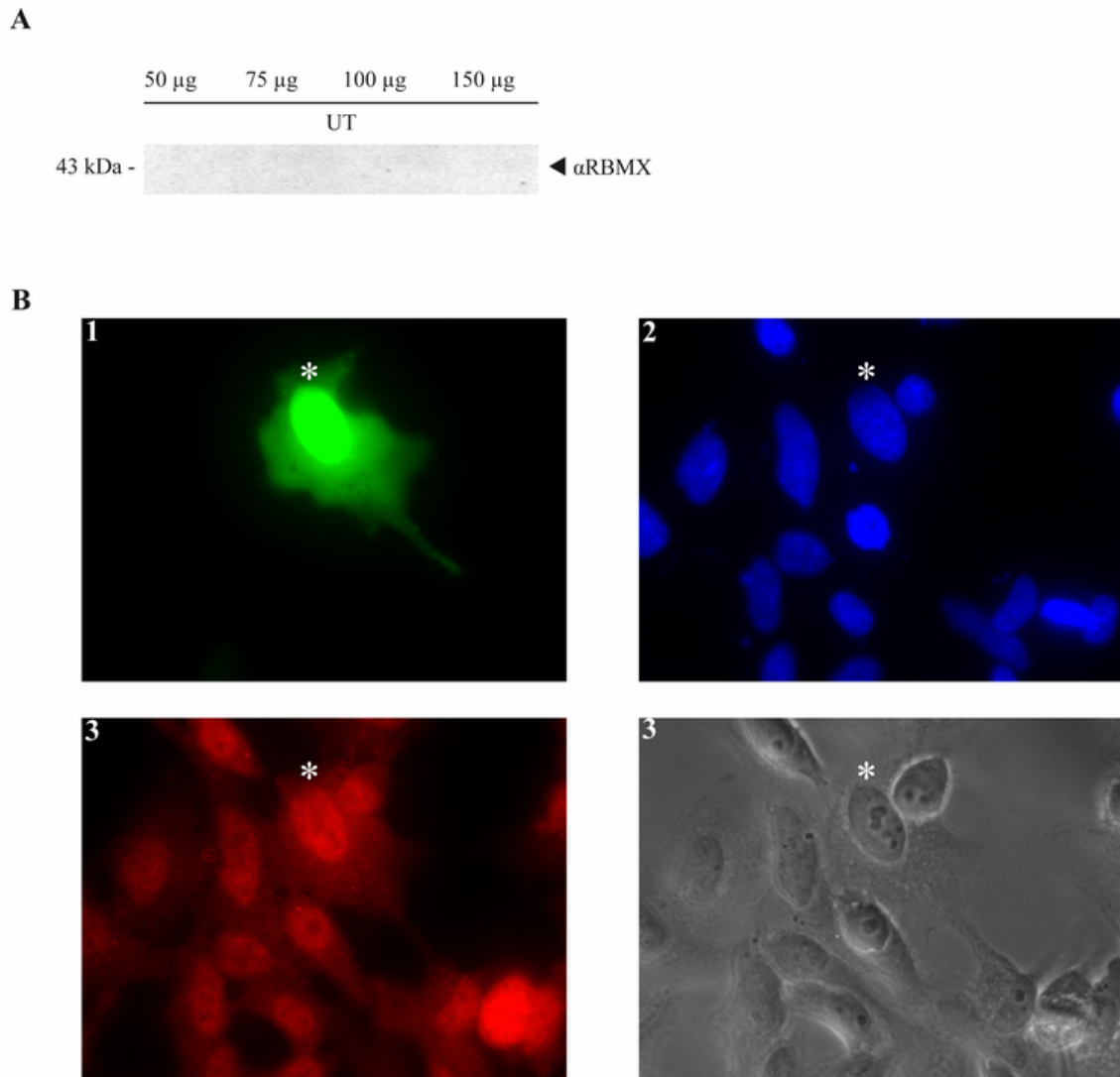


**Figure 3-6: Testing of the shRBMX plasmids in HeLa cells.**

**(A) Detection of RBMX on Western Blot.** Different protein amounts (50 - 150  $\mu$ g) of an UT HeLa lysate were tested on a Western Blot to detect RBMX. The protein was not detected in any condition on the blot, whereas the RBMX immunostainings displayed fluorescent signals (see (B)). So the shRBMX plasmids could not be tested for their downregulation of RBMX. Blot was probed for RBMX, which should result in a ~43 kDa band. RBMX could also not be detected in the  $\beta$ -Globin HeLa cell lines (see Figure 3-14). **(B) Immunocytochemistry.** Immunostainings to check whether RBMX downregulation could be made visible in fixed cells. Transfection and staining procedure as described in the *Methods section*. For description of pictures see also Figure 3-2. (1) HeLa cell transfected with the shRBMX plasmid (#308) strongly expressing EGFP is marked with \*. (2) DAPI staining. (3) Antibody staining for RBMX to visualise downregulation in transfected cells. There is no apparent reduction or depletion of RBMX visible, if the observed staining pattern is specific. (4) Phase contrast picture. UT, untransfected; #308, shRBMX plasmid;  $\alpha$ , anti.

## 1.5. ShRNA plasmids targeting RBM4

RBM4 is an RNA-binding protein of the RNA recognition motif (RRM) class and a splicing factor. RBM4 localizes in nuclear speckles and nucleoli, which supports its potential role in splicing or RNA processing (Markus, M. A. and Morris, B. J. 2006). These facts are also good indicators for a possible role of RBM4 in the NMD process.

The created shRBM4 plasmids were tested for their capacity of protein downregulation via Western Blot. **Figure 3-7A** and **B** show Western Blots displaying no downregulation of RBM4 protein (~43 kDa) upon transfection of conventional HeLa cells with the shRBM4 plasmids #320, #321, #343 and #344. According to the EGFP signals, transfections worked for all four plasmids. In the case of the shRNA constructs #343 and #344, the EGFP signals were quite low compared to those of plasmids #320 and #321. This indicated a lower transfection rate and EGFP expression upon transfection with #343 and #344. No RBM4 signal was detected on the Western Blot in **Figure 3-7B** (see *Discussion section*).

The shRNA sequences for plasmid #343 and #344 were chosen according to a recent study (Hock, J. et al. 2007), but did not downregulate RBM4 in our experiments. In this publication, the siRNA constructs were pre-transfected as 2'-O-methyl oligoribonucleotides into HeLa cells using EscortV (Sigma), according to the manufacturer's instructions.

Taken together, none of the designed and tested shRNA plasmids was able to reduce RBM4 expression and also inconsistencies with the RBM4 detection on the Western Blots occurred (see *Discussion section*).



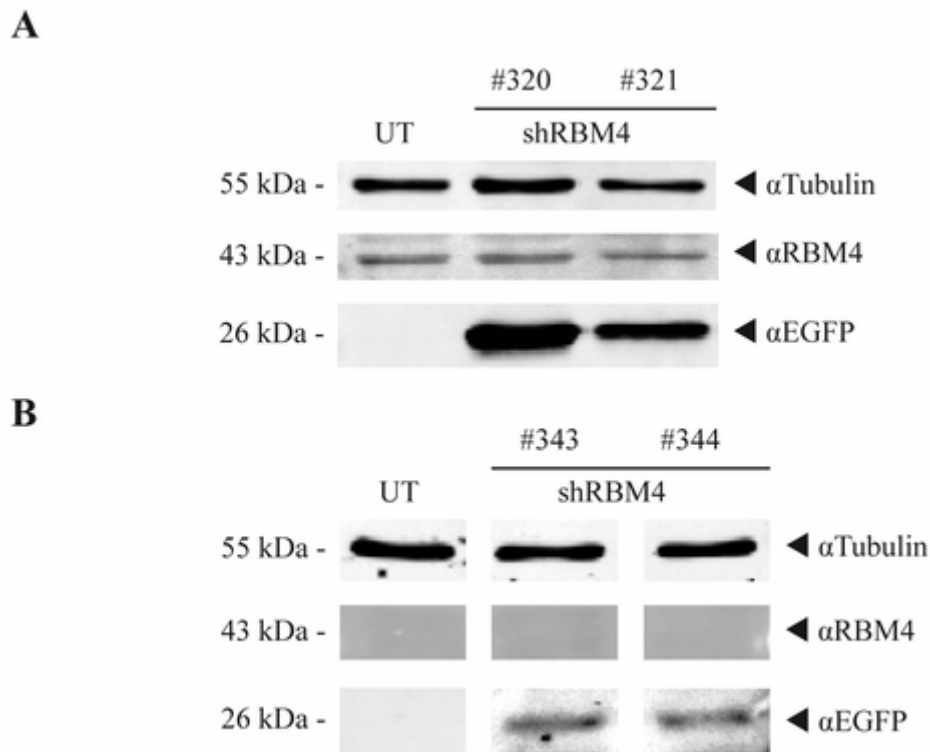


**Figure 3-7: Testing of the shRBM4 plasmids in HeLa cells.**

The Western Blots for testing RBM4 downregulation were quantified using the Odyssey® Application Software 2.1 (see manufacturer's manual). The protein levels of the transfected samples were compared to the levels of an UT control (=100%) and normalised to Tubulin. The corresponding molecular weights are indicated on the left side, the chosen antibodies for protein detection on the right side.

**(A) Test of protein downregulation on Western Blot.** Western Blot showing no downregulation of RBM4 protein (~43 kDa) upon transfection of HeLa cells with two different shRBM4 plasmids (#320 and #321).

**(B) Test of protein downregulation on Western Blot.** Western Blot showing no downregulation of RBM4 protein (~43 kDa) upon transfection of HeLa cells with two additional shRBM4 plasmids (#343 and #344). The RBM4 protein was not even detected on the Blot.

UT, untransfected; #320, shRBM4 plasmid; #321, shRBM4 plasmid; #343, shRBM4 plasmid; #344, shRBM4 plasmid; α, anti.

## 2. ESTABLISHMENT OF AN NMD ASSAY

To investigate the role of the selected candidate proteins in NMD, I set out in collaboration with Dr. Daniela Karra to establish an NMD assay (Daniela Karra, PhD thesis 2008) based on the method developed by Miles Wilkinson and coworkers (Carter, M. S. et al. 1995; Li, S. et al. 1997; Muhlemann, O. et al. 2001). For this assay, they transiently transfected HeLa cells with either a wild type (wt) or a PTC-containing NMD reporter construct (TCR- $\beta$  or  $\beta$ -Globin) to monitor the efficiency of the decay by NMD (Carter, M. S. et al. 1995; Li, S. et al. 1997).

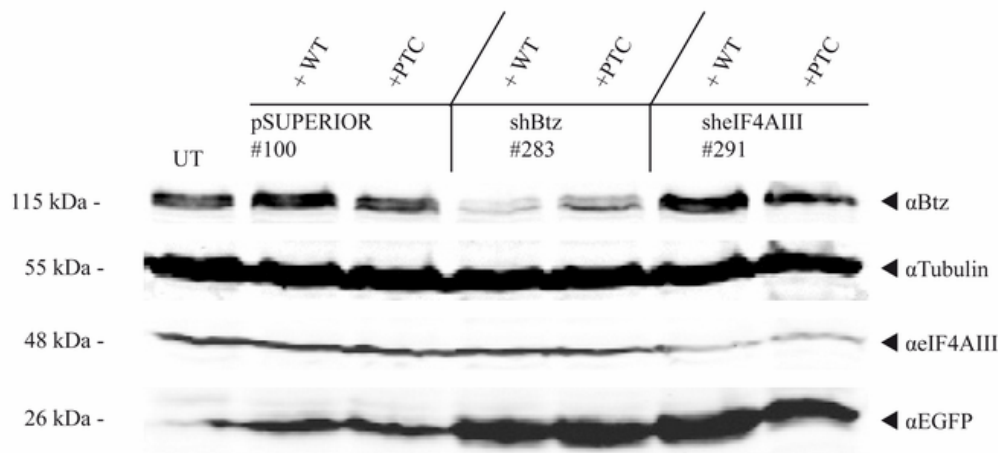
### 2.1. Essential controls for the NMD assay

Since it was already shown that the RNA-binding proteins Btz and eIF4AIII play a role in NMD, those proteins were chosen to serve as positive controls for the NMD assay (Ferraiuolo, M. A. et al. 2004; Palacios, I. M. et al. 2004). The corresponding shRNA plasmids were designed and tested for the NMD assay by Dr. Daniela Karra (Daniela Karra, PhD thesis 2008 and data not shown). The following shRNA plasmids served as positive controls in the NMD assay: shBtz (plasmid #283) and shEIF4AIII (plasmid #291); the empty pSUPERIOR vector (plasmid #100) as negative control. The shRNA plasmids, which should serve as NMD assay controls, were tested in HeLa cells. Dr. Daniela Karra also investigated their effect in hippocampal neurons during her PhD thesis.

Figure 3-8A shows a typical NMD assay experiment where HeLa cells were cotransfected with the controls and the WT or PTC TCR- $\beta$  constructs and the samples were compared to an untransfected, untreated control (UT). Downregulation of Btz (plasmid #283) and eIF4AIII (plasmid #291) protein upon transfection of conventional HeLa cells was clearly visible on the Western Blot. The shBtz usually showed a reduction of protein expression of ~ 50 – 60% upon transfection (Daniela Karra, PhD thesis 2008). The effect of the shEIF4AIII was found to be strongly dependent on the quality of the maxiprep, which is a crucial criterion for the obtained transfection efficiency, as was observed before for all transfections (Zeitelhofer, M. et al. 2008).

The control plasmid #100 had no effect on the Btz or eIF4AIII expression as expected. Some of the #100 + WT sample diffused into the UT slot. Therefore, the UT sample showed a residual EGFP signal. All transfections worked well according to the EGFP signal. Only the #100 control samples had weaker EGFP signals than the other samples. The immunofluorescence pictures in Figure 3-8B show a typical example of a high transfection efficiency obtained for the control plasmids. Conventional HeLa cells were cotransfected with shBtz (plasmid #283) and the wt TCR- $\beta$  construct (WT). Since EGFP is coexpressed together with the respective shRNA from the same plasmid, EGFP expression in cells is just a verification of the transfection with the shRNA plasmids and does not tell whether the TCR- $\beta$  plasmids are successfully transfected into the same cell as well. Obviously the expression levels of EGFP differ from cell to cell as can be seen in this picture. The phase contrast picture of the cells was used to check the cells' morphology and if they are alive.

A



B

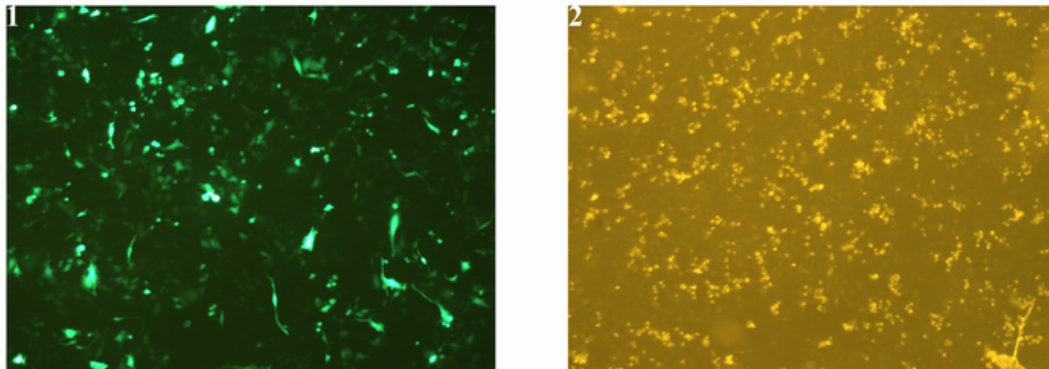


**Figure 3-8: Test of NMD assay controls and setup in conventional HeLa cells.**

**(A) Protein downregulation of NMD assay controls Btz and eIF4AIII.** Western Blot showing the downregulation of Btz (plasmid #283) and eIF4AIII (plasmid #291) protein upon cotransfection of conventional HeLa cells with the control shRNA plasmid and the WT or PTC TCR- $\beta$  construct. The TCR- $\beta$  constructs are used to monitor the effect on NMD, when a protein is depleted. The corresponding molecular weights are indicated on the left side, the chosen antibodies for protein detection on the right side. Levels of protein expression are compared to the protein levels of an untransfected control (=100%) and normalised to Tubulin. Some of the negative control (#100 + WT) sample diffused into the UT slot. Therefore, the UT sample shows a little EGFP signal. Control (#100) samples have weaker EGFP signals than the other samples. **(B) Pictures of transfected HeLa cells.** Pictures were taken with the Leica MZ 16F microscope (Leica) with 80x magnification (picture size 1781  $\mu\text{m}$  x 1331  $\mu\text{m}$ ). (1) HeLa cells, cotransfected with shBtz (plasmid #283) + WT, expressing EGFP. Expression levels of EGFP differ from cell to cell as can be seen here. Picture shows typically transfection efficiency for conventional HeLa cells. (2) Corresponding phase contrast picture to check the cells' morphologies and their physiological status.

UT, untransfected; WT, TCR- $\beta$  wt RNA without PTC; PTC, TCR- $\beta$  RNA with PTC; #100, empty pSUPERIOR plasmid; #283, shBtz plasmid; #291, sheIF4AIII plasmid;  $\alpha$ , anti.

## **2.2. Establishment of the NMD assay in conventional HeLa cells using TCR- $\beta$ reporter constructs**

Once effective shRNA plasmids targeting chosen candidates for the NMD assay were designed and tested (see *Methods section* and *1 Creation and testing of shRNAs for NMD assay candidates* in the *Results section*), they were used to investigate the role of the respective candidate in NMD. It is already known that if an essential component of the NMD machinery is lacking, the process is impaired (Sun, X. et al. 1998; Ferraiuolo, M. A. et al. 2004; Palacios, I. M. et al. 2004).

Upon knockdown of the respective candidate in conventional HeLa cells, the amounts of different TCR- $\beta$  mRNA reporter constructs (Carter, M. S. et al. 1995; Li, S. et al. 1997) are monitored. If a candidate protein is part of the NMD machinery, it will lead to an accumulation of TCR- $\beta$  mRNAs containing a PTC and therefore to an impairment of the NMD process.

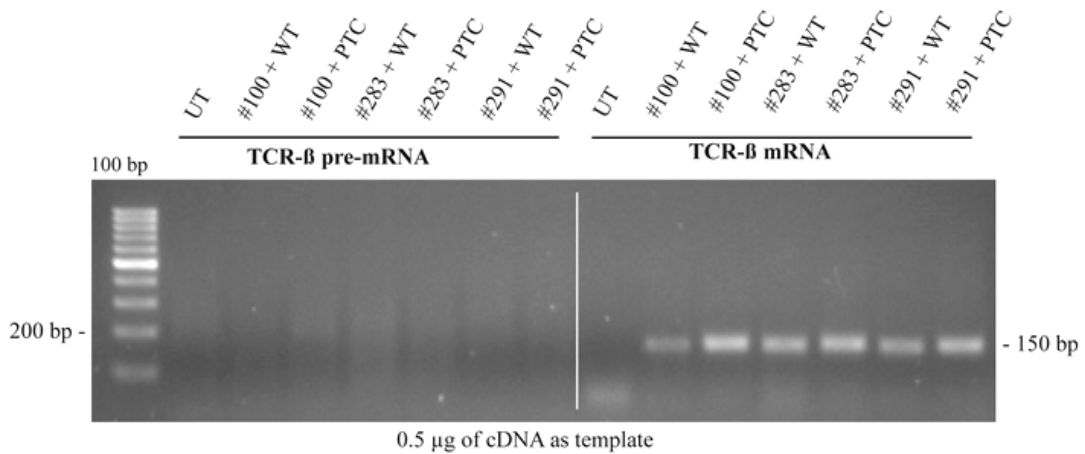
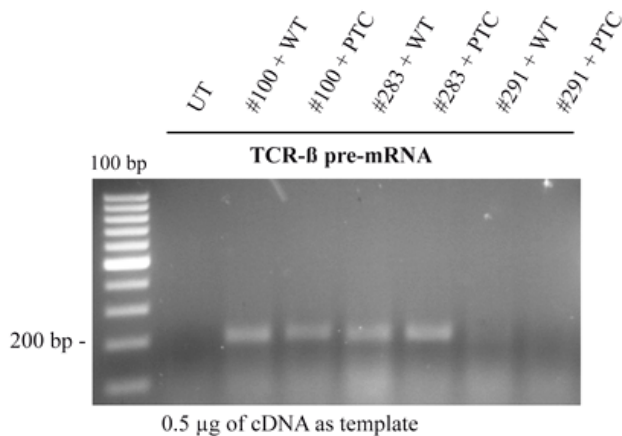
Conventional HeLa cells were therefore cotransfected with the shRNA plasmid targeting an NMD candidate and a plasmid for the expression of a wt TCR- $\beta$  construct without PTC (WT) or a TCR- $\beta$  construct with a PTC (PTC). RNA and protein were isolated with Trizol® Reagent (Invitrogen) from the samples 72 h after transfection. Protein downregulation of the NMD candidate was confirmed by Western Blot. The RNA was transcribed into cDNA and semiquantitative PCRs for the TCR- $\beta$  pre-mRNA (200 nt fragment) and mRNA (150 nt fragment) were performed in different PCR tubes. The PCR products were then checked and analysed on a 2% agarose gel.

### 2.2.1. Optimisation of semiquantitative PCR for TCR- $\beta$ pre-mRNA in HeLa cells

The following parameters had to be set up for the NMD assay. Foremost, the pre-mRNA product was found to be more sensitive when amplified by PCR. In one of the first experiments to set up the PCR conditions, the amplification of the TCR- $\beta$  mRNA cDNA worked, whereas the TCR- $\beta$  pre-mRNA product could not be amplified (**Figure 3-9A**). Two parameters were tested to detect the TCR- $\beta$  pre-mRNA PCR product: the amount of the template cDNA used for the PCR to optimize the sensitivity of the PCR reaction and the annealing temperature to increase the specificity of the PCR reaction and product.

Different cDNA template amounts (0.25 - 1.0  $\mu$ g) were tested for the PCR, but did not permit the detection of the expected pre-mRNA product (data not shown).

Bioinformatical analyses (using internet tools, e.g. Primer3) revealed that the TCR- $\beta$  pre-mRNA primer forms secondary structures. To dissolve those, different temperatures were tested to optimize the annealing of the primer to the template cDNA: 55°C, 58°C, 60°C and 62°C (data not shown with the exception of 60°C in **Figure 3-9B**). But only an annealing temperature of 60°C restored the successful amplification of the TCR- $\beta$  pre-mRNA, with the exception of the #291 samples (sheIF4AIII plasmid, positive control) (see *Discussion section*) in this particular experiment shown in **Figure 3-9B**. The untransfected HeLa cell control did not give a TCR- $\beta$  PCR product as expected.

**A No TCR-β pre-mRNA amplification, but TCR-β mRNA amplification****B Increase of annealing temperature for TCR-β pre-mRNA primers****Figure 3-9: Optimisation of semiquantitative PCR for TCR-β pre-mRNA in HeLa cells.**

PCRs were performed on cDNA templates of HeLa cells, cotransfected with the constructs indicated above each lane, to amplify either TCR-β pre-mRNA (200 bp) or TCR-β mRNA (150 bp) products. 30 µl of each PCR reaction including 6x Loading Dye (Fermentas) were separated on a 2% agarose gel in parallel with 15 µl of the GeneRuler™ 100 bp DNA Ladder (Fermentas). The untransfected HeLa cell sample (UT) served as negative control.

**(A) No TCR-β pre-mRNA amplification, but TCR-β mRNA amplification.** PCR for TCR-β pre-mRNA on cDNA did not work. Subsequent tests using different cDNA template amounts (0.25 - 1.0 µg) for PCR did not yield the expected pre-mRNA products (data not shown). **(B) Increase of annealing temperature for TCR-β pre-mRNA primers.** The annealing temperature for the TCR-β pre-mRNA primers was changed to 60°C. This successfully restored amplification of the TCR-β pre-mRNA products (with exception of the sheIF4AIII samples (#291)). Tested cDNA samples are the same as in (A).

UT, untransfected; WT, TCR-β wt RNA without PTC; PTC, TCR-β RNA with PTC; #100, empty pSUPERIOR plasmid; #283, shBtz plasmid; #291, sheIF4AIII plasmid.

### 2.2.2. Test of different RNA isolation kits

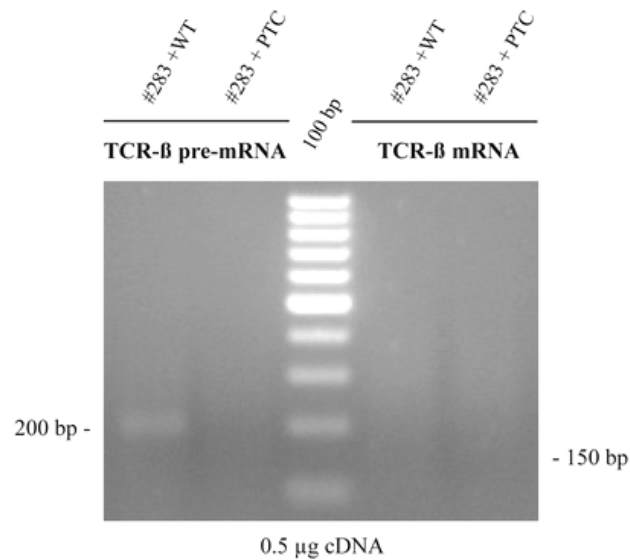
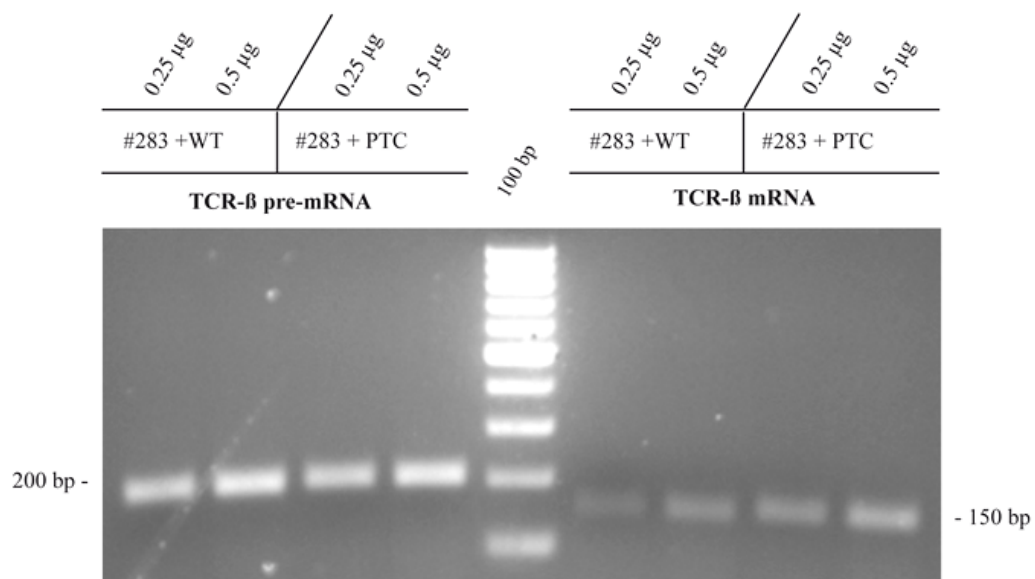
The quality of the RNA is crucial for the detection and quantification of the TCR- $\beta$  products by PCR. Therefore, different RNA isolation kits were tested as shown in **Figure 3-10A** and **B**. After RNA isolation, all samples were reverse transcribed using the M-MLV reverse transcriptase (H-) (Promega). The generated cDNA was then used to amplify TCR- $\beta$  PCR products which were analysed on a 2% agarose gel.

Although the RNeasy Midi Kit (Qiagen) is a phenol/chloroform-free RNA isolation procedure with a high degree of RNA stabilisation, it did not work well for the RNA isolation of our TCR- $\beta$  construct. Just a faint band of one pre-mRNA sample (#283 + WT) was visible on the gel picture (**Figure 3-10A**). But as the kit is designed to enrich RNAs >200 nt using a silica-gel membrane step, the TCR- $\beta$  RNAs were possibly excluded by size. So only in a single case, a faint band of the TCR- $\beta$  product could be detected.

The mirVana™ miRNA Isolation Kit (Ambion) combines organic extraction (acid-phenol/chloroform) and solid-phase extraction for RNA isolation over a broad size range. The purification was done for total RNA, which should also be very effective for small RNAs. A final purification step to enrich in small RNAs was not performed, because it would have excluded our 200 nt samples.

With the mirVana™ miRNA Isolation Kit, isolation of the desired TCR- $\beta$  RNA worked really well as shown in **Figure 3-10B**. The intensities of the bands were proportional to the used template amounts, which allowed quantification of the results (data not shown).



**A RNeasy Midi Kit – Qiagen****B mirVana™ miRNA Isolation Kit – Ambion****Figure 3-10: Test of different RNA isolation kits.**

PCRs were performed on cDNA templates of HeLa cells, cotransfected with the constructs indicated above each lane, to amplify either TCR-β pre-mRNA (200 bp) or TCR-β mRNA (150 bp) products. PCR products amplified from cDNA, were separated and analysed on a 2% agarose gel as described in Figure 3-9. RT-PCR was performed using the M-MLV Reverse Transcriptase (H-) (Promega) in all experiments. **(A) RNeasy Midi Kit – Qiagen.** Just a faint band of one pre-mRNA sample (#283 + WT) was seen once when using the RNeasy Midi Kit (Qiagen). **(B) mirVana™ miRNA Isolation Kit – Ambion.** In all cases, amplification of the TCR-β products was successful with the mirVana™ miRNA Isolation Kit (Ambion). Intensity of the bands was also proportional to the used template amounts. To confirm reproducibility, experiments were repeated yielding comparable results. WT, TCR-β wt RNA without PTC; PTC, TCR-β RNA with PTC; #283, shBtz plasmid.

### 2.2.3. Optimisation of template amounts and internal standards for normalisation

For further fine-tuning of the experimental setup, different template amounts were tested to find the quantitative and sensitive range of the PCR reaction (**Figure 3-11**). TCR- $\beta$  pre-mRNA was chosen for amplification, as it was more sensitive to changes in the experimental conditions. 0.25 -1.25  $\mu\text{g}$  cDNA template amounts were tested. The same cDNA samples were already previously used to amplify TCR- $\beta$  cDNA successfully (see **Figure 3-10**). The PCR of TCR- $\beta$  pre-mRNA worked for all used conditions. However, the intensities of the PCR bands were not at all or only poorly correlated to the template amounts. There was just one exception. Correlation between template amount and the intensity of the band was observed for the sample cotransfected with shBtz and the wt TCR- $\beta$  construct where 1.25 $\mu\text{g}$  were used as template for PCR (sample #283 + WT 1.25  $\mu\text{g}$ ).

So no obvious conclusion could be drawn concerning the quantitative PCR range and the precision of the semiquantitative PCR. Due to this reason, the integration of a housekeeping gene such as tubulin was tested as an internal PCR standard (last lane of each sample). GAPDH was also used to normalize the signal intensity (data not shown). This allows the quantification of the samples even in semiquantitative PCR reactions.

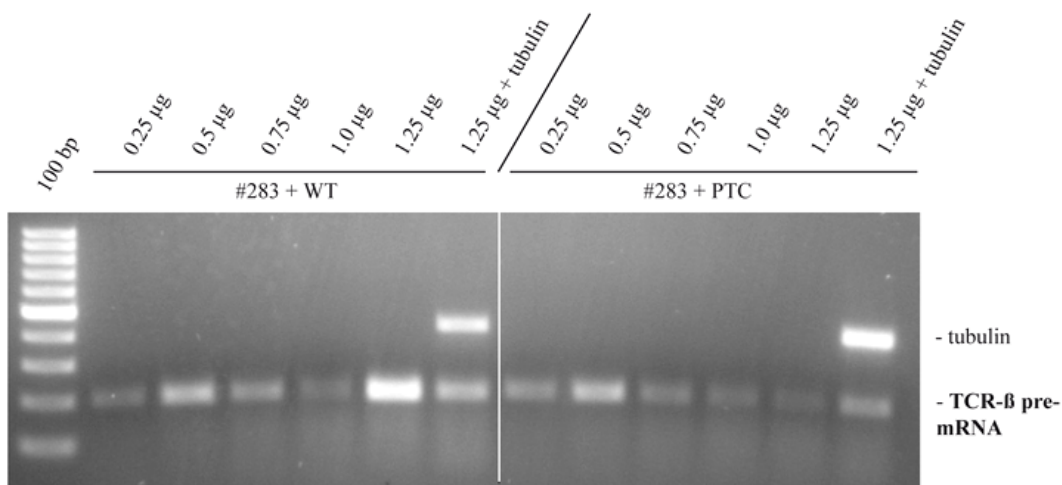


**Figure 3-11: Optimisation of template amounts and internal standards for normalisation.**

PCRs were performed on cDNA templates of HeLa cells, cotransfected with the constructs indicated above the gel picture, to amplify TCR- $\beta$  pre-mRNA (200 bp). The same cDNA samples were already successfully used before to amplify TCR- $\beta$  products. PCR products amplified from cDNA were separated and analysed on a 2% agarose gel as described in Figure 3-9. PCR of TCR- $\beta$  pre-mRNA worked for all conditions. In the last lane of each sample tubulin was also amplified as internal standard. WT, TCR- $\beta$  wt RNA without PTC; PTC, TCR- $\beta$  RNA with PTC; #283, shBtz plasmid.

#### 2.2.4. Optimisation of RT-PCR conditions

Since the integration of an internal standard was successful, different RT-PCR conditions were now tested to increase the sensitivity of the assay. Within the reverse transcriptase reaction, it is possible to enrich your target cDNA by using a specific primer instead of random primers, which were used in the reactions so far. RNA that was isolated with the mirVana™ miRNA Isolation Kit (Ambion), was in parallel reverse transcribed using the M-MLV reverse transcriptase (H-) (Promega) either using Random Primers (Promega) or the specific TCR- $\beta$  reverse primer. The resulting PCR products were then analysed on 2% agarose gels (**Figure 3-12**). Tubulin could still be amplified in the specific TCR- $\beta$  reverse primer reactions (see *Discussion section*). So as a next step, the bands on the gels could then be quantified to establish the normalisation of the PCR results via tubulin.

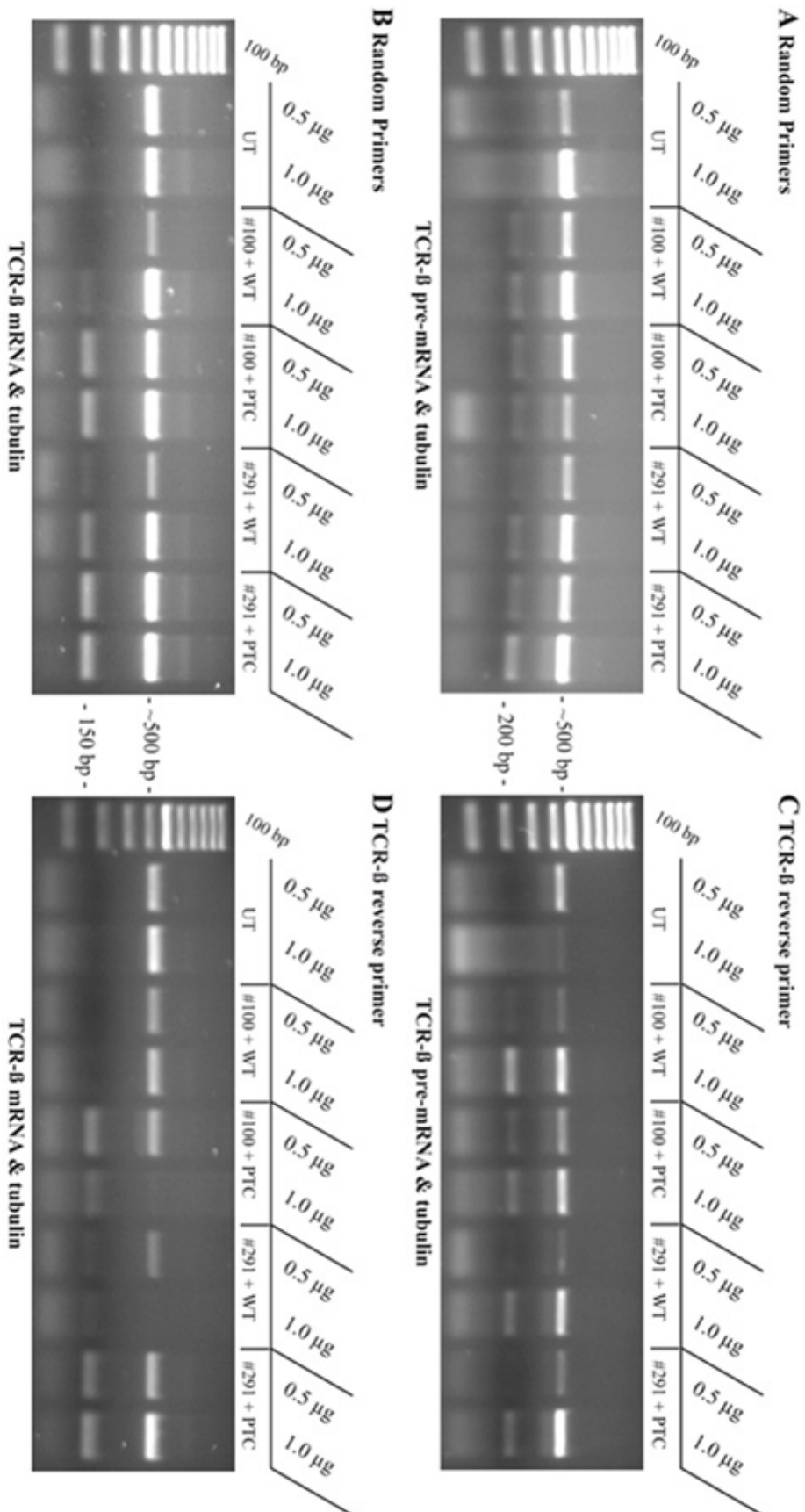


**Figure 3-12: Optimisation of RT-PCR conditions.**

PCRs were performed on cDNA templates of HeLa cells transfected with the constructs indicated above each lane. RNA was isolated with mirVana™ mRNA Isolation Kit (Ambion). RT-PCR was performed using either Random Primers (Promega) or TCR-β reverse primer. (A) TCR-β pre-mRNA (200 bp) and tubulin (~500 bp) amplified from cDNA created with Random Primers. (B) TCR-β mRNA (150 bp) and tubulin amplified from cDNA created with Random Primers. (C) TCR-β pre-mRNA and tubulin amplified from cDNA created with TCR-β reverse primer. (D) TCR-β mRNA and tubulin amplified from cDNA created with TCR-β reverse primer. UT, untransfected; WT, TCR-β wt RNA without PTC; PTC, TCR-β RNA with PTC; #100, empty pSUPERIOR plasmid; #291, shIF4AIII plasmid

The bands on the gels were quantified using the Quantity One software (Bio-Rad) (**Table 3-1A and B**). The measured values of the samples were normalised to the tubulin values. mRNAs with a PTC should be degraded in the negative control samples (#100), where NMD is intact, whereas incorrect RNAs should accumulate in the eIF4AIII knockdown samples (#291, positive control), where NMD is impaired. These expected results could not be experimentally verified, which might also indicate insufficient detection sensitivity of the semiquantitative PCR. But as the total RNA was isolated using the mirVana™ miRNA Isolation Kit, protein could not be isolated in parallel to analyse the protein downregulation upon transfection with the respective shRNA via Western Blot. So it was not possible to confirm whether the knockdown of the controls was sufficient in this experiment. Possibly, eIF4AIII was simply not sufficiently downregulated (#291 samples), which explains the obtained results concerning the NMD process.

**Table 3-1:** Test of tubulin as an internal standard

<b>A</b>					<b>B</b>				
<b>RT-PCR with Random Primers</b>					<b>RT-PCR with TCR-<math>\beta</math> reverse primer</b>				
<b>TCR-<math>\beta</math> pre-mRNA</b>					<b>TCR-<math>\beta</math> pre-mRNA</b>				
Results normalised to tubulin in %.					Results normalised to tubulin in %.				
Template amount	Volume INT*/mm <sup>2</sup>	Density INT*/mm <sup>2</sup>	Mean value		Template amount	Volume INT*/mm <sup>2</sup>	Density INT*/mm <sup>2</sup>	Mean value	
UT	0.5 $\mu$ g	0	0		UT	0.5 $\mu$ g	0	0	
	1.0 $\mu$ g	0	0			1.0 $\mu$ g	0	0	
100+WT	0.5 $\mu$ g	47.07	47.07	40.21	100+WT	0.5 $\mu$ g	82.47	82.47	78.06
	1.0 $\mu$ g	33.35	33.35			1.0 $\mu$ g	73.64	73.64	
100+PTC	0.5 $\mu$ g	45.24	45.24	52.34	100+PTC	0.5 $\mu$ g	67.97	67.97	65.53
	1.0 $\mu$ g	59.43	59.43			1.0 $\mu$ g	63.08	63.08	
291+WT	0.5 $\mu$ g	53.56	53.56	44.72	291+WT	0.5 $\mu$ g	75.74	75.74	68.06
	1.0 $\mu$ g	35.88	35.88			1.0 $\mu$ g	60.38	60.38	
291+PTC	0.5 $\mu$ g	46.15	46.15	42.46	291+PTC	0.5 $\mu$ g	66.16	66.16	55.29
	1.0 $\mu$ g	38.77	38.77			1.0 $\mu$ g	44.42	44.42	
<b>TCR-<math>\beta</math> mRNA</b>					<b>TCR-<math>\beta</math> mRNA</b>				
Results normalised to tubulin in %.					Results normalised to tubulin in %.				
Template amount	Volume INT*/mm <sup>2</sup>	Density INT*/mm <sup>2</sup>	Mean value		Template amount	Volume INT*/mm <sup>2</sup>	Density INT*/mm <sup>2</sup>	Mean value	
UT	0.5 $\mu$ g	0	0		UT	0.5 $\mu$ g	0	0	
	1.0 $\mu$ g	0	0			1.0 $\mu$ g	0	0	
100+WT	0.5 $\mu$ g	no band	no band	41.63	100+WT	0.5 $\mu$ g	no band	no band	no value
	1.0 $\mu$ g	41.63	41.63			1.0 $\mu$ g	no band	no band	
100+PTC	0.5 $\mu$ g	62.20	62.20	59.90	100+PTC	0.5 $\mu$ g	77.25	77.25	86.79
	1.0 $\mu$ g	57.59	57.59			1.0 $\mu$ g	96.33	96.33	
291+WT	0.5 $\mu$ g	75.91	75.91	67.31	291+WT	0.5 $\mu$ g	71.44	71.44	80.29
	1.0 $\mu$ g	58.71	58.71			1.0 $\mu$ g	89.14	89.14	
291+PTC	0.5 $\mu$ g	58.03	58.03	56.87	291+PTC	0.5 $\mu$ g	71.47	71.47	66.61
	1.0 $\mu$ g	55.71	55.71			1.0 $\mu$ g	61.75	61.75	

RNA was isolated with the miRvana™ miRNA Isolation Kit (Ambion). RT-PCR was either done using Random Primers (Promega) **(A)** or using specific TCR- $\beta$  reverse primers **(B)**. PCR products were analysed on a 2% agarose gel (see Figure 3-12). The bands on the gels were then quantified using the Quantity One software (Bio-Rad). Volume INT\*/mm<sup>2</sup> and Density INT\*/mm<sup>2</sup> values of the samples were normalised to the tubulin values. Results are given in %. Mean value is calculated for the results of 0.5  $\mu$ g and 1.0  $\mu$ g of the same sample. mRNAs with a PTC should accumulate in the shelfF4AIII samples (#291) where NMD is impaired. This effect is not visible in the data. UT, untransfected; WT, TCR- $\beta$  wt RNA without PTC; PTC, TCR- $\beta$  RNA with PTC; #100, empty pSUPERIOR plasmid; #291, shelfF4AIII plasmid

### 2.2.5. Variability of cotransfections

Cotransfections are usually performed to introduce 2 or more plasmids into HeLa cells. In theory, both plasmids should be equally taken up, if transfection worked. But in some of the experiments for the NMD assay, problems with cotransfection of the TCR- $\beta$  construct and the shRNA plasmid occurred in conventional HeLa cells (**Figure 3-13**). According to the PCR results in **Figure 3-13**, cells were only transfected with the shRNA plasmid, but not the TCR- $\beta$  plasmid. Since all shRNA plasmids also express EGFP, transfected cells were always checked for EGFP expression under the microscope and pictures were taken to monitor transfection efficiencies (data not shown). In contrast, expression of the TCR- $\beta$  plasmid could only be verified by PCR. Therefore, we chose HeLa cell lines with stable integrated NMD reporter constructs (in our case  $\beta$ -globin and TCR- $\beta$ ) for the subsequent experiments.

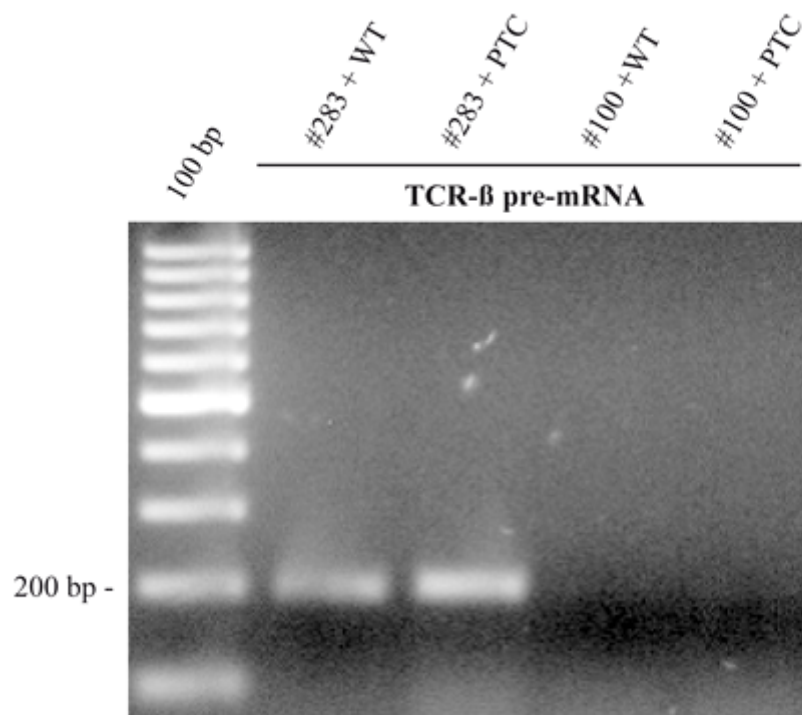


**Figure 3-13: Variability of cotransfections.**

RNA isolation was done using Trizol® Reagent (Invitrogen) and RT-PCR was performed to generate cDNA, using Random Primers and reagents from Promega. PCR products amplified from cDNA were separated and analysed on a 2% agarose gel as described in Figure 3-9. TCR- $\beta$  pre-mRNA (200 bp) could be amplified in the first 2 samples, but not in the last 2 ones, indicating that the WT and PTC plasmids were not cotransfected together with plasmid #100.

WT, TCR- $\beta$  wt RNA without PTC; PTC, TCR- $\beta$  RNA with PTC; #283, shBtz plasmid; #100, empty pSUPERIOR plasmid.

### **2.3. Cell lines stably expressing $\beta$ -Globin & real-time PCR**

The variability in the amount and quality of the isolated total RNA, the inconsistency in the cotransfection efficiency and the fact that a conventional PCR is only semiquantitative (Ferre, F. 1992; Kubista, M. et al. 2006; Blow, N. 2007), led us to set up quantitative real-time PCR. In this case, total RNA and protein isolation using the Trizol<sup>®</sup> Reagent (Invitrogen) is state-of-the-art (see <http://www.invitrogen.com>, e.g. (Albertini, V. et al. 2006)), since Trizol<sup>®</sup> does not interfere with the reaction.

To overcome the inconsistency of the cotransfection efficiencies in the conventional HeLa cells, 4 stable HeLa cell lines expressing NMD mRNA targets ( $\beta$ -globin or TCR- $\beta$ ) with or without PTC were used for the real-time PCR experiments, which were a generous gift from Dr. Oliver Mühlemann (Institute of Cell Biology, University of Bern, Switzerland).

In the remainder, the following two  $\beta$ -Globin cell lines were used to investigate the role of the candidates in NMD by real-time PCR: wt  $\beta$ -Globin HeLa cells without a PTC and NS39  $\beta$ -Globin HeLa cells containing a PTC (Thermann, R. et al. 1998). Two HeLa cell lines with a TCR- $\beta$  construct were also tested for the NMD assay: HeLa 290F without a PTC and HeLa 593C without a PTC (Muhlemann, O. et al. 2001).



### 2.3.1. Analysis of NMD assay candidates in TCR- $\beta$ and $\beta$ -Globin HeLa cell lines

The expression levels of the candidate proteins and the NMD assay controls Btz and eIF4AIII were analysed by Western Blots, shown in **Figure 3-14**. Total protein was isolated with Trizol<sup>®</sup> Reagent from stably transfected  $\beta$ -Globin and TCR- $\beta$  HeLa cell lines. The protein lysates from the cell lines were compared to a protein sample from conventional HeLa cells. Same volumes of the protein samples were loaded for Western Blots to yield comparable protein amounts. The first Western Blot was probed for Btz, DDX5, Tubulin, RBM4 and NPM1 (**Figure 3-14A**). On the second Western Blot, the expression levels of U5-116 kDa, Tubulin and eIF4AIII were analysed (**Figure 3-14B**). RBMX was also tested, but the antibody recognised a protein double band of a different size (<35 kDa, marked by an asterisk) than the expected 43 kDa of RBMX. The visible double band at <35 kDa, after the incubation with RBMX antibody, was even stronger for the 4 cell lines (see *Discussion section*).

According to the normalisation to the Tubulin signal, Btz was stronger expressed in the TCR- $\beta$  cell lines and much stronger expressed in the  $\beta$ -Globin cell lines, compared to wt conventional HeLa cells. The expression levels observed for DDX5, U5-116 kDa as well as for eIF4AIII were approximately the same in all tested cell lines. RBM4 proteins were nearly equally expressed in the conventional HeLa cells and the  $\beta$ -Globin cell lines, but a bit reduced in the TCR- $\beta$  cell lines. The strong expression of NPM1 in the stable cell lines, compared to conventional HeLa cells, was very surprising. The NPM1 signals were so prominent that the phosphorylated and the unphosphorylated form of NPM1 (Okuda, M. et al. 2000) could no longer be distinguished.

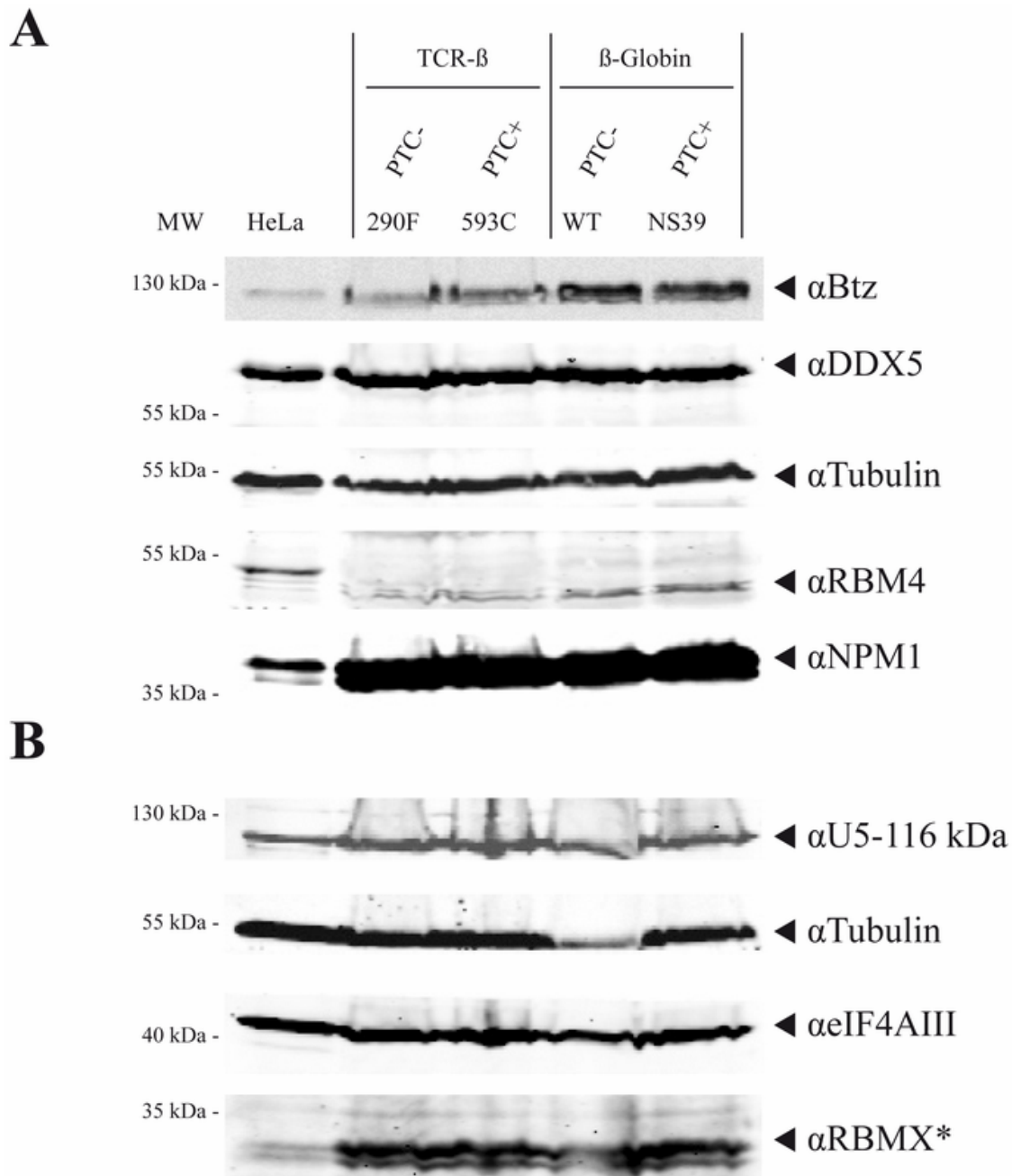


**Figure 3-14: Analysis of NMD assay candidates in TCR- $\beta$  and  $\beta$ -Globin HeLa cell lines.**

Protein isolations with Trizol® Reagent (Invitrogen) were separated on 10% SDS-PA gels for Western Blots. Protein expression of conventional HeLa cells was compared to protein expression of the stable HeLa cell lines. PageRuler™ Prestained Protein Ladder (Fermentas) was used to determine the molecular weight on the left (MW), where the size of the marker is depicted.  $\alpha$ Tubulin antibody was applied as loading control.

(A) Western Blot was probed for Btz (115 kDa), DDX5 (68 kDa), Tubulin (55 kDa), RBM4 (43 kDa) and NPM1 (38 kDa). NPM1 displayed the characteristic double bands, described in Figure 3-2.

(B) Western Blot was probed for U5-116 kDa (116 kDa), Tubulin and eIF4AIII (48 kDa). RBMX (43 kDa) was also tested, but antibody recognised a double band of different size <35 kDa (\*).

MW, molecular weight marker (PageRuler™ Prestained Protein Ladder - Fermentas); HeLa, conventional HeLa cell sample; TCR- $\beta$ , stable TCR- $\beta$  HeLa cell line;  $\beta$ -Globin, stable  $\beta$ -Globin HeLa cell line; PTC, premature termination codon; PTC-, without PTC; PTC+, with PTC;  $\alpha$ , anti.

### 2.3.2. NPM1 downregulation in wt $\beta$ -Globin HeLa cells

The designed shRNA plasmids that had already been tested in conventional HeLa cells, were tested for their efficiency in downregulating the corresponding protein in the stable cell lines.

72 h after transfection, downregulation of NPM1 in the stable cell lines was not sufficient (data not shown). Since the shRNA plasmids for NPM1 (#312 and #317) were very efficient in the conventional HeLa cells, I decided to examine the protein turnover and downregulation of the respective protein in the stable cell lines (**Figure 3-15**). Wt  $\beta$ -Globin HeLa cells were transfected with a shNPM1 plasmid (#317) and downregulation was allowed to take place for 4 or 5 days. Protein lysates of transfected cells were then analysed by Western Blot and compared to an untransfected control sample (**Figure 3-15A**). The Western Blot was probed for Btz, Tubulin, NPM1 and EGFP. The EGFP signals on the Western Blot confirmed the successful transfection with the shNPM1 plasmid (#317).

Quantification of the Western Blot revealed a slight downregulation of NPM1 after 5 days to 68.94% (**Figure 3-15B**). Compared to the 17.94% NPM1 expression obtained with the same plasmid in conventional HeLa cell after 72 h of downregulation, the achieved effect was quite marginal. The expression level of Btz was not influenced by the shNPM1 plasmid, as expected.

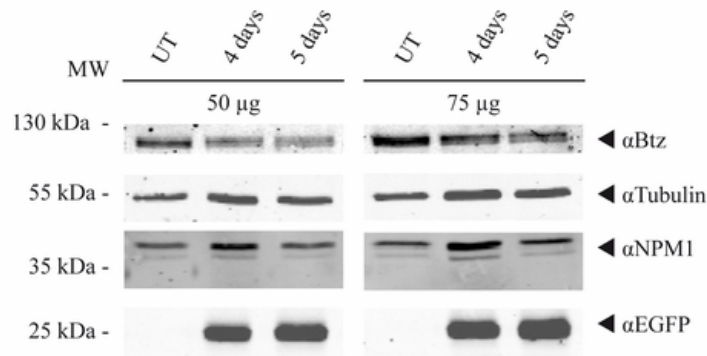
Afterwards, immunocytochemistry was performed in wt  $\beta$ -Globin HeLa cells to investigate, whether the NPM1 downregulation after 5 days was visible in single cells (**Figure 3-16**). The wt  $\beta$ -Globin HeLa cells were transfected with the shNPM1 plasmid (#317) and strongly expressed EGFP. The observed transfection efficiencies in the wt  $\beta$ -Globin HeLa cells were lower than the usually obtained transfection rates in conventional HeLa cells (data not shown). The nuclei were intact and the morphology of the cells was normal, which indicated that the cells were not stressed and alive. The antibody staining for NPM1 (Yung, B. Y. et al. 1990; Iggo, R. D. et al. 1991; Bocker, T. et al. 1995; Wu, M. H. et al. 1995; Nozawa, Y. et al. 1996; Zatsepina, O. V. et al. 1997; Cordell, J. L. et al. 1999), to visualize downregulation in transfected cells, is shown in red. The transfected cells were clearly depleted of NPM1 and also the speckles of NPM1 were reduced or absent in the nuclei. Furthermore, the puncta of NPM1 in the untransfected

cells were less prominent than those in conventional HeLa cells (**Figure 3-3C**), but that in general the nuclear area was more intensely red, which might indicate the higher expression level of NPM1 in the  $\beta$ -Globin cells. As the NPM1 downregulation was quite low with just 31.06% reduction on the Western Blot, downregulation judged by immunostaining also seemed to be a little weaker as for the conventional HeLa cells (**Figure 3-3C**). This is easy to see in the white squares which indicate a 3x magnification of one cell area.

Therefore, the immunocytochemistry experiment confirmed that NPM1 can also be downregulated in stable HeLa cell lines. In contrast to the obvious NPM1 knockdown visualized by immunostaining, no significant downregulation was observed via Western Blot. This might be due to the observed lower transfection efficiency in the stable HeLa cells compared to the wt cells (see *Discussion section*).

Antibiotic selection has been used previously in NMD assay experiments (e.g. (Chan, W. K. et al. 2007; Stalder, L. et al. 2007)). Via selection, low transfection efficiencies in the stable cell lines can be compensated, because only cells containing the desired plasmids survive the procedure. Therefore, it is easier to monitor the effect of the knockdown of a candidate protein, because there will be less background signal of untransfected cells. Hence, as a next step neomycin selection was performed on the  $\beta$ -Globin cell lines, as all the shRNA plasmids had a neomycin resistance gene.

A



B

### Efficiency of NPM1 downregulation after 4 and 5 days (plasmid #317)

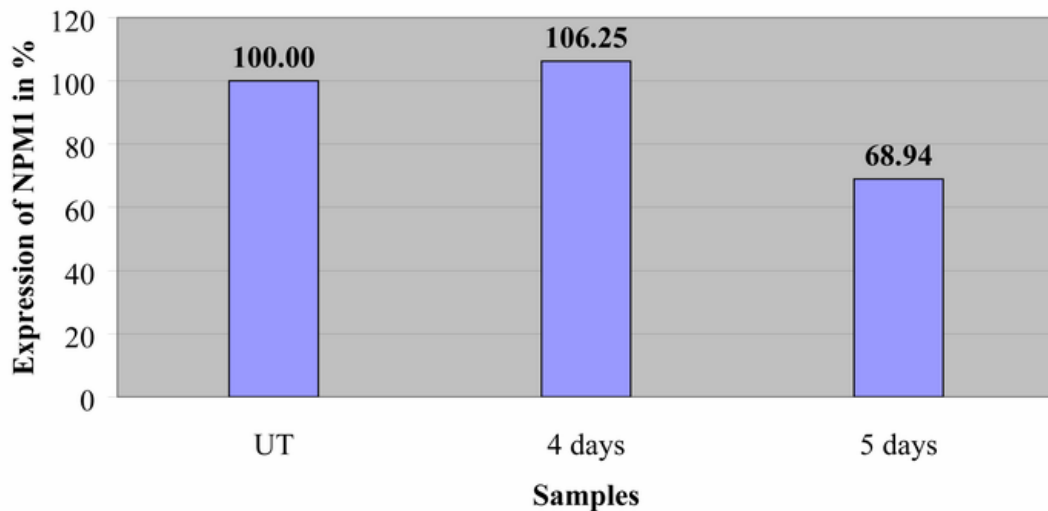


**Figure 3-15: Time course of NPM1 downregulation in wt β-Globin HeLa cells.**

**(A) Western Blots.** Samples of wt β-Globin HeLa cells were transfected with the shNPM1 plasmid (#317) and downregulation was allowed to take place for 4 or 5 days (not 3 days as in previous experiments). Protein lysates of an untreated and two transfected (#317) samples were then separated on a 10% SDS-PA gel for Western Blot. PageRuler™ Prestained Protein Ladder (Fermentas) was used to determine the molecular weight (MW). The size of the marker is depicted on the left. EGFP signals show successful transfection with the shNPM1 plasmid (#317). Western Blot was probed for Btz (115 kDa), Tubulin (55 kDa), NPM1 (38 kDa) and EGFP (26 kDa). **(B) Quantification of downregulation.** Quantification was done using the Odyssey® Application Software 2.1 (LI-COR® Biosciences). Expression levels of NPM1 samples were normalised to Tubulin and compared to the UT sample (=100%). Downregulation of NPM1 for 5 days resulted in a reduced expression level of 68.94%. MW, molecular weight marker (PageRuler™ Prestained Protein Ladder - Fermentas); UT, untransfected wt β-Globin HeLa cell sample; 4 days, 4 days of transfection and downregulation with shNPM1 #317; 5 days, 5 days of transfection and downregulation with shNPM1 #317; α, anti.

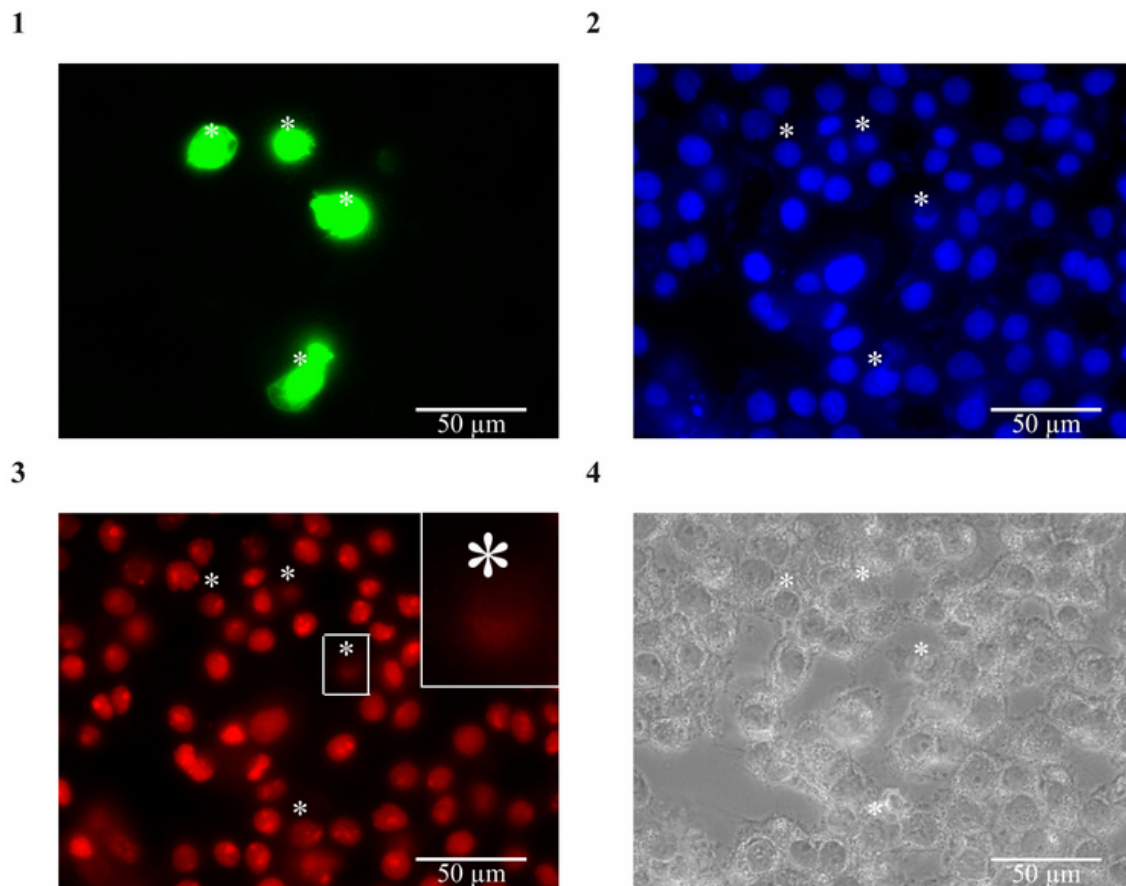


**Figure 3-16: 5 days of NPM1 downregulation in wt  $\beta$ -Globin HeLa cells.**

Wt  $\beta$ -Globin HeLa cells were transfected and immunostained as described in the *Methods section* to visualise the downregulation of NPM1 visible in fixed cells.

(1) HeLa cells transfected with the shNPM1 plasmid (#317) expressing EGFP are marked with \*. (2) DAPI staining of the DNA to visualise nuclei. (3) Antibody staining for NPM1 to visualise downregulation in transfected cells. Transfected HeLa cells are clearly depleted of NPM1: the puncta of NPM1 in the nuclei are reduced or abolished. The inset on the left indicates a 3fold magnification of the selected cell area. (4) Corresponding phase contrast picture to investigate the cells' morphologies and their physiological status.

### 2.3.3. Neomycin selection to enrich transfected cells

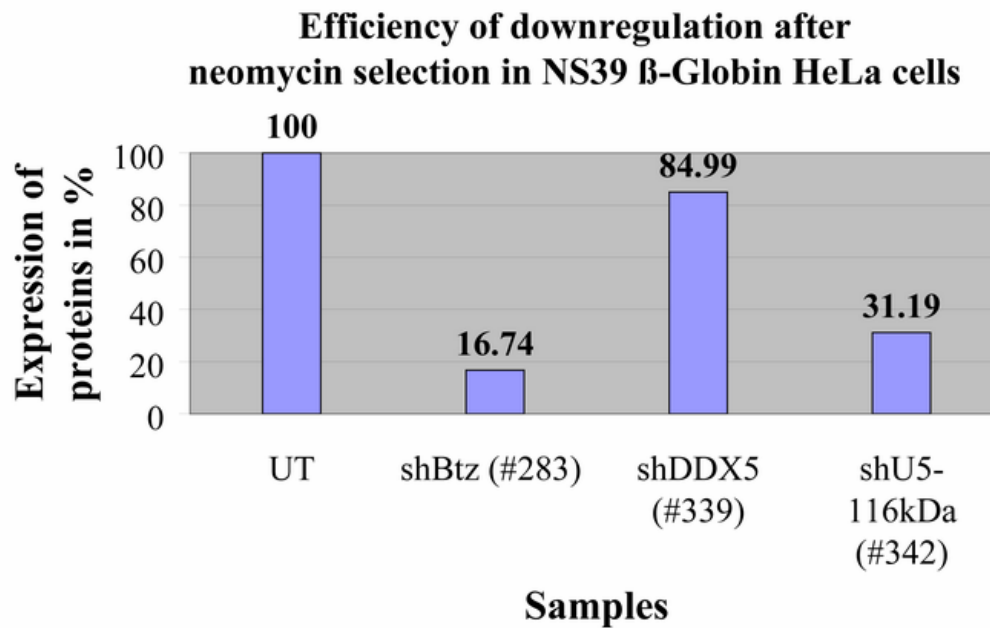
As downregulation for 3 - 5 days was not sufficient on Western Blot to considerably downregulate the candidate proteins to be tested in the NMD assay (**Figures 3-15, 3-16** and data not shown), neomycin selection was performed to enrich for transfected  $\beta$ -Globin HeLa cells (**Figure 3-17**). Transfections with the respective shRNA plasmids were done as usual and were followed by a neomycin selection procedure (see *Methods section* and the pSUPERIOR.neo+gfp vector manual (OligoEngine)). The final neomycin concentration of 600  $\mu\text{g/ml}$  was identified to be sufficient for selection within 7 days.

First, the empty pSUPERIOR.neo+gfp vector, shBtz (plasmid #283), shNPM1 (plasmid #312 and #317), shDDX5 (plasmid #339) and shU5-116 kDa (plasmid #342), which were tested successfully in conventional HeLa cells, were transfected into wt and NS39  $\beta$ -Globin HeLa cells. After transfection, neomycin selection was performed as described and total RNA and proteins were then isolated using Trizol<sup>®</sup> Reagent. Before samples were analysed by real-time PCR, Western Blots were performed (data not shown) to determine the knockdown efficiency of the respective protein. Quantification of the downregulation of the respective candidate proteins by Western Blots (**Figure 3-17A**) revealed that the shBtz (expression level of 16.74%), the shDDX5 (expression level of 84.99%) and the shU5-116 kDa (expression level of 31.19%) downregulated their corresponding protein in the NS39  $\beta$ -Globin HeLa cells. In the wt  $\beta$ -Globin HeLa cells, only the shBtz showed a reduction in Btz protein expression of 53.88%. The two shNPM1 plasmids (#312 and #317) did not affect the expression level of NPM1 in both cell lines.

**Figure 3-17B** shows examples of NS39  $\beta$ -Globin HeLa cells transfected with shBtz (plasmid #283) after 7 days of neomycin selection, to prove the efficiency of the selection procedure. The EGFP picture shows a typical example for usually obtained transfection efficiencies. The combined EGFP and phase contrast picture demonstrates that the transfected cells survived the selection. In contrast, untransfected cells rounded up, died and swam around in the medium.

Pictures were taken for all samples during the experiments (data not shown) to monitor the efficiencies of the neomycin selection.

A



B

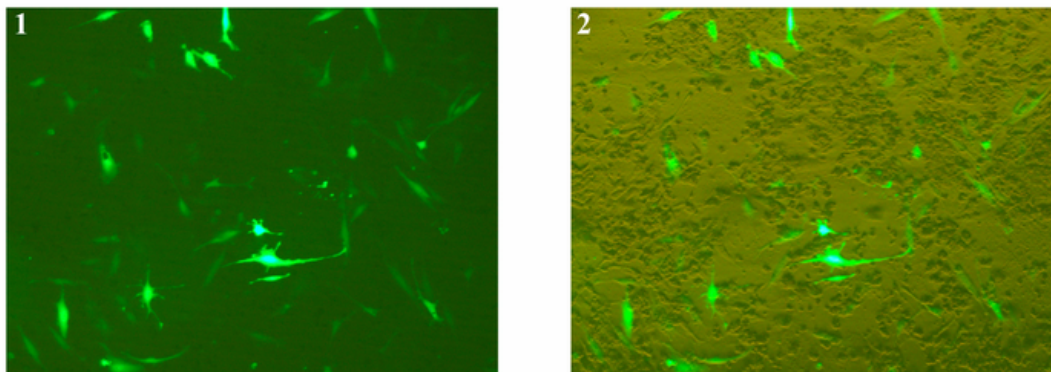


**Figure 3-17: Neomycin selection to enrich HeLa cells.**

**(A) Quantification of downregulation of NMD assay candidates on Western Blots after neomycin selection.** Quantification was done using the Odyssey® Application Software 2.1 (see manufacturer's manual). Protein levels of samples are always compared to an untransfected control (=100%) and normalised to Tubulin. The following three shRA plasmids: shBtz, shDDX5 and shU5-116 kDa downregulated their corresponding proteins in NS39  $\beta$ -Globin HeLa cells. **(B) Pictures of HeLa cells after transfection and neomycin selection.** Pictures were taken with the Leica MZ 16F microscope (Leica) and an 80x magnification (picture size 1781  $\mu$ m x 1331  $\mu$ m). (1) NS39  $\beta$ -Globin HeLa cells transfected with shBtz (plasmid #283) expressing EGFP. (2) EGFP and phase contrast picture of NS39  $\beta$ -Globin HeLa cells transfected with shBtz (plasmid #283). Transfected cells survived the selection, whereas untransfected cells were rounded, died and swam around in the medium.

UT, untransfected; #283, shBtz plasmid; #339, shDDX5 plasmid; #342, shU5-116 kDa plasmid.



### 2.3.4. Establishment of the real-time PCR

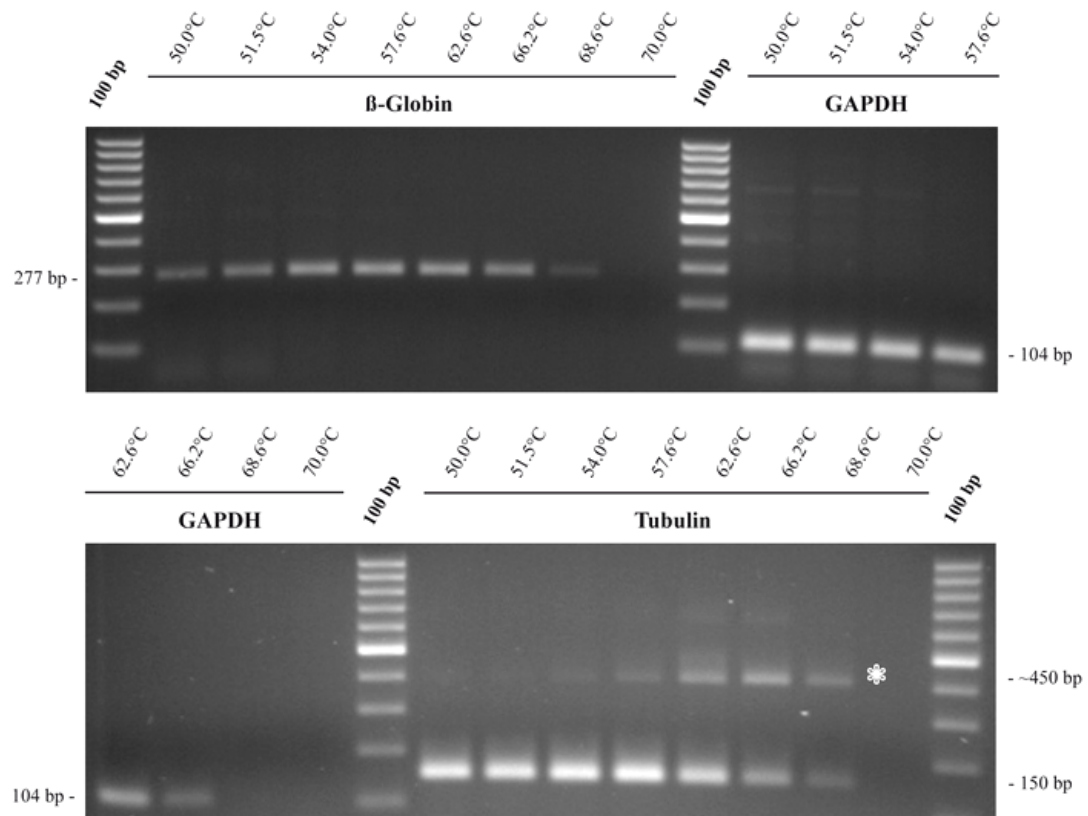
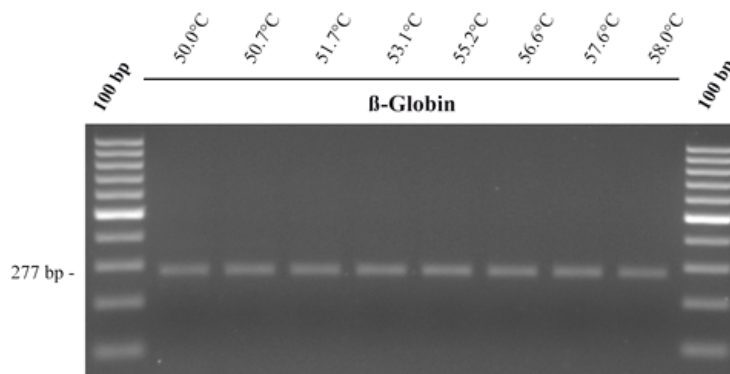
In parallel to the tests of the shRNA plasmids in the stable  $\beta$ -Globin cell lines, the optimal conditions for the real-time PCR were determined in these cells. The following parameters were optimised: template amounts (tested from 200 - 800 ng), primer concentrations and the setup for the dilution series. In addition, the real-time PCR cycle scheme was also fine tuned. The establishment was done for the stable  $\beta$ -Globin cell lines which should be investigated using specific  $\beta$ -globin primers. GAPDH and tubulin primers were utilised for normalisation.

One important parameter for all PCRs is to determine the optimal annealing temperature of all used primer pairs (**Figure 3-18A and B**). First, the primers were analysed for secondary structures with different internet tools (e.g. Primer3). Secondly, temperature gradient PCRs were performed as described in the *Methods section*, to find the best annealing temperature for all primers. For this purpose, 400 nM of each primer (800 nM per primer pair) was tested on 0.5  $\mu$ g total cDNA from untreated wt  $\beta$ -Globin HeLa cells. Each primer pair was analysed separately in different PCR tubes, but the reactions were run at the same time using the same PCR machine and the same PCR program. The quality of the resulting PCR products was analysed via agarose gel electrophoreses. **Figure 3-18A** shows the results of the temperature gradient from 50°C - 70°C for  $\beta$ -globin (PCR product size: 277 bp), GAPDH (PCR product size: 104 bp) and tubulin (PCR product: size 150 bp) primers. A secondary product of ~450 bp at 54.0°C - 68.6°C was amplified by the tubulin primers (**Figure 3-18A**). Single PCR products with the expected size were obtained using the  $\beta$ -globin or GAPDH primers, respectively.

In **Figure 3-18B**, a temperature gradient from 50°C - 58°C for  $\beta$ -globin (PCR product size: 277 bp) primers was tested, to narrow down the temperature range for the annealing. The detected PCR product of  $\beta$ -globin was specific over the whole range. The same gradient was also done for the tubulin primers (data not shown), showing their specificity for the same temperature range. According to the data, an annealing temperature of 55°C was used in all following real-time PCR experiments.

Beside the quality also the quantity of the primers is a very important parameter for real-time PCR. Primer concentrations were optimised using total cDNA from untreated wt  $\beta$ -Globin HeLa cells (**Figure 3-19**). Once 200 ng cDNA were identified to serve as best template amount (data not shown), 200 nM, 250 nM, 300 nM, 350 nM and 400 nM

primer concentration were tested for the housekeeping genes GAPDH and tubulin. For  $\beta$ -globin, only 300 nM and 350 nM were examined. The PCRs were performed using the real-time PCR program, described in the *Methods section*. Afterwards, the PCR products were checked for their quality and purity on 2% agarose gels. The results of the gel pictures were compared to real-time PCR parameter results (efficiency,  $R^2$ , slope). In addition, a concentration of 100 nM per primer was also tested with nearly the same results, efficiency and quality as 200 nM primer concentration (data not shown). Based on these results, the optimal real-time PCR conditions were determined for all three genes, which yielded similar real-time PCR parameter results, especially the efficiencies very close to each other.

**A Temperature gradient 50°C - 70°C****B Temperature gradient 50°C - 58°C****Figure 3-18: Optimisation of annealing temperature for real-time PCR primers.**

18  $\mu$ l of PCR reactions including 6x Loading Dye (Fermentas) were separated on a 2% agarose gel in parallel with 15  $\mu$ l of the GeneRuler™ 100 bp DNA Ladder (Fermentas). Primers (400 nM each) were tested on 0.5  $\mu$ g total cDNA from untreated wt  $\beta$ -Globin HeLa cells. PCR products were analysed for quality and purity on the gel. **(A) Temperature gradient 50°C - 70°C.** Temperature gradient from 50°C - 70°C for  $\beta$ -globin (PCR product size: 277 bp), GAPDH (PCR product size: 104 bp) and tubulin (PCR product: size 150 bp) primers. The tubulin primers give also a secondary product of ~450 bp at 54.0°C - 68.6°C, marked with a white \*. **(B) Temperature gradient 50°C - 58°C.** Temperature gradient from 50°C - 58°C for  $\beta$ -globin (PCR product size: 277 bp) primers to narrow down the temperature range. PCR product is specific over the whole range. The same gradient was also done for tubulin primers (data not shown) showing their specificity for the same temperature range. 55°C was subsequently used for real-time PCR.

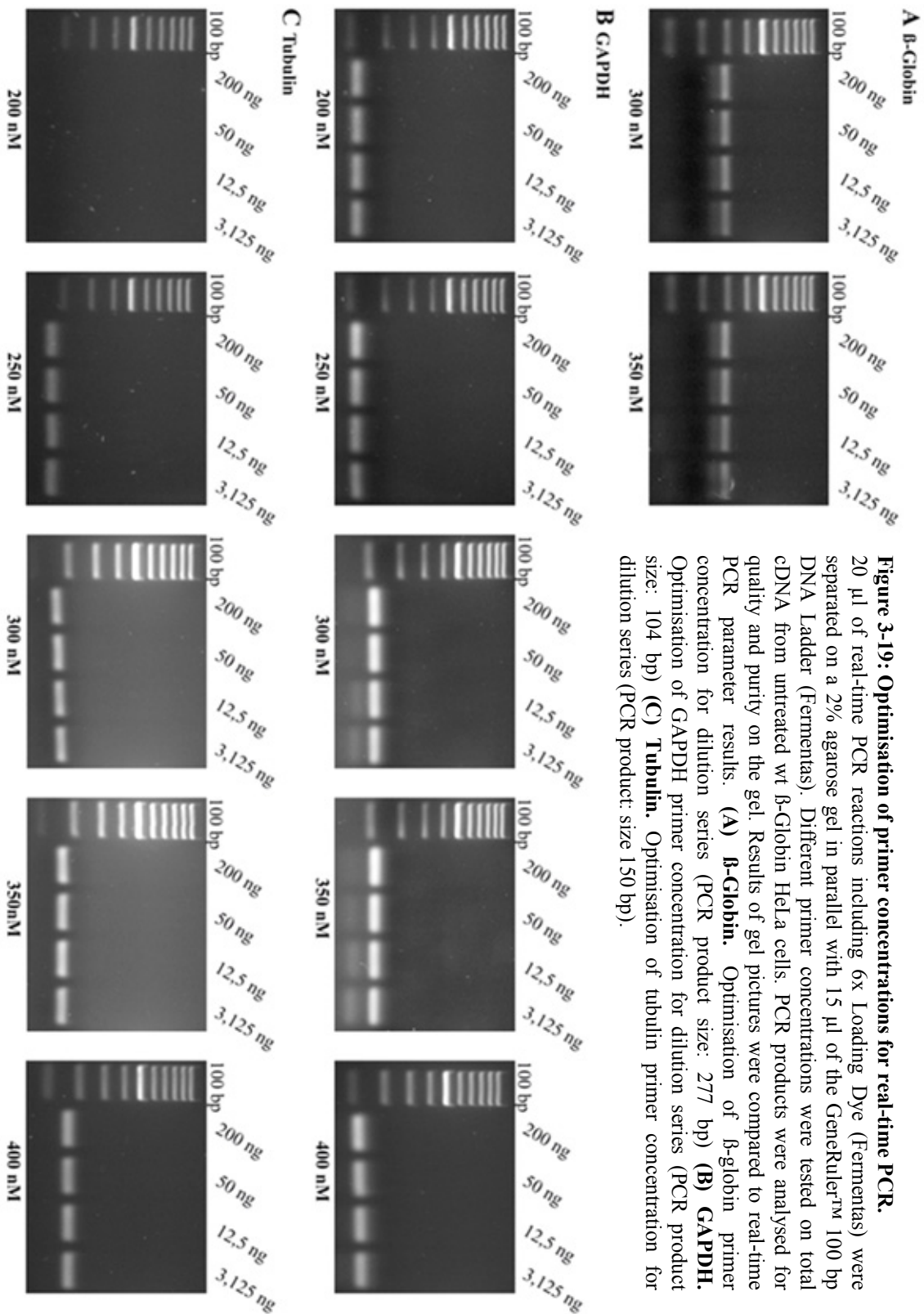


**Figure 3-19: Optimisation of primer concentrations for real-time PCR.** 20 µl of real-time PCR reactions including 6x Loading Dye (Fermentas) were separated on a 2% agarose gel in parallel with 15 µl of the GeneRuler™ 100 bp DNA Ladder (Fermentas). Different primer concentrations were tested on total cDNA from untreated wt β-Globin HeLa cells. PCR products were analysed for quality and purity on the gel. Results of gel pictures were compared to real-time PCR parameter results. (A) **β-Globin**. Optimisation of β-globin primer concentration for dilution series (PCR product size: 277 bp) (B) **GAPDH**. Optimisation of GAPDH primer concentration for dilution series (PCR product size: 104 bp) (C) **Tubulin**. Optimisation of tubulin primer concentration for dilution series (PCR product: size 150 bp).

### 2.3.5. Real-time PCR of $\beta$ -Globin HeLa cell lines after neomycin selection

First, the efficiencies of protein downregulation with the shRNA plasmids after neomycin selection were tested in the  $\beta$ -Globin cell lines (**Figure 3-17A**). Secondly, the downregulated samples after neomycin selection were now tested under the optimised real-time PCR conditions for their effects on the NMD process. In detail, they were analysed for their efficiency of decay of the  $\beta$ -globin constructs and therefore on the expression level of these constructs (**Figure 3-20**).

Real-time PCR was performed as described in 2.3.4 and the *Methods section*. 300 nM  $\beta$ -globin primer as well as 400 nM GAPDH and tubulin primer were used respectively per reaction. All samples were tested in triplicates. The obtained real-time data was analysed using the iQ5 Optical System Software (Version 2.0, Bio-Rad) and the  $\Delta\Delta C_t$  method. Finally, all shRNA samples were normalised to untransfected cells (UT sample with Normalised Fold Expression = 1). It is important to note the different scaling of the diagrams, which were drawn using the iQ5 Optical System Software.

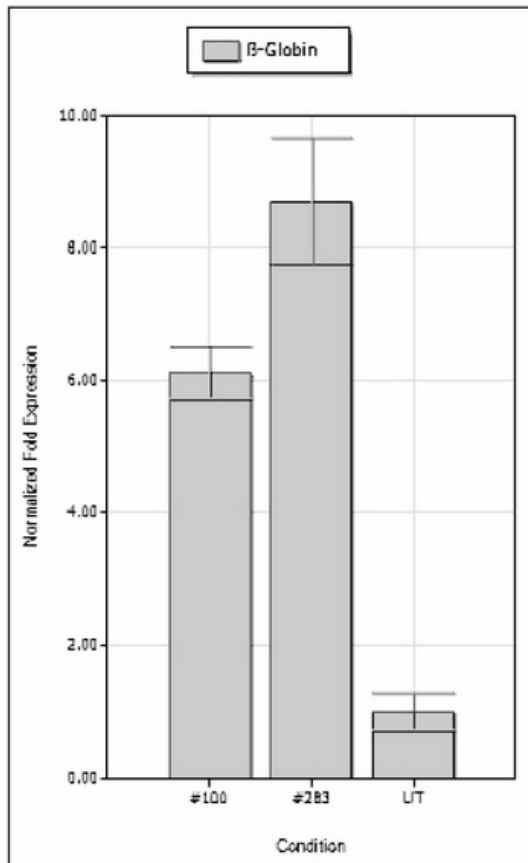
**Figure 3-20A** displays the real-time PCR results for the wt  $\beta$ -Globin HeLa cell line. The parameters of this reaction were  $E = 104.7\%$ ,  $R^2 = 0.989$  and  $\text{slope} = -3.215$ . The depletion of Btz (plasmid #283) down to 46.12% residual protein expression led to a  $\sim 9$ fold increase of wt  $\beta$ -globin expression. But also the transfection with the empty pSUPERIOR.neo+gfp vector resulted in a  $\sim 6$ fold increase of expression (see *Discussion section*).

The results for the NS39  $\beta$ -Globin cell line are shown in **Figure 3-20B**.  $E = 106.7\%$ ,  $R^2 = 0.964$  and  $\text{slope} = -3.171$  were the real-time parameters for this PCR reaction. The reduction of U5-116 kDa (plasmid #342) to 31.19% protein expression had nearly the same effect as the depletion of Btz (plasmid #283) to 16.74% protein expression with a  $\sim 10$ fold increase of NS39  $\beta$ -globin expression. It was surprising that the increase in expression of  $\beta$ -globin was nearly the same for the wt and the NS39 cell line, if Btz had been knocked down.

Although DDX5 is only reduced by 15.01%, it led to a drastic  $> 40$ fold increase of NS39  $\beta$ -globin. This indicated that the NMD process was strongly impaired in DDX5 depleted cells. But as the knockdown of DDX5 with plasmid #339 did not work in the

wt  $\beta$ -Globin cell line, which would have been an important control, no firm conclusion can be drawn from this real-time data set yet.

**A** wt  $\beta$ -Globin HeLa cells



**B** NS39  $\beta$ -Globin HeLa cells

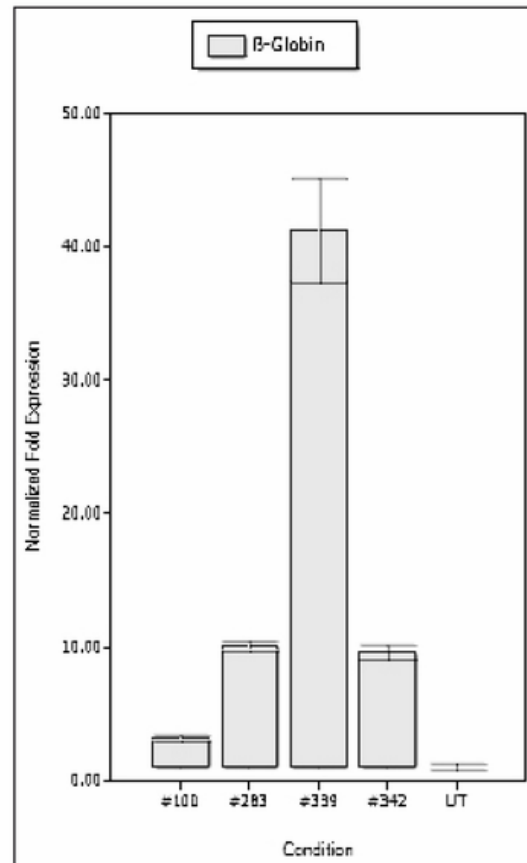


**Figure 3-20: Real-time PCR of  $\beta$ -Globin HeLa cell lines after neomycin selection.**

Real-time PCR was performed using 200 ng cDNA (RNA isolation with Trizol® Reagent) as template. Samples were tested for  $\beta$ -globin cDNA levels. GAPDH and tubulin were used as internal standards for normalisation. 300 nM  $\beta$ -globin primer and 400 nM GAPDH and tubulin primers were used per reaction. Samples were tested in triplicates. Real-time data was analysed using the iQ5 Optical System Software (Version 2.0, Bio-Rad) and the  $\Delta\Delta C_t$  method. ShRNA samples were normalised to UT (Normalised Fold Expression = 1). Note the different scaling of the diagrams. **(A) wt  $\beta$ -Globin HeLa cells.**  $E = 104.7\%$ ;  $R^2 = 0.989$ ; slope = -3.215; The depletion of Btz (plasmid #283) leads to a  $\sim 9x$  increase of wt  $\beta$ -globin expression, but also the transfection with the empty pSUPERIOR.neo+gfp vector results in a  $\sim 6x$  increase of expression. **(B) NS39  $\beta$ -Globin HeLa cells.**  $E = 106.7\%$ ;  $R^2 = 0.964$ ; slope = -3.171; The reduction of U5-116 kDa (plasmid #342) shows nearly the same effect as the depletion of Btz (plasmid #283) with a  $\sim 10x$  increase of NS39  $\beta$ -globin expression. The knockdown of DDX5 (plasmid # 339) even leads to a  $> 40x$  increase of NS39  $\beta$ -globin expression. This indicates that NMD is impaired under these conditions.

UT, untransfected; #100, empty pSUPERIOR vector; #283, shBtz plasmid; #339, shDDX5 plasmid; #342, shU5-116 kDa plasmid.

### 3. TEST OF DESIGNED shRNA PLASMIDS IN E17 RAT HIPPOCAMPAL NEURONS

The next step was to adapt the NMD assay, which was established in HeLa cells, for hippocampal neurons. This would allow us to identify the NMD machinery in neurons, which has not been investigated so far.

All designed shRNA plasmids which I had created for the NMD assay and also other projects in the laboratory and which worked in human HeLa cells were now tested in embryonic

day 17 (E17) rat hippocampal neurons. This should also be a first effort to start an NMD assay in neurons. Neurons were nucleofected with the Nucleoector II (Amaxa) (see *Methods section*). The O-003 programme was used and 10 µg and 20 µg plasmid DNA, respectively, were tested for their transfection efficiencies.

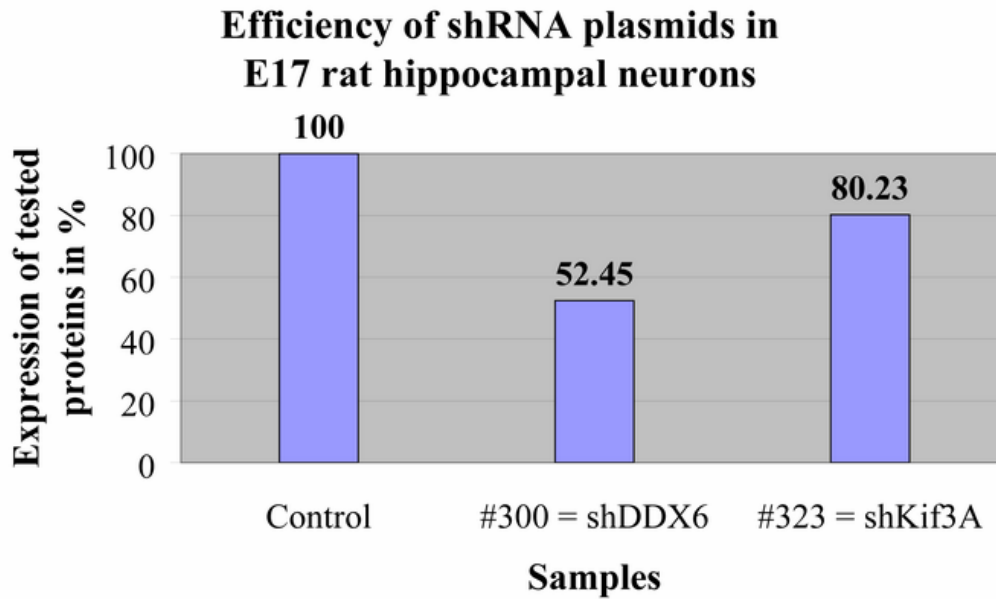
**Figure 3-21A** shows the quantification of the downregulation on Western Blots. This was achieved by using the Odyssey® Application Software 2.1 (see manufacturer's manual). All shRNA samples were compared to a control (=100% protein expression). Untransfected or not downregulated samples served as controls. Only the shDDX6 (plasmid #300) downregulated its corresponding protein to 52.45% protein expression as well as the shKif3A (plasmid #323) which downregulated the Kif3A protein to 80.23%.

The shNPM1 (#312 and #317) and shDDX5 (# 399) plasmids were also tested, but did not downregulate their corresponding proteins (data not shown). Interestingly, the NPM1 protein was not even detectable on Western Blots (see *Discussion section*).

**Figure 3-21B** shows the maximal obtained transfection efficiency upon nucleofection with 20 µg plasmid DNA. In this case, the neurons expressing EGFP were transfected with shDDX5 (plasmid #339).

Although all tested shRNA plasmids were designed to target rat and human sequences, none of the plasmids working in HeLa cells displayed downregulation of the respective protein in rat hippocampal neurons. So further shRNA plasmids have to be designed and tested in order to start an NMD assay also in rat neurons.

A



B

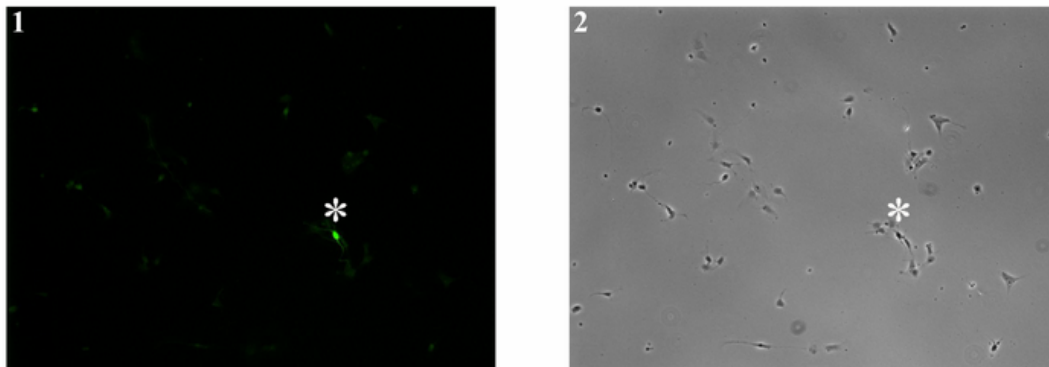


**Figure 3-21: Test of shRNA plasmids in rat hippocampal neurons.**

**(A) Quantification of downregulation on Western Blots.** Rat embryonic day 17 (E17) neurons were nucleofected with the Nucleoector II (Amaxa). The O-003 programme was used and 10  $\mu$ g and 20  $\mu$ g plasmid DNA were tested for their transfection efficiency. Quantification was done using the Odyssey® Application Software 2.1 (see manufacturer's manual). Protein levels of samples are compared to a control (=100%) and normalised to Tubulin. ShNPM1 plasmids (# 312 and #317) and shDDX5 plasmid (# 339) were also tested, but did not downregulate their corresponding proteins (data not shown).

**(B) Picture of nucleofected E17 rat hippocampal neurons.** For the testing of five generated shRNA plasmids, the maximal obtained transfection efficiency upon nucleofection with 20  $\mu$ g plasmid DNA is shown. (1) Transfected rat hippocampal neuron expressing EGFP marked with \*. (2) Phase contrast picture.

Control, untransfected or not downregulated samples; #300, shDDX6 plasmid; #323, shKif3A plasmid.



# DISCUSSION

The intention of this diploma thesis was to establish an NMD assay in order to investigate the role of putative players in the NMD process. Therefore, shRNA plasmids were created against selected protein candidates to study their function in NMD. HeLa cells were then depleted of these protein candidates and the effect of the protein knockdown on the NMD process was monitored.

## 1. TRANSFECTION OF shRNA PLASMIDS

For the design of the shRNAs, the selection of the shRNA sequence by hand with the computer program Lasergene from DNASTAR (Version 7.1.0 (44)) was found to be as successful as the design with the used tool “Stealth™ RNAi“ of the “BLOCK-iT™ RNAi Designer” from Invitrogen.

Although all shRNAs were designed specifically for their respective target, not all of them were successfully downregulating their corresponding protein. It remains unclear, why a particular sequence worked as shRNA, whereas others failed to do so. Some of the used and previously published criteria to increase the success of the shRNA design are mentioned in the *Methods section*. For each candidate protein, several shRNA plasmids had to be generated and tested to identify at least one that was working. Interestingly, also the sequences of the shRBM4 plasmids #343 and 344 which were taken from a publication where they were introduced as 2'-O-methyl oligoribonucleotides into HeLa cells did not downregulate the respective protein. As the same sequence was used, it may also make a difference whether a plasmid or an oligo is used for transfection and protein knockdown.

The presence of 2'-O-methylation protects the oligos against intracellular nuclease digestion and increases their stability against alkaline hydrolysis (Sproat, B. S. et al. 1989). The 2'-O-alkylation also increases the affinity for the target, due to a decrease of non-specific binding because of optimised thermodynamics and reduced steric

hindrance (Iribarren, A. M. et al. 1990). Therefore, oligonucleotides might be more successful in downregulation of their target protein.

Also the secondary structures of the target mRNA is important for the successful downregulation via siRNA. The 3-dimensional structure of the target influences its accessibility for the siRNA. So the successful binding of the siRNA to its target is crucial and obligatory for the protein knockdown.

Furthermore, I observed that impurities of the plasmid DNA interfere with a successful transfection (data not shown and (Zeitelhofer, M. et al. 2008)). Maybe, because they encumber the formation of lipid vesicles around the DNA at all or they just hinder the formation of vesicles of the right size which are taken up by the cell.

Variability of the cotransfection was also observed (see **Figure 3-13**). In theory, two or more plasmids can be taken up by a single cell during the transfection. I tried to cotransfect conventional HeLa cells using a plasmid with a TCR- $\beta$  construct and an additional shRNA plasmid, and observed that cotransfections did not always work. As all shRNA plasmids had an EGFP gene, successful transfections of the shRNA plasmids were monitored by microscopy and Western blotting. The semiquantitative PCRs analysed via agarose gel electrophoreses revealed that the TCR- $\beta$  construct was not always present in the cells. But as only 100 ng of TCR- $\beta$  DNA (Dr. Corinna Giorgi - personal correspondence) compared to 7.5  $\mu$ g of shRNA plasmid DNA were transfected, it is quite obvious that the cotransfection of the two plasmids often did not work due to the present DNA amounts. More than 100 ng of the TCR- $\beta$  DNA should not be transfected or otherwise the NMD process could be overloaded, as it is just an “emergency mechanism” to get rid of incorrect RNAs.

Polyethylenimine (PEI) (see *Material section*) was also tested as an alternative to the FuGENE<sup>®</sup> HD Transfection Reagent (Roche) for the transfection of HeLa cells. The cationic polymer PEI was chosen, because it is gentle and efficient for gene transfer into a variety of cell types, especially HeLa cells ((Boussif, O. et al. 1995) and <http://www.sigmaldrich.com>). A PEI:DNA ratio of 3:1 [ $\mu$ l: $\mu$ g] was used. The PEI was found to have a cytotoxic activity on the cells which were dying shortly after transfection. This observed circumstance concerning cytotoxicity of PEI was confirmed by a literature search (Boussif, O. et al. 1995; Neu, M. et al. 2005; Hunter, A. C. 2006).

## 2. DOWNREGULATION AND DETECTION OF SELECTED PROTEIN CANDIDATES

The protein candidates for the NMD assay and their knockdown with the respective shRNAs were detected via Western Blots and immunocytochemistry. Specificity of the observed protein expression and localisation patterns was verified via literature search wherever possible. The outcome of the experiments, concerning the verifiability of the expression and/or depletion of a protein and the subcellular localisation of the protein candidates, is discussed below.

### 2.1. DDX5 detection with immunocytochemistry

Whereas DDX5 downregulation was confirmed via Western Blot, it was not visible in the performed immunostainings (**Figure 3-4C**), although the same antibody was used as for the Western Blot analysis. It is possible and often encountered that antibodies working well on Western Blots do not work for immunocytochemistry and vice versa (Harlow E. and Lane D.; *Antibodies: A Laboratory Manual*; Cold Spring Harbor Laboratory; Cold Spring Harbor; 1988 and Harlow E. and Lane D.; *Using Antibodies: A Laboratory Manual*; Cold Spring Harbor Laboratory; Cold Spring Harbor; 1999). Different explanations for this are possible.

Maybe this is due to the reduced accessibility of the epitope for the antibody in fixed specimens on coverslips. Therefore, the antibodies can not find their target as easily and quickly as on a Western Blot where the denatured proteins are presented on a membrane.

Also the fixation method has an influence of the later accessibility of the epitopes. The chemicals used for fixation (4% PFA) may interfere with the accessibility or integrity of the epitopes.

Another explanation could be that the used antibody is not specific therefore yielding ambiguous staining patterns. The members of the DEAD-box (DDX) family are highly conserved (e.g. (Luking, A. et al. 1998; Fuller-Pace, F. V. 2006; Linder, P. 2006)). Thus, it is possible that the used, particular antibody is also recognizing other members of this family. In addition to DDX5, the DDX5 antibody also recognises a second

protein band on the Western Blot (data not shown). This might be either DDX3 or DDX17, which are highly related to DDX5 (Luking, A. et al. 1998; Abdelhaleem, M. 2005; Barbosa-Morais, N. L. et al. 2006; Fuller-Pace, F. V. 2006). The latter two RNA helicases share 90% amino acid identity across the conserved core (Ogilvie, V. C. et al. 2003) and exist as a heterodimer in the cell (Lamm, G. M. et al. 1996). Due to these facts, the used antibody can maybe not distinguish between these two or respectively three proteins.

In summary, DDX5 was clearly reduced on the Western Blot, according to the band of the right molecular weight, but the downregulation of the protein was maybe not visible in the immunostaining, because the antibody did not only recognise DDX5 but possibly also DDX17 and/or DDX3.

## **2.2. U5-116 kDa detection with immunocytochemistry**

Only one paper reported the subcellular localisation of U5-116 kDa in HeLa cells, showing a staining pattern with a predominantly nuclear localisation of U5-116 kDa, where the nucleoli and the cytoplasm were largely unstained (Fabrizio, P. et al. 1997).

In contrast, the performed immunostainings for this thesis displayed a slightly aberrant staining pattern where the protein is equally distributed in the cell, with a slightly higher concentration in the nucleus (**Figure 3-5C**). Upon downregulation, U5-116 kDa seemed to be reduced in the cell periphery but unchanged in the nucleus. Interestingly, the used antibody is the same as in Fabrizio et al. (1997).

U5-116 kDa shows a high degree of homology with the ribosomal elongation factor EF-2 (Fabrizio, P. et al. 1997). Thus, a possible explanation for the obtained staining pattern in this thesis is that the antibody recognises both proteins - U5-116 kDa and EF-2. But the specificity of the antibody was already confirmed in the mentioned publication (Fabrizio, P. et al. 1997)

EF-2 has a molecular weight of approximately 95 kDa on a Western Blot (e.g. (Carroll, M. et al. 2004; Devost, D. et al. 2005)). A band of the size for EF-2 was visible after incubation with the U5-116 kDa antibody (data not shown). But it is also possible that the observed bands on the Western Blots are just degradation products. The additional band is not present on the Western Blots made from HeLa lysates by

Fabrizio et al. with the same antibody (Fabrizio, P. et al. 1997). Therefore, I conclude that the bands on my Western Blots are rather degradation products than isoforms or related proteins.

### 2.3. RBMX and RBM4 detection on Western Blots

RBMX and in some experiments RBM4 were not detectable via Western Blot. It is already known that both proteins mainly localise in the nucleus (Elliott, D. J. 2004; Markus, M. A. and Morris, B. J. 2006).

RBMX (~43 kDa) could not be detected in conventional HeLa cells via Western Blot by the used commercial antibody (see *Material section*), even if high protein amounts were tested (**Figure 3-6A**). The protein candidate could also not be detected in the TCR-  $\beta$  and  $\beta$ -Globin HeLa cell lines (see **Figure 3-14**), but the antibody recognised a double band of a different size (<35 kDa) (see **Figure 3-14B** and 2.2.1 in the *Results section*). Therefore, the shRBMX plasmids could not be tested for their downregulation of RBMX in HeLa cells by Western blotting.

Interestingly the same antibody used for Western Blots gave a reproducible staining pattern for RBMX in the immunocytochemistry. This indicates that the RBMX antibody did not work for Western Blots but for immunocytochemistry. In this case, as well as for the DDX5 antibody, the used antibodies did not work equally well for Western Blot and immunofluorescence. In contrast, the DDX5 antibody seemed to work for Western blotting but not for immunostaining.

The used RBMX antibody recognised a protein double band (< 35 kDa) on the Western Blot from the stable HeLa cell lines and gave a reproducible pattern in the immunostaining of conventional HeLa cells. One explanation of these findings is that different isoforms of RBMX exist which are recognised by the commercial antibody. This would confirm the specificity of the used RBMX antibody.

This assumption is attenuated by the fact that no RBMX signal was detected on Western Blots made from conventional HeLa cells. Thus, if there are different RBMX isoforms, which lead to a specific immunostaining pattern of conventional HeLa cells, their signal should also be detectable via Western Blot. This, however, is not the case.

Another explanation is that RBMX may be very instable when isolated. If the protein was then also expressed at a higher level in the stable compared to the conventional HeLa cells, this could explain the signal (< 35 kDa) on the Western Blot from the stable cell lines (**Figure 3-14**). This would also illustrate why RBMX is still detectable by immunofluorescence, under the assumption that RBMX is not degraded or altered upon fixation.

If the staining pattern for RBMX was specific, it indicated that most RBMX protein was concentrated in the nuclei and just a minor portion of the protein was present in the cell periphery. This could confirm that the RBMX concentration in the cell lysate from the cytoplasm was simply too low for detection by Western Blot, because the buffer used to lyse the conventional HeLa cells in this diploma project was not strong enough to break up the nuclei as well.

This assumption was strengthened by the protein isolations from the stable HeLa cell lines (**Figure 3-14**) which were performed with Trizol<sup>®</sup> Reagent that is potent enough to break up the nuclei. Nevertheless, the protein was still not detectable on the Western Blot. This indicates that the RBMX protein is not or just at a minor level expressed in HeLa cells, which can not be confirmed via literature, because nothing has been published about the expression of RBMX in HeLa cells or different tissues yet. There is just one publication ascertaining that RBMX is ubiquitously expressed in humans (Lingenfelter, P. A. et al. 2001). On the Western Blots of the stable HeLa cells, a double band <35 kDa was recognised by the used antibody. These bands can again represent RBMX isoforms.

Another possible explanation is that as the RBMX protein is a member of the RNA-binding motif (RBM) family and these proteins have highly conserved domains. So the used RBMX antibody is maybe not selective enough and recognises also other protein family members.

In some experiments, RBM4 was also not detectable via Western Blot in HeLa cells (**Figure 3-7B**). A literature search revealed that RBM4 is mainly localised in the nucleus in a cell (Markus, M. A. and Morris, B. J. 2006). The used lysis buffer did not break up the nuclei. Therefore, the protein concentration in the cytoplasm might simply be too low to detect it via Western Blot in some cases, depending on distinct factors such as stress, expression level and distribution of RBM4. This hypothesis was

confirmed by experiments with proteins which were isolated from stable HeLa cell lines (**Figure 3-14**) using Trizol<sup>®</sup> Reagent that broke up nuclei. In this experiment, RBM4 signals were detectable on the Western Blots.

### **3. OPTIMISATION OF RNA ISOLATION & PCR SETUPS**

The used RNA isolation kits and procedures (see **Figure 3-10**) had a significant impact on the obtained quality and quantity of RNA. Furthermore, this was also a crucial factor for the reproducibility of the semiquantitative PCR for the respective cDNA.

Variability in the amplification of the TCR- $\beta$  pre-mRNA was a significant problem at the beginning of this diploma thesis (**Figure 3-9A**). Bioinformatical analyses revealed that the TCR- $\beta$  pre-mRNA primer may actually form secondary structures. So optimisation of the semiquantitative PCR of the TCR- $\beta$  pre-mRNA construct was necessary to permit the PCR product. Finally, an increase of the annealing temperature to 60°C restored the successful amplification of the TCR- $\beta$  pre-mRNA product (**Figure 3-9B**), with the exception of the eIF4AIII depleted samples (#291) in this particular experiment. Maybe the #291 samples were degraded or contaminated with a PCR inhibitor during the troubleshooting, as the tested #291 samples in **Figure 3-9A** and **B** were the same. This can be possible, because the wt and PTC TCR- $\beta$  samples, cotransfected with the same shRNA plasmid (#291 in this case) were always treated in parallel. So contaminations could be spread between these two samples.

Finally, 60°C annealing temperature for the TCR- $\beta$  pre-mRNA primer were stringent enough to reduce secondary structures and still allowed annealing of the primer to the cDNA. Therefore, 60°C annealing temperature enabled successful amplification of the TCR- $\beta$  pre-mRNA product.

The reverse transcription PCR was also optimised for the NMD assay to increase the sensitivity of the analysis (**Figure 3-12** and **Table 3-1**). Therefore, RT-PCR with Random Primers and the specific TCR- $\beta$  reverse primer, to enrich the target cDNA, were compared. In addition, tubulin was tested as an internal PCR standard for

normalisation of the PCR results.

The RT-PCR using specific primers lead to an enrichment of the target cDNA, but interestingly tubulin could still be amplified from the cDNA after the specific TCR- $\beta$  reverse primer reaction. Two explanations are possible for the successful amplification of tubulin. First, the specific TCR- $\beta$  reverse primer binds to the RNA and the RNA is reverse transcribed. So the RNA coding for tubulin is also amplified, as it is on the same RNA to which the primer bound. Reverse transcription is made in one direction from the primer to the end of the RNA, thereby also amplifying the tubulin sequence. Secondly, it is also possible that the tubulin primers are not specific and by chance create a PCR fragment of the expected size.

## **4. COMPARISON OF CONVENTIONAL & STABLE HELA CELLS**

Since variability of cotransfection was observed in conventional HeLa cells, HeLa cell lines with stable NMD reporter constructs were used for the real-time PCR experiments. The shRNA plasmids of the candidate proteins working in conventional HeLa cells were tested for their efficiency of protein knockdown in the stable cell lines. Thereby, the following differences between conventional and stable HeLa cell lines were observed.

In general, the observed transfection efficiencies with stable HeLa cell lines were much lower than with conventional HeLa cells. Although transfections were exactly performed the same way in all HeLa cell lines, transfection efficiencies, even using the same maxiprep DNA, were lower in the stable cell lines. In addition, the obtained transfection efficiencies were in general lower for the wt  $\beta$ -Globin cells compared to the NS39  $\beta$ -Globin cells (data not shown). We observed that the stable cell lines were growing faster than conventional HeLa cells. So less stable HeLa cells than conventional cells were plated for transfection, to have a similar confluence of all HeLa cells, when they were transfected.

It was also surprising that plasmids working in conventional HeLa cells, downregulated the respective protein less or they did not even downregulate the protein candidate at all



in the stable cell lines (**Figure 3-15** and **3-16** and data not shown). This was very astonishing, as all cell lines were HeLa cells with just one difference: some expressed a stable construct and the others not.

These findings indicate that there are differences in the expression pattern and also transfection of conventional and stable HeLa cells. As HeLa cells are cancer cell lines, even distinct conventional HeLa cell batches might have different genetic backgrounds due to spontaneous mutations. This might explain their different features and reactions to the introduction of transgenes.

## 5. NEOMYCIN SELECTION

Since the shRNA plasmids working in conventional HeLa cells (**Figure 3-2 – 3-5**) did not sufficiently downregulate their respective protein in the stable HeLa cell lines even after 5 days (**Figure 3-15** and **3-16** and data not shown), neomycin selection was performed to enrich for successfully transfected cells (see *2.3.3 Neomycin selection to enrich transfected cells* in the *Results* section).

It was surprising that even 7 days of neomycin selection did not sufficiently knockdown the protein candidates (**Figure 3-17** and data not shown). Unfortunately, only the downregulation of Btz worked in the wt  $\beta$ -Globin cell line. In the NS39  $\beta$ -Globin cell line, Btz, DDX5 and U5-116 kDa were downregulated, but still to a minor extent than observed in conventional HeLa cells.

The antibiotics neomycin and geneticin (G418) are usually really effective tools for selection (e.g. (Muhlemann, O. et al. 2001)). Although selection seemed to work according to the taken pictures of the cell samples (**Figure 3-17**), not all protein candidates were depleted in both cell lines or were reduced at all. This finding is also discussed in *4 Comparison of conventional & stable HeLa cells* in this section.

Interestingly, NPM1 was even upregulated after neomycin selection compared to the control (data not shown), when tested via Western Blot. Neomycin as well as geneticin block protein synthesis and therefore also interfere with cell growth.

The phenomenon of translational upregulation upon introduction of miRNAs in growth-arrested cells was recently published (Vasudevan, S. et al. 2007). As there is no structural differences in siRNAs and miRNAs (Rana, T. M. 2007), they could possibly both mediate translational activation as well.

## 6. PRELIMINARY NMD ASSAY RESULTS

Real-time PCR was then performed for the samples where the respective protein was sufficiently downregulated after neomycin selection (**Figure 3-20**). These samples were the shBtz (#283) and the empty pSUPERIOR sample (#100) for the wt  $\beta$ -Globin cell line as well as the shBtz (#283), the shDDX5 (#339), the shU5-116 kDa (#342) and the empty pSUPERIOR sample (#100) for the NS39  $\beta$ -Globin cell line. The PCR results were normalised to the  $\beta$ -globin levels in untreated controls. The reduction of U5-116 kDa protein expression had nearly the same effect as the depletion of Btz protein expression with a  $\sim 10$ fold increase of NS39  $\beta$ -globin expression, although U5-116 kDa was twice as highly expressed as Btz. This preliminary data indicates that U5-116 kDa probably plays an important role in NMD if it has such an impressive effect on the  $\beta$ -globin construct amount compared to Btz.

It was surprising that the fold increase in  $\beta$ -globin expression was nearly the same for the wt and the NS39 cell line, if Btz had been knocked down, because the downregulation efficiency varied from 46.12% residual protein expression in the wt to 16.74% residual protein expression in the NS39  $\beta$ -Globin cell line. I would have expected that the fold increase in expression is higher than  $\sim 10$  in the NS39 cells, if you take away Btz protein to a higher extent and thereby impair NMD. This in turn should lead to an accumulation of aberrant NS39  $\beta$ -globin mRNA.

The DDX5 protein seemed to have the strongest effect on NMD in the first, preliminary real-time experiment performed in this thesis. Even a minor depletion of DDX5 by 15.01% resulted in  $> 40$ fold increase of NS39  $\beta$ -globin. In DDX5 depleted NS39 cells,  $\beta$ -globin accumulates and is no longer degraded. This indicates that NMD is impaired as well as that DDX5 possibly plays a role in NMD. Unfortunately, the knockdown of DDX5 with plasmid #339 did not work in the wt  $\beta$ -Globin cell line. This will be an essential control to perform. Therefore, no firm conclusion can yet be drawn from this

preliminary real-time data about the role of DDX5 in the NMD process.

Interestingly, also the transfection with the empty pSUPERIOR.neo+gfp vector (#100), which served as negative control, resulted in a ~ 6fold increase in the wt and a ~ 3fold increase of  $\beta$ -globin expression in the NS39  $\beta$ -Globin HeLa cells. Literature search for evaluation of the experiments showed that some aminoglycoside antibiotics can also interfere with and block NMD to a certain extent under not fully understood conditions (reviewed in (Holbrook, J. A. et al. 2004; Behm-Ansmant, I., Kashima, I. et al. 2007)). Therefore, it might be better to normalise the real-time PCR results to the samples transfected with the empty pSUPERIOR.neo+gfp vector (#100) instead of the untreated samples (UT). As all samples were treated the same with geneticin for antibiotic selection, the normalisation of the results to the empty pSUPERIOR.neo+gfp vector samples statistically eliminates the possible inhibiting effect of the antibiotic selection on NMD and visualises the specific effect of the tested candidate. Normalised to the pSUPERIOR.neo+gfp vector sample (#100), the treatment of the wt  $\beta$ -Globin cells with the shBtz led to a 1.42fold increase of wt  $\beta$ -globin expression. In NS39  $\beta$ -Globin cells, the depletion of Btz results in 3.15x increase, the reduction of DDX5 in a 12.88fold increase and the depletion of U5-116 kDa in a 2.99fold increase of NS39  $\beta$ -globin level normalised to the negative control sample (#100). Upon this normalisation, the different reductions of Btz in the wt and the NS39  $\beta$ -Globin cell line would negatively correlate with the change in expression of  $\beta$ -globin, which was not the case when the samples were normalised to the untreated control.

## 7. CONCLUSIONS & PROSPECTS

The goal was to establish the NMD assay first in HeLa cells, because this was fast and experimentally easy to set up. In a second step, which would follow now this diploma thesis, the assay can then be modified and adapted for primary rat hippocampal neurons. Therefore, the shRNAs were designed to target human and rat sequences whenever possible.

As HeLa cells are cancer cells which have been cultivated for a long time, the use of

primary, non-mutated rat hippocampal neurons might be even more physiological for the investigation of NMD.

All designed shRNA plasmids for the NMD assay and also other projects in the laboratory were tested by Dr. Daniela Karra and myself in embryonic day 17 rat hippocampal neurons (data not shown and **Figure 3-21**). **Figure 3-21** shows successful downregulation of DDX6 (plasmid #300) and Kif3A (plasmid #323). Unfortunately, none of the shRNA plasmids for candidates of the NMD assay depleted the respective protein.

Interestingly, the NPM1 protein, which was a promising candidate in HeLa cells, was not even detectable via Western Blots made from neuronal lysates after nucleofection, although the used antibody also recognises rat NPM1 (according to the manufacturer). NPM1 is a predominantly nucleolar protein (Feuerstein, N. et al. 1987; Schmidt-Zachmann, M. S. et al. 1987), also in neurons (Kalita, K. et al. 2008). Even the use of a more concentrated lysis buffer, e.g. the 2x Laemmli Buffer, which usually lyses the nuclei, did not result in NPM1 signals on the blots. This might indicate that it is just expressed at a very low level in E17 rat hippocampal neurons. The assumption can not be confirmed via literature, because nothing is published yet about NPM1 expression in E17 rat hippocampal or young neurons.

So, unfortunately none of the shRNA plasmids of the candidates for the NMD assay could downregulate its corresponding protein in rat hippocampal neurons. As the shRNA sequences were designed to recognise human and rat protein isoforms, it is unclear why some worked in HeLa cells but not in rat neurons. Different facts and assumptions might explain this finding.

In general, it is a demanding issue to reach transfection efficiencies in neurons which are high enough to visualise genetic alterations via Western blotting. So the obtained transfection rates in these experiments, which were monitored via EGFP expression, were maybe too low to detect downregulation on the Western Blot.

HeLa cells are differentiated, genetically instable cancer cells, whereas the used E17 rat hippocampal neurons are undifferentiated, primary and non-mutated cells. This could also influence the effect of a given shRNA plasmid in these two cell types. However, we do not have detailed knowledge about the pathway(s) leading to the uptake of the DNA into the nucleus. So we can only speculate that there are some differences, like different required factors or distinct pathways that influence the uptake, intracellular

processing and effect of the shRNA plasmids.

In general, neurons are more sensitive to any kind of stress than other cell types. This is also a reason why high transfection efficiencies are difficult to reach in neurons. For protection and maintenance of their intracellular composition, neurons may synthesise higher concentrations or a different subset of nucleases compared to HeLa cells. Therefore, in some cases introduced DNA would simply be degraded, before it can mediate its action.

So in order to start the NMD assay also in hippocampal neurons, further shRNA plasmids have to be designed and tested for their downregulation of the protein candidates in neurons.

## **8. ARRIVAL AT HYPOTHESIS**

Btz as an essential component of the EJC plays a central and crucial role in NMD (Palacios, I. M. et al. 2004) and is upregulated in most cancer cell lines (e.g. (Degot, S. et al. 2002)). These are interesting facts which might indicate that cancer cells try to overcome its derailing metabolism and the production of aberrant transcripts by upregulation of decay factors like Btz. This might bring transient help to clean the cell from abnormal or harmful transcripts and proteins. But at a certain point, this rescue attempt fails. The decay pathways are then overloaded with aberrant substrates and can't get rid of it as fast as required anymore. Harmful or non-functional proteins accumulate and mediate their action which further destabilises the cell and interferes or blocks important processes. This might then results in the cell's death, if essential reactions necessary for survival are encumbered.

But one principal question remains: Why do the decay pathways fail to clear up the cell before the mutations causing the production of the aberrant transcripts are repaired? Of course, this is clearly depending on the severity and quantity of mutations in the cell's genome. But let me speculate about another essential factor which might influence the time course of the cell's decline. Phosphorylation, for example, like other modifications of executive factors in the decay pathways seems to be crucial for the initiation and successful completion of the degradation, especially in NMD (e.g. (Chang, Y. F. et al. 2007)). Modifications on molecules are also necessary to elicit or upregulate the

expression of the executive factors in the beginning. These regulatory modifications require a sufficient supply of the cell with micronutrients. The uptake and especially the distribution of micronutrients are for sure impaired in a cell, where normal metabolism and transport is overloaded and blocked by non-functional transcripts and proteins. The depletion of micronutrient storages and the restriction of the supply with nutrients might be an important factor for the collapse of the cell's decay and metabolism leading to cell death in the end. This interesting model explaining the role of decay pathways like NMD in diseases (e.g. cancer) is supported by a recently published paper. In this publication, the MAPK pathway is linked to the expression and function of essential decay factors in fibroblast-like cells (Ha, J. E. et al. 2008). After stimulation of the cells with granulocyte-macrophage colony-stimulating factor (GM-CSF), the mitogen-activated protein kinase (MAPK) pathway is activated and especially the subfamilies p38 and JNK are dramatically phosphorylated. These events lead to the upregulation of Btz via transcriptional and post-translational control. Finally, Btz initiates or upregulates the expression of anti-apoptotic factors promoting cell survival. Thereby, this publication also points out the importance and essential functions of modification, especially phosphorylation, of signal and effector molecules. To maintain and support these cellular processes a sufficient supply with micronutrients is obligatory.

Another recently published minireview discusses the role of the EJC in translational activation and repression (Le Hir, H. et al. 2008), thereby also underscoring the important role of phosphorylation in these signalling pathways.

However, RNA decay is for sure a very important and central issue in cells. It is a quality control for its metabolism and prevents the development of many diseases. So it is a rewarding research topic for the future to investigate the interactions and key players in RNA decay, especially in NMD, in detail.

## ACKNOWLEDGEMENT

First of all, I want to thank Prof. Dr. Michael Kiebler for the opportunity to do my diploma thesis in his laboratory. I am also very thankful for his supervision, support, advice and for his critical and constructive comments on the manuscript.

Especially, I want to thank Dr. Daniela Karra, my supervisor at the bench, for providing me with an interesting diploma thesis topic and introducing me further into the world of science. I was able to learn a lot from and through her. Moreover, I am thankful to her for the proofreading and comments on the manuscript.

I am also grateful for the support and help of the amazing team and people in the laboratory. They were always open for my needs, my wishes and a discussion and contributed to a lot of funny as well as exciting hours in the laboratory.

Furthermore, I appreciate a lot the mentoring and advice from Dr. Ralf Dahm and Dr. Paolo Macchi which they gave to me, whenever I longed for it.

Last but not least, I want to thank my family, especially my parents, and friends for their love and support.

## APPENDIX I: ZUSAMMENFASSUNG

„Nonsense-mediated mRNA decay“ (NMD) ist ein Mechanismus zur Regulierung der Genexpression auf post-transkriptioneller Ebene in Eukaryonten. Neben der Quantitätsdient NMD auch der Qualitätskontrolle von Transkripten. Letztere Funktion umfasst die Beseitigung fehlerhafter RNAs mit einem verfrühten Stop-Codon, auch „Premature termination codon“ (PTC) genannt. Andernfalls würden diese RNAs zur Bildung verkürzter Proteine mit möglicherweise für die Zelle gefährlichen Funktionen führen, wie es bei Krankheiten, wie z. B. Krebs, oft der Fall ist.

In meiner Diplomarbeit untersuchte ich ausgewählte Proteine näher auf ihre Rolle in NMD. Zu diesem Zweck etablierte ich einen funktionellen Assay in verschiedenen HeLa-Zelllinien. NMD ist nicht voll funktionsfähig, wenn bestimmte NMD-Komponenten – wie z. B. Barentsz (Btz) oder eIF4AIII – fehlen. Es kommt zur Anhäufung fehlerhafter, PTC-enhaltender Transkripte, da jene nicht länger durch NMD abgebaut werden. Deshalb dienten diese beiden Proteine als Positivkontrollen für die Etablierung des Assays. Es galt im Folgenden, den Einfluss von fünf potentiellen Protein-Protein-Interaktoren des RNA-Bindeproteins Btz auf NMD zu testen: Nucleophosmin 1 (NPM1), DEAD-Box-Polypeptide 5 (DDX5), U5-116 kDa, RNA-Binding-Motif-Protein - X-linked (RBMX) und RNA-Binding-Motif-Protein 4 (RBM4). Ich stellte gegen diese Proteine gerichtete „Short hairpin RNA (shRNA)“-Plasmide her und testete sie. Danach verminderte ich die Expressionslevels der entsprechenden Proteine in HeLa-Zellen mittels ihrer shRNA-Plasmide und überprüfte, ob dies zur Akkumulierung von PTC-enhaltenden NMD-Reporter-Konstrukten führt, wie im Fall des Btz-Knockdowns. Hierfür wurden die Expressionslevels und somit der Abbau von eigens eingebrachten T-Zellrezeptor- $\beta$  (TCR- $\beta$ ) - und  $\beta$ -Globin-NMD-Reporter-Konstrukten mit und ohne PTC über semiquantitative und Real-time-PCR verglichen. Zusätzlich wurde eine Neomycin/G418-Selektion durchgeführt, um erfolgreich transfizierte Zellen anzureichern. Die ersten Real-time-PCR-Daten lassen auf eine wichtige Rolle von DDX5 und U5-116 kDa in NMD schließen, da ihre Reduktion zur Anhäufung PTC-enhaltender Transkripte führte. Für NPM1, RBMX und RBM4 konnten noch keine Aussagen getroffen werden, weil die entsprechenden shRNA-Plasmide in den verwendeten stabilen HeLa-Zelllinien keine Reduktion



entsprechender Proteinslevels bewirkten. Weitere Experimente zur Untersuchung dieser Proteine sind daher notwendig.

Zusammenfassend lässt sich festhalten, dass es mir in meiner Diplomarbeit gelungen ist, mit den potentiellen Btz-Interaktoren DDX5 und U5-116 kDa zwei weitere Proteine zu identifizieren, die eine Rolle in NMD spielen.

## APPENDIX II: REFERENCES

- Abdelhaleem, M. (2005). "RNA helicases: regulators of differentiation." Clin Biochem **38**(6): 499-503.
- Achsel, T., Ahrens, K., Brahms, H., Teigelkamp, S. and Luhrmann, R. (1998). "The human U5-220kD protein (hPrp8) forms a stable RNA-free complex with several U5-specific proteins, including an RNA unwindase, a homologue of ribosomal elongation factor EF-2, and a novel WD-40 protein." Mol Cell Biol **18**(11): 6756-66.
- Albertini, V., Jain, A., Vignati, S., Napoli, S., Rinaldi, A., Kwee, I., Nur-e-Alam, M., Bergant, J., Bertoni, F., Carbone, G. M., Rohr, J. and Catapano, C. V. (2006). "Novel GC-rich DNA-binding compound produced by a genetically engineered mutant of the mithramycin producer *Streptomyces argillaceus* exhibits improved transcriptional repressor activity: implications for cancer therapy." Nucleic Acids Res **34**(6): 1721-34.
- Amrani, N., Ganesan, R., Kervestin, S., Mangus, D. A., Ghosh, S. and Jacobson, A. (2004). "A faux 3'-UTR promotes aberrant termination and triggers nonsense-mediated mRNA decay." Nature **432**(7013): 112-8.
- Anders, K. R., Grimson, A. and Anderson, P. (2003). "SMG-5, required for *C.elegans* nonsense-mediated mRNA decay, associates with SMG-2 and protein phosphatase 2A." EMBO J **22**(3): 641-50.
- Azzalin, C. M. and Lingner, J. (2006). "The double life of UPF1 in RNA and DNA stability pathways." Cell Cycle **5**(14): 1496-8.
- Ballut, L., Marchadier, B., Baguet, A., Tomasetto, C., Seraphin, B. and Le Hir, H. (2005). "The exon junction core complex is locked onto RNA by inhibition of eIF4AIII ATPase activity." Nat Struct Mol Biol **12**(10): 861-9.
- Barbosa-Morais, N. L., Carmo-Fonseca, M. and Aparicio, S. (2006). "Systematic genome-wide annotation of spliceosomal proteins reveals differential gene family expansion." Genome Res **16**(1): 66-77.
- Behm-Ansmant, I., Gatfield, D., Rehwinkel, J., Hilgers, V. and Izaurralde, E. (2007). "A conserved role for cytoplasmic poly(A)-binding protein 1 (PABPC1) in nonsense-mediated mRNA decay." EMBO J **26**(6): 1591-601.

- Behm-Ansmant, I., Kashima, I., Rehwinkel, J., Sauliere, J., Wittkopp, N. and Izaurralde, E. (2007). "mRNA quality control: an ancient machinery recognizes and degrades mRNAs with nonsense codons." FEBS Lett **581**(15): 2845-53.
- Behrens, S. E. and Luhrmann, R. (1991). "Immunoaffinity purification of a [U4/U6.U5] tri-snRNP from human cells." Genes Dev **5**(8): 1439-52.
- Blow, N. (2007). "PCR's next frontier." Nat Methods **4**(10): 869-75
- Bocker, T., Bittinger, A., Wieland, W., Buettner, R., Fauser, G., Hofstaedter, F. and Ruschoff, J. (1995). "In vitro and ex vivo expression of nucleolar proteins B23 and p120 in benign and malignant epithelial lesions of the prostate." Mod Pathol **8**(3): 226-31.
- Bond, A. T., Mangus, D. A., He, F. and Jacobson, A. (2001). "Absence of Dbp2p alters both nonsense-mediated mRNA decay and rRNA processing." Mol Cell Biol **21**(21): 7366-79.
- Bono, F., Ebert, J., Lorentzen, E. and Conti, E. (2006). "The crystal structure of the exon junction complex reveals how it maintains a stable grip on mRNA." Cell **126**(4): 713-25.
- Borer, R. A., Lehner, C. F., Eppenberger, H. M. and Nigg, E. A. (1989). "Major nucleolar proteins shuttle between nucleus and cytoplasm." Cell **56**(3): 379-90.
- Boussif, O., Lezoualc'h, F., Zanta, M. A., Mergny, M. D., Scherman, D., Demeneix, B. and Behr, J. P. (1995). "A versatile vector for gene and oligonucleotide transfer into cells in culture and in vivo: polyethylenimine." Proc Natl Acad Sci U S A **92**(16): 7297-301.
- Brocke, K. S., Neu-Yilik, G., Gehring, N. H., Hentze, M. W. and Kulozik, A. E. (2002). "The human intronless melanocortin 4-receptor gene is NMD insensitive." Hum Mol Genet **11**(3): 331-5.
- Brummelkamp, T. R., Bernards, R. and Agami, R. (2002). "Stable suppression of tumorigenicity by virus-mediated RNA interference." Cancer Cell **2**(3): 243-7.
- Brummelkamp, T. R., Bernards, R. and Agami, R. (2002). "A system for stable expression of short interfering RNAs in mammalian cells." Science **296**(5567): 550-3.

- Carroll, M., Warren, O., Fan, X. and Sossin, W. S. (2004). "5-HT stimulates eEF2 dephosphorylation in a rapamycin-sensitive manner in *Aplysia* neurites." J Neurochem **90**(6): 1464-76.
- Carter, M. S., Doskow, J., Morris, P., Li, S., Nhim, R. P., Sandstedt, S. and Wilkinson, M. F. (1995). "A regulatory mechanism that detects premature nonsense codons in T-cell receptor transcripts in vivo is reversed by protein synthesis inhibitors in vitro." J Biol Chem **270**(48): 28995-9003.
- Carter, M. S., Li, S. and Wilkinson, M. F. (1996). "A splicing-dependent regulatory mechanism that detects translation signals." EMBO J **15**(21): 5965-75.
- Chan, W. K., Huang, L., Gudikote, J. P., Chang, Y. F., Imam, J. S., MacLean, J. A., 2nd and Wilkinson, M. F. (2007). "An alternative branch of the nonsense-mediated decay pathway." EMBO J **26**(7): 1820-30.
- Chang, Y. F., Imam, J. S. and Wilkinson, M. F. (2007). "The nonsense-mediated decay RNA surveillance pathway." Annu Rev Biochem **76**: 51-74.
- Chomczynski, P. and Sacchi, N. (1987). "Single-step method of RNA isolation by acid guanidinium thiocyanate-phenol-chloroform extraction." Anal Biochem **162**(1): 156-9.
- Chu, C. Y. and Rana, T. M. (2006). "Translation repression in human cells by microRNA-induced gene silencing requires RCK/p54." PLoS Biol **4**(7): e210.
- Cordell, J. L., Pulford, K. A., Bigerna, B., Roncador, G., Banham, A., Colombo, E., Pelicci, P. G., Mason, D. Y. and Falini, B. (1999). "Detection of normal and chimeric nucleophosmin in human cells." Blood **93**(2): 632-42.
- Degot, S., Le Hir, H., Alpy, F., Kedinger, V., Stoll, I., Wendling, C., Seraphin, B., Rio, M. C. and Tomasetto, C. (2004). "Association of the breast cancer protein MLN51 with the exon junction complex via its speckle localizer and RNA binding module." J Biol Chem **279**(32): 33702-15.
- Degot, S., Regnier, C. H., Wendling, C., Chenard, M. P., Rio, M. C. and Tomasetto, C. (2002). "Metastatic Lymph Node 51, a novel nucleo-cytoplasmic protein overexpressed in breast cancer." Oncogene **21**(28): 4422-34.

- Delbridge, M. L., Lingenfelter, P. A., Disteche, C. M. and Graves, J. A. (1999). "The candidate spermatogenesis gene RBMY has a homologue on the human X chromosome." *Nat Genet* **22**(3): 223-4.
- Devost, D., Girotti, M., Carrier, M. E., Russo, C. and Zingg, H. H. (2005). "Oxytocin induces dephosphorylation of eukaryotic elongation factor 2 in human myometrial cells." *Endocrinology* **146**(5): 2265-70.
- Dichmann, D. S., Fletcher, R. B. and Harland, R. M. (2008). "Expression cloning in *Xenopus* identifies RNA-binding proteins as regulators of embryogenesis and Rbmx as necessary for neural and muscle development." *Dev Dyn* **237**(7): 1755-66.
- Elliott, D. J. (2004). "The role of potential splicing factors including RBMY, RBMX, hnRNP-G-T and STAR proteins in spermatogenesis." *Int J Androl* **27**(6): 328-34.
- Fabrizio, P., Laggerbauer, B., Lauber, J., Lane, W. S. and Luhrmann, R. (1997). "An evolutionarily conserved U5 snRNP-specific protein is a GTP-binding factor closely related to the ribosomal translocase EF-2." *EMBO J* **16**(13): 4092-106.
- Ferraiuolo, M. A., Lee, C. S., Ler, L. W., Hsu, J. L., Costa-Mattioli, M., Luo, M. J., Reed, R. and Sonenberg, N. (2004). "A nuclear translation-like factor eIF4AIII is recruited to the mRNA during splicing and functions in nonsense-mediated decay." *Proc Natl Acad Sci U S A* **101**(12): 4118-23.
- Ferre, F. (1992). "Quantitative or semi-quantitative PCR: reality versus myth." *PCR Methods Appl* **2**(1): 1-9.
- Feuerstein, N. and Mond, J. J. (1987). "Identification of a prominent nuclear protein associated with proliferation of normal and malignant B cells." *J Immunol* **139**(6): 1818-22.
- Filipowicz, W. (2005). "RNAi: the nuts and bolts of the RISC machine." *Cell* **122**(1): 17-20.
- Fire, A., Xu, S., Montgomery, M. K., Kostas, S. A., Driver, S. E. and Mello, C. C. (1998). "Potent and specific genetic interference by double-stranded RNA in *Caenorhabditis elegans*." *Nature* **391**(6669): 806-11.
- Frischmeyer, P. A. and Dietz, H. C. (1999). "Nonsense-mediated mRNA decay in health and disease." *Hum Mol Genet* **8**(10): 1893-900.

- Fukuhara, N., Ebert, J., Unterholzner, L., Lindner, D., Izaurralde, E. and Conti, E. (2005). "SMG7 is a 14-3-3-like adaptor in the nonsense-mediated mRNA decay pathway." Mol Cell **17**(4): 537-47.
- Fuller-Pace, F. V. (2006). "DExD/H box RNA helicases: multifunctional proteins with important roles in transcriptional regulation." Nucleic Acids Res **34**(15): 4206-15.
- Gao, Q., Das, B., Sherman, F. and Maquat, L. E. (2005). "Cap-binding protein 1-mediated and eukaryotic translation initiation factor 4E-mediated pioneer rounds of translation in yeast." Proc Natl Acad Sci U S A **102**(12): 4258-63.
- Gehring, N. H., Kunz, J. B., Neu-Yilik, G., Breit, S., Viegas, M. H., Hentze, M. W. and Kulozik, A. E. (2005). "Exon-junction complex components specify distinct routes of nonsense-mediated mRNA decay with differential cofactor requirements." Mol Cell **20**(1): 65-75.
- Gehring, N. H., Neu-Yilik, G., Schell, T., Hentze, M. W. and Kulozik, A. E. (2003). "Y14 and hUpf3b form an NMD-activating complex." Mol Cell **11**(4): 939-49.
- Gjerset, R. A. (2006). "DNA damage, p14ARF, nucleophosmin (NPM/B23), and cancer." J Mol Histol **37**(5-7): 239-51.
- Grisendi, S., Bernardi, R., Rossi, M., Cheng, K., Khandker, L., Manova, K. and Pandolfi, P. P. (2005). "Role of nucleophosmin in embryonic development and tumorigenesis." Nature **437**(7055): 147-53.
- Ha, J. E., Choi, Y. E., Jang, J., Yoon, C. H., Kim, H. Y. and Bae, Y. S. (2008). "FLIP and MAPK play crucial roles in the MLN51-mediated hyperproliferation of fibroblast-like synoviocytes in the pathogenesis of rheumatoid arthritis." FEBS J **275**(14): 3546-55.
- He, F., Li, X., Spatrick, P., Casillo, R., Dong, S. and Jacobson, A. (2003). "Genome-wide analysis of mRNAs regulated by the nonsense-mediated and 5' to 3' mRNA decay pathways in yeast." Mol Cell **12**(6): 1439-52.
- He, L. and Hannon, G. J. (2004). "MicroRNAs: small RNAs with a big role in gene regulation." Nat Rev Genet **5**(7): 522-31.

- Hock, J., Weinmann, L., Ender, C., Rudel, S., Kremmer, E., Raabe, M., Urlaub, H. and Meister, G. (2007). "Proteomic and functional analysis of Argonaute-containing mRNA-protein complexes in human cells." EMBO Rep **8**(11): 1052-60.
- Holbrook, J. A., Neu-Yilik, G., Gehring, N. H., Kulozik, A. E. and Hentze, M. W. (2006). "Internal ribosome entry sequence-mediated translation initiation triggers nonsense-mediated decay." EMBO Rep **7**(7): 722-6.
- Holbrook, J. A., Neu-Yilik, G., Hentze, M. W. and Kulozik, A. E. (2004). "Nonsense-mediated decay approaches the clinic." Nat Genet **36**(8): 801-8.
- Hsieh, A. C., Bo, R., Manola, J., Vazquez, F., Bare, O., Khvorova, A., Scaringe, S. and Sellers, W. R. (2004). "A library of siRNA duplexes targeting the phosphoinositide 3-kinase pathway: determinants of gene silencing for use in cell-based screens." Nucleic Acids Res **32**(3): 893-901.
- Hunter, A. C. (2006). "Molecular hurdles in polyfectin design and mechanistic background to polycation induced cytotoxicity." Adv Drug Deliv Rev **58**(14): 1523-31.
- Hutvagner, G. and Zamore, P. D. (2002). "A microRNA in a multiple-turnover RNAi enzyme complex." Science **297**(5589): 2056-60.
- Iggo, R. D., Jamieson, D. J., MacNeill, S. A., Southgate, J., McPheat, J. and Lane, D. P. (1991). "p68 RNA helicase: identification of a nucleolar form and cloning of related genes containing a conserved intron in yeasts." Mol Cell Biol **11**(3): 1326-33.
- Iribarren, A. M., Sproat, B. S., Neuner, P., Sulston, I., Ryder, U. and Lamond, A. I. (1990). "2'-O-alkyl oligoribonucleotides as antisense probes." Proc Natl Acad Sci U S A **87**(19): 7747-51.
- Ishigaki, Y., Li, X., Serin, G. and Maquat, L. E. (2001). "Evidence for a pioneer round of mRNA translation: mRNAs subject to nonsense-mediated decay in mammalian cells are bound by CBP80 and CBP20." Cell **106**(5): 607-17.
- Isken, O., Kim, Y. K., Hosoda, N., Mayeur, G. L., Hershey, J. W. and Maquat, L. E. (2008). "Upf1 phosphorylation triggers translational repression during nonsense-mediated mRNA decay." Cell **133**(2): 314-27.

- Izaurrealde, E., Lewis, J., Gamberi, C., Jarmolowski, A., McGuigan, C. and Mattaj, I. W. (1995). "A cap-binding protein complex mediating U snRNA export." Nature **376**(6542): 709-12.
- Kahlina, K., Goren, I., Pfeilschifter, J. and Frank, S. (2004). "p68 DEAD box RNA helicase expression in keratinocytes. Regulation, nucleolar localization, and functional connection to proliferation and vascular endothelial growth factor gene expression." J Biol Chem **279**(43): 44872-82.
- Kalita, K., Makonchuk, D., Gomes, C., Zheng, J. J. and Hetman, M. (2008). "Inhibition of nucleolar transcription as a trigger for neuronal apoptosis." J Neurochem.
- Kashima, I., Yamashita, A., Izumi, N., Kataoka, N., Morishita, R., Hoshino, S., Ohno, M., Dreyfuss, G. and Ohno, S. (2006). "Binding of a novel SMG-1-Upf1-eRF1-eRF3 complex (SURF) to the exon junction complex triggers Upf1 phosphorylation and nonsense-mediated mRNA decay." Genes Dev **20**(3): 355-67.
- Keeling, K. M., Lanier, J., Du, M., Salas-Marco, J., Gao, L., Kaenjak-Angeletti, A. and Bedwell, D. M. (2004). "Leaky termination at premature stop codons antagonizes nonsense-mediated mRNA decay in *S. cerevisiae*." RNA **10**(4): 691-703.
- Kim, Y. K., Furic, L., Desgroseillers, L. and Maquat, L. E. (2005). "Mammalian Staufen1 recruits Upf1 to specific mRNA 3'UTRs so as to elicit mRNA decay." Cell **120**(2): 195-208.
- Kubista, M., Andrade, J. M., Bengtsson, M., Forootan, A., Jonak, J., Lind, K., Sindelka, R., Sjoback, R., Sjogreen, B., Strombom, L., Stahlberg, A. and Zoric, N. (2006). "The real-time polymerase chain reaction." Mol Aspects Med **27**(2-3): 95-125.
- Kumar, L. D. and Clarke, A. R. (2007). "Gene manipulation through the use of small interfering RNA (siRNA): from in vitro to in vivo applications." Adv Drug Deliv Rev **59**(2-3): 87-100.
- Laemmli, U. K. (1970). "Cleavage of structural proteins during the assembly of the head of bacteriophage T4." Nature **227**(5259): 680-5.
- Lamm, G. M., Nicol, S. M., Fuller-Pace, F. V. and Lamond, A. I. (1996). "p72: a human nuclear DEAD box protein highly related to p68." Nucleic Acids Res **24**(19): 3739-47.



- Le Hir, H., Gatfield, D., Izaurralde, E. and Moore, M. J. (2001). "The exon-exon junction complex provides a binding platform for factors involved in mRNA export and nonsense-mediated mRNA decay." EMBO J **20**(17): 4987-97.
- Le Hir, H. and Seraphin, B. (2008). "EJCs at the heart of translational control." Cell **133**(2): 213-6.
- Lejeune, F., Ishigaki, Y., Li, X. and Maquat, L. E. (2002). "The exon junction complex is detected on CBP80-bound but not eIF4E-bound mRNA in mammalian cells: dynamics of mRNP remodeling." EMBO J **21**(13): 3536-45.
- Li, Q., Imataka, H., Morino, S., Rogers, G. W., Jr., Richter-Cook, N. J., Merrick, W. C. and Sonenberg, N. (1999). "Eukaryotic translation initiation factor 4AIII (eIF4AIII) is functionally distinct from eIF4AI and eIF4AII." Mol Cell Biol **19**(11): 7336-46.
- Li, S., Leonard, D. and Wilkinson, M. F. (1997). "T cell receptor (TCR) mini-gene mRNA expression regulated by nonsense codons: a nuclear-associated translation-like mechanism." J Exp Med **185**(6): 985-92.
- Lin, J. C., Hsu, M. and Tarn, W. Y. (2007). "Cell stress modulates the function of splicing regulatory protein RBM4 in translation control." Proc Natl Acad Sci U S A **104**(7): 2235-40.
- Linder, P. (2006). "Dead-box proteins: a family affair--active and passive players in RNP-remodeling." Nucleic Acids Res **34**(15): 4168-80.
- Lingenfelter, P. A., Delbridge, M. L., Thomas, S., Hoekstra, H. E., Mitchell, M. J., Graves, J. A. and Disteche, C. M. (2001). "Expression and conservation of processed copies of the RBMX gene." Mamm Genome **12**(7): 538-45.
- Lippman, Z. and Martienssen, R. (2004). "The role of RNA interference in heterochromatic silencing." Nature **431**(7006): 364-70.
- Luking, A., Stahl, U. and Schmidt, U. (1998). "The protein family of RNA helicases." Crit Rev Biochem Mol Biol **33**(4): 259-96.
- Lykke-Andersen, J., Shu, M. D. and Steitz, J. A. (2000). "Human Upf proteins target an mRNA for nonsense-mediated decay when bound downstream of a termination codon." Cell **103**(7): 1121-31.

- Ma, X. M., Yoon, S. O., Richardson, C. J., Julich, K. and Blenis, J. (2008). "SKAR links pre-mRNA splicing to mTOR/S6K1-mediated enhanced translation efficiency of spliced mRNAs." Cell **133**(2): 303-13.
- Maquat, L. E. (2005). "Nonsense-mediated mRNA decay in mammals." J Cell Sci **118**(Pt 9): 1773-6.
- Maquat, L. E. and Carmichael, G. G. (2001). "Quality control of mRNA function." Cell **104**(2): 173-6.
- Maquat, L. E. and Li, X. (2001). "Mammalian heat shock p70 and histone H4 transcripts, which derive from naturally intronless genes, are immune to nonsense-mediated decay." RNA **7**(3): 445-56.
- Markus, M. A., Heinrich, B., Raitskin, O., Adams, D. J., Mangs, H., Goy, C., Ladomery, M., Sperling, R., Stamm, S. and Morris, B. J. (2006). "WT1 interacts with the splicing protein RBM4 and regulates its ability to modulate alternative splicing in vivo." Exp Cell Res **312**(17): 3379-88.
- Markus, M. A. and Morris, B. J. (2006). "Lark is the splicing factor RBM4 and exhibits unique subnuclear localization properties." DNA Cell Biol **25**(8): 457-64.
- Matzke, M. A. and Matzke, A. J. (2004). "Planting the seeds of a new paradigm." PLoS Biol **2**(5): E133.
- Meister, G. and Tuschl, T. (2004). "Mechanisms of gene silencing by double-stranded RNA." Nature **431**(7006): 343-9.
- Morris, C., Wittmann, J., Jack, H. M. and Jalinot, P. (2007). "Human INT6/eIF3e is required for nonsense-mediated mRNA decay." EMBO Rep **8**(6): 596-602.
- Mort, M., Ivanov, D., Cooper, D. N. and Chuzhanova, N. A. (2008). "A meta-analysis of nonsense mutations causing human genetic disease." Hum Mutat.
- Muhlemann, O., Mock-Casagrande, C. S., Wang, J., Li, S., Custodio, N., Carmo-Fonseca, M., Wilkinson, M. F. and Moore, M. J. (2001). "Precursor RNAs harboring nonsense codons accumulate near the site of transcription." Mol Cell **8**(1): 33-43.

- Napoli, C., Lemieux, C. and Jorgensen, R. (1990). "Introduction of a Chimeric Chalcone Synthase Gene into Petunia Results in Reversible Co-Suppression of Homologous Genes in trans." Plant Cell **2**(4): 279-289.
- Neu-Yilik, G., Gehring, N. H., Hentze, M. W. and Kulozik, A. E. (2004). "Nonsense-mediated mRNA decay: from vacuum cleaner to Swiss army knife." Genome Biol **5**(4): 218.
- Neu, M., Fischer, D. and Kissel, T. (2005). "Recent advances in rational gene transfer vector design based on poly(ethylene imine) and its derivatives." J Gene Med **7**(8): 992-1009.
- Nozawa, Y., Van Belzen, N., Van der Made, A. C., Dinjens, W. N. and Bosman, F. T. (1996). "Expression of nucleophosmin/B23 in normal and neoplastic colorectal mucosa." J Pathol **178**(1): 48-52.
- Ogilvie, V. C., Wilson, B. J., Nicol, S. M., Morrice, N. A., Saunders, L. R., Barber, G. N. and Fuller-Pace, F. V. (2003). "The highly related DEAD box RNA helicases p68 and p72 exist as heterodimers in cells." Nucleic Acids Res **31**(5): 1470-80.
- Okuda, M., Horn, H. F., Tarapore, P., Tokuyama, Y., Smulian, A. G., Chan, P. K., Knudsen, E. S., Hofmann, I. A., Snyder, J. D., Bove, K. E. and Fukasawa, K. (2000). "Nucleophosmin/B23 is a target of CDK2/cyclin E in centrosome duplication." Cell **103**(1): 127-40.
- Paddison, P. J., Caudy, A. A., Bernstein, E., Hannon, G. J. and Conklin, D. S. (2002). "Short hairpin RNAs (shRNAs) induce sequence-specific silencing in mammalian cells." Genes Dev **16**(8): 948-58.
- Pal, M., Ishigaki, Y., Nagy, E. and Maquat, L. E. (2001). "Evidence that phosphorylation of human Upf1 protein varies with intracellular location and is mediated by a wortmannin-sensitive and rapamycin-sensitive PI 3-kinase-related kinase signaling pathway." RNA **7**(1): 5-15.
- Palacios, I. M., Gatfield, D., St Johnston, D. and Izaurralde, E. (2004). "An eIF4AIII-containing complex required for mRNA localization and nonsense-mediated mRNA decay." Nature **427**(6976): 753-7.
- Palaniswamy, V., Moraes, K. C., Wilusz, C. J. and Wilusz, J. (2006). "Nucleophosmin is selectively deposited on mRNA during polyadenylation." Nat Struct Mol Biol **13**(5): 429-35.

- Palauqui, J. C., Elmayan, T., Pollien, J. M. and Vaucheret, H. (1997). "Systemic acquired silencing: transgene-specific post-transcriptional silencing is transmitted by grafting from silenced stocks to non-silenced scions." EMBO J **16**(15): 4738-45.
- Plasterk, R. H. (2002). "RNA silencing: the genome's immune system." Science **296**(5571): 1263-5.
- Pulak, R. and Anderson, P. (1993). "mRNA surveillance by the *Caenorhabditis elegans* smg genes." Genes Dev **7**(10): 1885-97.
- Qing, Y., Yingmao, G., Lujun, B. and Shaoling, L. (2008). "Role of Npm1 in proliferation, apoptosis and differentiation of neural stem cells." J Neurol Sci **266**(1-2): 131-7.
- Rana, T. M. (2007). "Illuminating the silence: understanding the structure and function of small RNAs." Nat Rev Mol Cell Biol **8**(1): 23-36.
- Reynolds, A., Leake, D., Boese, Q., Scaringe, S., Marshall, W. S. and Khvorova, A. (2004). "Rational siRNA design for RNA interference." Nat Biotechnol **22**(3): 326-30.
- Roth, M. J., Tanese, N. and Goff, S. P. (1985). "Purification and characterization of murine retroviral reverse transcriptase expressed in *Escherichia coli*." J Biol Chem **260**(16): 9326-35.
- Ruiz-Echevarria, M. J., Gonzalez, C. I. and Peltz, S. W. (1998). "Identifying the right stop: determining how the surveillance complex recognizes and degrades an aberrant mRNA." EMBO J **17**(2): 575-89.
- Saxena, S., Jonsson, Z. O. and Dutta, A. (2003). "Small RNAs with imperfect match to endogenous mRNA repress translation. Implications for off-target activity of small inhibitory RNA in mammalian cells." J Biol Chem **278**(45): 44312-9.
- Schell, T., Kulozik, A. E. and Hentze, M. W. (2002). "Integration of splicing, transport and translation to achieve mRNA quality control by the nonsense-mediated decay pathway." Genome Biol **3**(3): REVIEWS1006.

- Schmidt-Zachmann, M. S., Hugle-Dorr, B. and Franke, W. W. (1987). "A constitutive nucleolar protein identified as a member of the nucleoplasmin family." EMBO J **6**(7): 1881-90.
- Shibuya, T., Tange, T. O., Sonenberg, N. and Moore, M. J. (2004). "eIF4AIII binds spliced mRNA in the exon junction complex and is essential for nonsense-mediated decay." Nat Struct Mol Biol **11**(4): 346-51.
- Soulard, M., Della Valle, V., Siomi, M. C., Pinol-Roma, S., Codogno, P., Bauvy, C., Bellini, M., Lacroix, J. C., Monod, G., Dreyfuss, G. and et al. (1993). "hnRNP G: sequence and characterization of a glycosylated RNA-binding protein." Nucleic Acids Res **21**(18): 4210-7.
- Sproat, B. S., Lamond, A. I., Beijer, B., Neuner, P. and Ryder, U. (1989). "Highly efficient chemical synthesis of 2'-O-methyloligoribonucleotides and tetrabiotinylated derivatives; novel probes that are resistant to degradation by RNA or DNA specific nucleases." Nucleic Acids Res **17**(9): 3373-86.
- Stalder, L. and Muhlemann, O. (2007). "Transcriptional silencing of nonsense codon-containing immunoglobulin micro genes requires translation of its mRNA." J Biol Chem **282**(22): 16079-85.
- Stevenson, R. J., Hamilton, S. J., MacCallum, D. E., Hall, P. A. and Fuller-Pace, F. V. (1998). "Expression of the 'dead box' RNA helicase p68 is developmentally and growth regulated and correlates with organ differentiation/maturation in the fetus." J Pathol **184**(4): 351-9.
- Sun, X., Perlick, H. A., Dietz, H. C. and Maquat, L. E. (1998). "A mutated human homologue to yeast Upf1 protein has a dominant-negative effect on the decay of nonsense-containing mRNAs in mammalian cells." Proc Natl Acad Sci U S A **95**(17): 10009-14.
- Svitkin, Y. V., Herdy, B., Costa-Mattioli, M., Gingras, A. C., Raught, B. and Sonenberg, N. (2005). "Eukaryotic translation initiation factor 4E availability controls the switch between cap-dependent and internal ribosomal entry site-mediated translation." Mol Cell Biol **25**(23): 10556-65.
- Tabara, H., Grishok, A. and Mello, C. C. (1998). "RNAi in *C. elegans*: soaking in the genome sequence." Science **282**(5388): 430-1.

- Takemoto, T., Nishio, Y., Sekine, O., Ikeuchi, C., Nagai, Y., Maeno, Y., Maegawa, H., Kimura, H. and Kashiwagi, A. (2007). "RBMX is a novel hepatic transcriptional regulator of SREBP-1c gene response to high-fructose diet." FEBS Lett **581**(2): 218-22.
- Tange, T. O., Shibuya, T., Jurica, M. S. and Moore, M. J. (2005). "Biochemical analysis of the EJC reveals two new factors and a stable tetrameric protein core." RNA **11**(12): 1869-83.
- Thermann, R., Neu-Yilik, G., Deters, A., Frede, U., Wehr, K., Hagemeyer, C., Hentze, M. W. and Kulozik, A. E. (1998). "Binary specification of nonsense codons by splicing and cytoplasmic translation." Embo J **17**(12): 3484-94.
- Tsend-Ayush, E., O'Sullivan, L. A., Grutzner, F. S., Onnebo, S. M., Lewis, R. S., Delbridge, M. L., Marshall Graves, J. A. and Ward, A. C. (2005). "RBMX gene is essential for brain development in zebrafish." Dev Dyn **234**(3): 682-8.
- Unterholzner, L. and Izaurralde, E. (2004). "SMG7 acts as a molecular link between mRNA surveillance and mRNA decay." Mol Cell **16**(4): 587-96.
- van Blokland, R., van der Geest, N., Mol, J., Kooter, J. (1994). "Transgene-mediated suppression of chalcone synthase expression in *Petunia hybrida* results from an increase in RNA turnover." Plant J. **6**(6): 861-877.
- van Eeden, F. J., Palacios, I. M., Petronczki, M., Weston, M. J. and St Johnston, D. (2001). "Barentsz is essential for the posterior localization of oskar mRNA and colocalizes with it to the posterior pole." J Cell Biol **154**(3): 511-23.
- Vasudevan, S., Tong, Y. and Steitz, J. A. (2007). "Switching from repression to activation: microRNAs can up-regulate translation." Science **318**(5858): 1931-4.
- Venables, J. P., Elliott, D. J., Makarova, O. V., Makarov, E. M., Cooke, H. J. and Eperon, I. C. (2000). "RBMX, a probable human spermatogenesis factor, and other hnRNP G proteins interact with Tra2beta and affect splicing." Hum Mol Genet **9**(5): 685-94.
- Voinnet, O. and Baulcombe, D. C. (1997). "Systemic signalling in gene silencing." Nature **389**(6651): 553.

- Wang, J., Vock, V. M., Li, S., Olivas, O. R. and Wilkinson, M. F. (2002). "A quality control pathway that down-regulates aberrant T-cell receptor (TCR) transcripts by a mechanism requiring UPF2 and translation." J Biol Chem **277**(21): 18489-93.
- Weber, M., Moller, K., Welzeck, M. and Schorr, J. (1995). "Short technical reports. Effects of lipopolysaccharide on transfection efficiency in eukaryotic cells." Biotechniques **19**(6): 930-40.
- Wilkins, C., Dishongh, R., Moore, S. C., Whitt, M. A., Chow, M. and Machaca, K. (2005). "RNA interference is an antiviral defence mechanism in *Caenorhabditis elegans*." Nature **436**(7053): 1044-7.
- Wilkinson, M. F. and Shyu, A. B. (2002). "RNA surveillance by nuclear scanning?" Nat Cell Biol **4**(6): E144-7.
- Wu, L. and Belasco, J. G. (2008). "Let me count the ways: mechanisms of gene regulation by miRNAs and siRNAs." Mol Cell **29**(1): 1-7.
- Wu, M. H., Lam, C. Y. and Yung, B. Y. (1995). "Translocation of nucleophosmin from nucleoli to nucleoplasm requires ATP." Biochem J **305** ( Pt 3): 987-92.
- Ye, K. (2005). "Nucleophosmin/B23, a multifunctional protein that can regulate apoptosis." Cancer Biol Ther **4**(9): 918-23.
- Yung, B. Y. (2007). "Oncogenic role of nucleophosmin/B23." Chang Gung Med J **30**(4): 285-93.
- Yung, B. Y., Bor, A. M. and Yang, Y. H. (1990). "Immunolocalization of phosphoprotein B23 in proliferating and non-proliferating HeLa cells." Int J Cancer **46**(2): 272-5.
- Zamore, P. D. (2002). "Ancient pathways programmed by small RNAs." Science **296**(5571): 1265-9.
- Zatsepina, O. V., Todorov, I. T., Philipova, R. N., Krachmarov, C. P., Trendelenburg, M. F. and Jordan, E. G. (1997). "Cell cycle-dependent translocations of a major nucleolar phosphoprotein, B23, and some characteristics of its variants." Eur J Cell Biol **73**(1): 58-70.

Zeitelhofer, M., Karra, D., Macchi, P., Tolino, M., Thomas, S., Schwarz, M., Kiebler, M. and Dahm, R. (2008). "Dynamic interaction between P-bodies and transport ribonucleoprotein particles in dendrites of mature hippocampal neurons." J Neurosci **28**(30): 7555-62.

## **THESES**

Daniela Karra, PhD thesis 2008

Johanna Barbara Munding, PhD thesis 2006

## **INTERNET REFERENCES**

<http://www.oligoengine.com>

<http://www.fermentas.com>

<http://rnaidesigner.invitrogen.com/rnaiexpress/>

<http://www.ncbi.nlm.nih.gov/>

<http://www.ensembl.org/index.html>

<http://www.ihop-net.org>

<http://www.expasy.org>

<http://www.invitrogen.com>

<http://www.sigmaaldrich.com>

## **TEXTBOOKS**

Harlow E. and Lane D.; Antibodies: A Laboratory Manual; Cold Spring Harbor Laboratory; Cold Spring Harbor; 1988.

Harlow E. and Lane D.; Using Antibodies: A Laboratory Manual; Cold Spring Harbor Laboratory; Cold Spring Harbor; 1999.

Sambrook J., Fritsch E. F., Maniatis T.; Molecular Cloning: A Laboratory Manual; Cold Spring Harbor Laboratory; Cold Spring Harbor; 1989.

## **MEETINGS**

Chan, W., Gudikote, J. P. and Wilkinson, M. F. (2005). "TCR nonsense-mediated decay is insensitive to UPF3b depletion." Presented at "Eukaryotic mRNA Processing" Cold Spring Harbor, NY



## APPENDIX III: CURRICULUM VITAE

<b>Personal Information</b>	
Surname, Firstnames Address Nationality Date and place of birth Gender	Kieweg, Ingrid Daniela Vogeltenn 19, 4654 Bad Wimsbach-Neydharting, Austria Austrian citizenship 22.05.1984 in Wels, Upper Austria Female
<b>Education and Training</b>	
2002  1994-2002  1992-1994 1990-1992	School leaving examination passed with distinction (grade point average of 1.0); thesis in chemistry as part of school leaving examination, topic: "Homöopathie - Wirkungsweise und Wirksamkeit" Grammar school in Lambach with supplementary tuitions in chemistry, physics and biology (grade point average during whole school career of 1.0) Elementary school in Bad Wimsbach-N. Elementary school in Wels
<b>Academic Studies</b>	
July 2007-June 2008  2002-2008	Diploma thesis in the Division of Neuronal Cell Biology at the Center for Brain Research of the Medical University of Vienna under supervision of O. Univ.-Prof. Dr. Michael Kiebler; topic: "Analysis and characterisation of five novel Barentsz interactors in the context of nonsense-mediated mRNA decay" Study "Molecular Biology" (A 490) at the University of Vienna; specialisations: Genetics, Cell Biology, Neurosciences
<b>Scientific Work Experiences and Traineeships</b>	
March-April 2007  July and December 2006  December 2005	Division of Neuronal Cell Biology at the Center for Brain Research of the Medical University of Vienna under supervision of O. Univ.-Prof. Dr. Paolo Macchi and O. Univ.-Prof. Dr. Michael Kiebler Department of Molecular Cell Biology on the Campus Vienna Biocenter under supervision of Univ.-Ass. Mag. Dr. Christina Abrahamsberg and O. Univ.-Prof. Dr. Gerhard Wiche University course „Basics of Neuroscience“ at the Center for Brain Research of the Medical University of Vienna

<b>Techniques</b>	
	<ul style="list-style-type: none"> <li>• Able to work sterile and non-sterile</li> <li>• Able to work with DNA, RNA and proteins</li> <li>• Cell culture: cell lines and primary cultures (primary macrophages, neurons)</li> <li>• Cloning</li> <li>• PCR, RT-PCR, Real-time PCR</li> <li>• Transfection</li> <li>• Design of siRNAs and other bioinformatic techniques</li> <li>• Immunocytochemistry</li> <li>• Microscopy</li> <li>• Western Blots</li> <li>• Antibody expression in <i>E. coli</i> and purification (chromatography: affinity, gel filtration, size exclusion)</li> <li>• Course of histology and embryology</li> </ul>
<b>Languages</b>	
Mother tongue Foreign Languages	German Excellent English, elementary Italian
<b>Skills and competences</b>	
2007	Author of the study “Differences in urbane navigation between men and women” of the Institute of Anthropology of the University of Vienna
2006-2007	Member of the scientific network “Molecular Biology Society” (MBS)
2006	Excellence scholarships of the University of Vienna
2004-2005	Private tutor in Chemistry, Physics, Mathematics, English and German for 2 years at the private lesson agency “SOS Nachhilfe Wels” (Upper Austria)
1999	Participation in the Olympiad of Mathematics
1998-2001	3 years of voluntary social work in child and youth care
1998-2001	Successful participation in literature contests e.g. competition „Europäisches Jahr der Sprachen 2001” of the University of Salamanca (Spain) and the Institute for Romanic Studies of the University of Salzburg (Austria), contribution „Regengrau”